USGS
science for a changing world

Prepared in cooperation with the Oklahoma Water Resources Board

Hydrogeology, Numerical Simulation of Groundwater Flow, and Effects of Future Water Use and Drought for Reach 1 of the Washita River Alluvial Aquifer, Roger Mills and Custer Counties, Western Oklahoma, 1980–2015

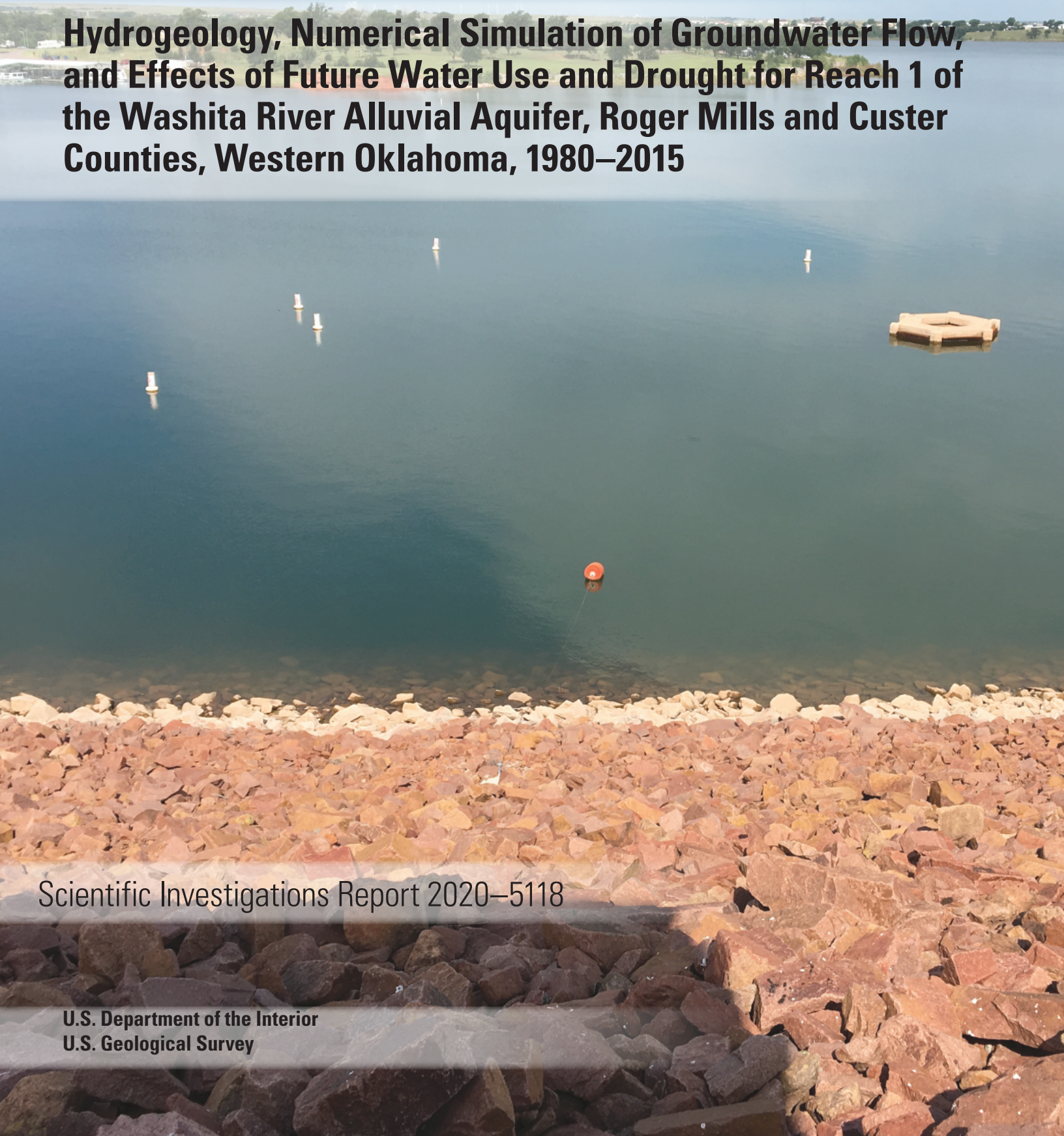

Scientific Investigations Report 2020–5118

U.S. Department of the Interior
U.S. Geological Survey

Front cover: Photograph showing Foss Reservoir and Outlet Works Intake Structure during an Annual Site Inspection, June 30, 2016. Photograph by Anna Hoag, P.E., Civil Engineer, Bureau of Reclamation.

Back cover: Photograph showing Foss Reservoir and Outlet Works Intake Structure during the Foss Dam Comprehensive Review, March 11, 2015. Photograph by Adam Milligan, Civil Engineering Technician, Bureau of Reclamation.

Hydrogeology, Numerical Simulation of Groundwater Flow, and Effects of Future Water Use and Drought for Reach 1 of the Washita River Alluvial Aquifer, Roger Mills and Custer Counties, Western Oklahoma, 1980–2015

By John H. Ellis, Derek W. Ryter, Leland T. Fuhrig, Kyle W. Spears, Shana L. Mashburn, and Ian M.J. Rogers

Prepared in cooperation with the Oklahoma Water Resources Board

Scientific Investigations Report 2020–5118

U.S. Department of the Interior
U.S. Geological Survey

U.S. Department of the Interior
DAVID BERNHARDT, Secretary

U.S. Geological Survey
James F. Reilly II, Director

U.S. Geological Survey, Reston, Virginia: 2020

Suggested citation:
Ellis, J.H., Ryter, D.W., Fuhrig, L.T., Spears, K.W., Mashburn, S.L., and Rogers, I.M.J., 2020, Hydrogeology, numerical simulation of groundwater flow, and effects of future water use and drought for reach 1 of the Washita River alluvial aquifer, Roger Mills and Custer Counties, western Oklahoma, 1980–2015: U.S. Geological Survey Scientific Investigations Report 2020–5118, 81 p., https://doi.org/10.3133/sir20205118.

Associated data for this publication:
Ellis, J.H., Ryter, D.W., Fuhrig, L.F., Mashburn, S.L., and Rogers, I., 2020, MODFLOW-NWT model used in simulation of groundwater flow, and analysis of projected water use for the Washita River alluvial aquifer, western Oklahoma: U.S. Geological Survey data release, https://doi.org/10.5066/P9PKMG6U.

ISSN 2328-0328 (online)

Acknowledgments

This study was conducted as part of the U.S. Geological Survey (USGS) Cooperative Matching Funds program in cooperation with the Oklahoma Water Resources Board (OWRB). The authors thank Christopher Neel, Geologist, OWRB Water Resources, for help with defining study objectives and providing hydrogeologic and water-use permit data. The authors also thank Daniel Clement of Burns & McDonnell Engineering Company, Inc., for providing reports and information on the groundwater investigation performed for the City of Clinton, Oklahoma.

The authors thank USGS employees Kyle Rennell and Nicole Paizis, for help in the field and with data management.

Contents

Figures

Tables

Conversion Factors

U.S. customary units to International System of Units

Multiply	By	To obtain
	Length	
inch (in.)	2.54	centimeter (cm)
foot (ft)	0.3048	meter (m)
mile (mi)	1.609	kilometer (km)
	Area	
acre	4,047	square meter (m^2)
acre	0.004047	square kilometer (km^2)
square foot (ft^2)	929.0	square centimeter (cm^2)
square foot (ft^2)	0.09290	square meter (m^2)
square mile (mi^2)	259.0	hectare (ha)
square mile (mi^2)	2.590	square kilometer (km^2)
	Volume	
acre-foot (acre-ft)	1,233	cubic meter (m^3)
	Flow rate	
acre-foot per year (acre-ft/yr)	1,233	cubic meter per year (m^3/yr)
acre-foot per year (acre-ft/yr)	0.001233	cubic hectometer per year (hm^3/yr)
foot per second (ft/s)	0.3048	meter per second (m/s)
cubic foot per second (ft^3/s)	0.02832	cubic meter per second (m^3/s)
cubic foot per day (ft^3/d)	0.02832	cubic meter per day (m^3/d)
gallon per minute (gal/min)	0.06309	liter per second (L/s)
inch per year (in/yr)	25.4	millimeter per year (mm/yr)
	Hydraulic conductivity	
foot per day (ft/d)	0.3048	meter per day (m/d)
	Hydraulic gradient	
foot per mile (ft/mi)	0.1894	meter per kilometer (m/km)
	Transmissivity	
foot squared per day (ft^2/d)	0.09290	meter squared per day (m^2/d)

Temperature in degrees Fahrenheit (°F) may be converted to degrees Celsius (°C) as follows:
°C = (°F – 32) / 1.8.

Datum

Vertical coordinate information is referenced to the North American Vertical Datum of 1988 (NAVD 88), unless otherwise noted.

Horizontal coordinate information is referenced to the North American Datum of 1983 (NAD 83).

Altitude, as used in this report, refers to distance above the vertical datum.

Supplemental Information

Specific conductance is given in microsiemens per centimeter at 25 degrees Celsius (µS/cm at 25 °C).

Concentrations of chemical constituents in water are given in either milligrams per liter (mg/L) or micrograms per liter (µg/L).

Abbreviations

BFI	base-flow index
COOP	cooperative observer (NOAA station)
DEM	digital elevation model
EPS	equal-proportionate share
ET	evapotranspiration
ETg	saturated-zone evapotranspiration
GHB	General-Head Boundary
HVSR	horizontal-to-vertical spectral ratio
Lidar	light detection and ranging
MAY	maximum annual yield
NHDPlus	National Hydrography Dataset Plus
NOAA	National Oceanographic and Atmospheric Administration
NRCS	Natural Resources Conservation Service
NWIS	National Water Information System
OWRB	Oklahoma Water Resources Board
RMSE	root-mean-square error
SFR2	Streamflow-Routing Package, version 2
SVD	singular value decomposition
SVDA	singular value decomposition-assist
SWB	Soil-Water-Balance (code)
USGS	U.S. Geological Survey
WTF	water-table fluctuation

Hydrogeology, Numerical Simulation of Groundwater Flow, and Effects of Future Water Use and Drought for Reach 1 of the Washita River Alluvial Aquifer, Roger Mills and Custer Counties, Western Oklahoma, 1980–2015

By John H. Ellis,[1] Derek W. Ryter,[1] Leland T. Fuhrig,[1] Kyle W. Spears,[2] Shana L. Mashburn,[1] and Ian M.J. Rogers[1]

Abstract

The Washita River alluvial aquifer is a valley-fill and terrace alluvial aquifer along the valley of the Washita River in western Oklahoma that provides a productive source of groundwater for agricultural irrigation and water supply. The Oklahoma Water Resources Board (OWRB) has designated the westernmost section of the aquifer in Roger Mills and Custer Counties, Okla., as reach 1 of the Washita River alluvial aquifer; reach 1 is the focus of this report. The OWRB issued an order on November 13, 1990, that established the maximum annual yield (MAY; 120,320 acre-feet per year [acre-ft/yr]) and equal-proportionate-share (EPS) pumping rate (2.0 acre-feet per acre per year [(acre-ft/acre)/yr]) for reach 1 of the Washita River alluvial aquifer. The MAY and EPS were based on hydrologic investigations that evaluated the effects of potential groundwater withdrawals on groundwater availability in the Washita River alluvial aquifer. Every 20 years, the OWRB is statutorily required to update the hydrologic investigation on which the MAY and EPS were based. Because 30 years have elapsed since the last order was issued, the U.S. Geological Survey, in cooperation with the OWRB, conducted a new hydrologic investigation and evaluated the effects of potential groundwater withdrawals on groundwater flow and availability in the Washita River alluvial aquifer.

The Washita River is the primary source of inflow to Foss Reservoir, a Bureau of Reclamation reservoir constructed in 1961 for flood control, water supply, and recreation. Foss Reservoir provides water for Bessie, Clinton, New Cordell, and Hobart, Okla. Nearly 98 percent of the total groundwater use from the Washita River alluvial aquifer during 1967 to 2015 was for irrigation; other uses of groundwater in the study area include public supply, mining, and agriculture.

A hydrogeologic framework was developed for the Washita River alluvial aquifer and included the physical characteristics of the aquifer, the geologic setting, the hydraulic properties of hydrogeologic units, the potentiometric surface (water table), and groundwater-flow directions at a scale that captures the regional controls on groundwater flow. The Washita River alluvial aquifer consists of alluvium and terrace deposits that were transported primarily by water and range from clay to gravel in size. The terrace includes windblown deposits of silt size and, in some cases, contains gravel laid down at several levels along former courses of present-day rivers.

A conceptual flow model is a simplified description of the aquifer system that includes hydrologic boundaries, major inflow and outflow sources of the groundwater-flow system, and a conceptual water budget with the estimated mean flows between those hydrologic boundaries. During the study period 1980–2015, mean annual groundwater withdrawals, predominantly used for agricultural irrigation, totaled 5,502 acre-ft/yr, or 14 percent of aquifer outflows. When applied across the 132-square-mile aquifer area used for modeling purposes (84,366 acres), mean annual recharge of 3.15 inches per year corresponds to a mean annual recharge volume of 22,169 acre-ft/yr, or 56 percent of aquifer inflows. The annual saturated-zone evapotranspiration outflow was 11,828 acre-ft/yr for the Washita River alluvial aquifer, or about 30 percent of aquifer outflows. For the Washita River alluvial aquifer, lateral flow was 17,157 acre-ft/yr, or 44 percent of the aquifer inflows. The conceptual flow model and hydrogeologic framework were used to conceptualize, design, and build the numerical groundwater-flow model.

A numerical groundwater-flow model of the Washita River alluvial aquifer was constructed by using MODFLOW-2005. The Washita River alluvial aquifer groundwater-model grid was spatially discretized into 350-foot (ft) cells and two layers. Layer 1 represented the undifferentiated alluvium and terrace deposits of Quaternary

[1]U.S. Geological Survey.

[2]Oklahoma State University.

age, and layer 2 represented the bedrock of Permian age, which was given a uniform nominal thickness of 100 ft. The groundwater-simulation period was temporally discretized into 433 monthly transient stress periods, representing January 1980 to December 2015. An initial 365-day steady-state stress period was configured to represent mean annual inflows and outflows from the Washita River alluvial aquifer for the study period. The groundwater-flow model was calibrated manually and by automated adjustment of model inputs by using PEST++. Calibration targets for the Washita River alluvial aquifer model included groundwater-level observations and reservoir-stage observations, as well as base-flow and stream-seepage estimates.

Three groundwater-availability scenarios were used in the calibrated groundwater model to (1) estimate the EPS pumping rate that retains the saturated thickness that meets the minimum 20-year life of the aquifer, (2) quantify the effects of projected pumping rates on groundwater storage over a 50-year period, and (3) evaluate how projected pumping rates extended 50 years into the future and sustained hypothetical drought conditions over a 10-year period affect base flow and groundwater in storage. The results of the groundwater-availability scenarios could be used by the OWRB to reevaluate the established MAY of groundwater from the Washita River alluvial aquifer.

EPS scenarios for the Washita River alluvial aquifer were run for periods of 20, 40, and 50 years. The 20-, 40-, and 50-year EPS pumping rates under normal recharge conditions were 1.7, 1.6, and 1.6 (acre-ft/acre)/yr, respectively. Given the aquifer area used for modeling purposes (84,366 acres), these rates correspond to annual yields of 142,579, 134,986, and 134,986 acre-ft/yr, respectively. Groundwater storage at the end of the 20-year EPS scenario was about 281,000 acre-feet (acre-ft), or about 306,000 acre-ft (52 percent) less than the starting storage. Considering the land-surface area of the Washita River alluvial aquifer and using a specific yield of 0.12, this decrease in storage was equivalent to a mean groundwater-level decline of about 30 ft. The Washita River downstream from Foss Reservoir and most of the streams in the study area were dry at the end of the 20-year EPS scenario. Foss Reservoir stage was below the dead-pool stage of 1,597 ft after about 7 years of pumping in the 20-year EPS scenario.

Four projected 50-year groundwater-use scenarios were used to simulate the effects of selected well withdrawal rates on groundwater storage in the Washita River alluvial aquifer. These four scenarios used (1) no groundwater use, (2) groundwater use at the 2015 pumping rate, (3) mean groundwater use for the simulation period, and (4) increasing groundwater use. Groundwater storage after 50 years with no groundwater use was 545,249 acre-ft, or 693 acre-ft (0.1 percent) greater than the initial groundwater storage; this groundwater storage increase is equivalent to a mean groundwater-level increase of 0.1 ft. Groundwater storage at the end of the 50-year period with 2015 pumping rates was 543,831 acre-ft, or 723 acre-ft (0.1 percent) less than the initial storage; this groundwater storage decrease is equivalent to a mean groundwater-level decrease of 0.1 ft. Groundwater storage after 50 years with the mean pumping rate for the study period was 543,202 acre-ft, or 1,349 acre-ft (0.2 percent) less than the initial groundwater storage; this groundwater storage decrease is equivalent to a mean groundwater-level decrease of 0.1 ft. Groundwater storage at the end of the 50-year period with an increasing demand groundwater-pumping rate, which was 38 percent greater than the 2015 groundwater-pumping rate, was 542,584 acre-ft, or 1,967 acre-ft (0.4 percent) less than the initial storage; this groundwater storage decrease is equivalent to a mean groundwater-level decrease of 0.2 ft.

A hypothetical 10-year-drought scenario was used to simulate the effects of a prolonged period of reduced recharge on groundwater storage in the Washita River alluvial aquifer and Foss Reservoir stage and storage. To simulate the hypothetical drought, recharge in the calibrated model was reduced by 50 percent during the simulated drought period (1983–1992). Groundwater storage at the end of the drought period in December 1992 was 562,000 acre-ft, or 36,000 acre-ft (6 percent) less than the groundwater storage of the calibrated groundwater model (598,000 acre-ft). At the end of the hypothetical drought, the largest changes in saturated thickness (as great as 43.5 ft) were in the area upgradient from Foss Reservoir, particularly in the terrace at the model boundary. Substantial decreases in the Foss Reservoir stage began during the fall of 1985 in conjunction with base-flow decreases of up to 100 percent at U.S. Geological Survey streamgage 07324200 Washita River near Hammon, Okla. These lake-stage declines outpaced groundwater-level declines in the surrounding aquifer. The minimum Foss Reservoir storage simulated during the drought period was 77,954 acre-ft, which was a decrease of 46 percent from the non-drought storage.

Introduction

Total water demand in west-central Oklahoma is projected to increase by approximately 38 percent from 2010 to 2060 because of increasing irrigation demand and oil and gas operations, during which surface-water and groundwater shortfalls are predicted (Oklahoma Water Resources Board [OWRB], 2012b). Because of increasing water demands, depletion of water in the High Plains aquifer to the west, and recurring droughts, effective water-resource management of surface-water and groundwater resources is essential (Gutentag and others, 1984). A priority recommendation of the Oklahoma Comprehensive Water Plan (OWRB, 2012a) was to complete updates of hydrologic investigations and to analyze groundwater and surface-water interactions in selected aquifers in Oklahoma. The Washita River alluvial aquifer is a valley-fill and terrace alluvial aquifer along the Washita

River and its tributaries in west-central Oklahoma (fig. 1). The Washita River alluvial aquifer provides water primarily for irrigation purposes; other uses of groundwater in the study area include public supply, mining, and agriculture. This report provides results from an updated hydrogeologic investigation for reach 1 of the Washita River alluvial aquifer (fig. 1).

The 1973 Oklahoma Water Law (82 OK Stat § 82-1020.5) requires the OWRB to conduct hydrologic investigations of the State's aquifers (called groundwater basins in the statutes) to support a determination of the maximum annual yield (MAY) for each groundwater basin (Oklahoma Senate, 2019). The MAY is defined as the amount of fresh groundwater that can be withdrawn annually while ensuring a minimum 20-year life of the aquifer (OWRB, 2017b). For alluvium and terrace aquifers such as the Washita River alluvial aquifer, the groundwater basin-life requirement is satisfied if, after 20 years of MAY withdrawals, 50 percent of the groundwater basin retains a saturated thickness of at least 5 feet (ft). When a MAY has been established, the amount of land owned or leased by a well permit applicant determines the annual volume of water allocated to that well permit. The annual volume of water allocated per acre of land is known as the equal-proportionate-share (EPS) pumping rate.

For reach 1 of the Washita River alluvial aquifer, the OWRB issued a final order on November 13, 1990, that established the MAY (120,320 acre-feet per year [acre-ft/yr]) and the EPS pumping rate (2.0 acre-feet per acre per year [(acre-ft/acre)/yr]) (OWRB, 2012b). The MAY and EPS were based on hydrologic investigations by Kent and others (1984) that used a numerical groundwater-flow model (hereinafter, "Trescott groundwater model") from Trescott and others (1976) to evaluate the effects of potential groundwater withdrawals on groundwater availability in the Washita River alluvial aquifer. Every 20 years, the OWRB is statutorily required to update the hydrologic investigation on which the MAY and EPS were based. Because 20 years have elapsed since the 1990 final order was issued, the U.S. Geological Survey (USGS), in cooperation with the OWRB, conducted an updated hydrologic investigation and evaluated the potential effects of groundwater availability by using a new numerical groundwater-flow model. Results of the groundwater-availability model scenarios support efforts by the OWRB to reevaluate the MAY of groundwater from the Washita River alluvial aquifer.

Purpose and Scope

The purpose of this report is to describe a hydrologic investigation of the Washita River alluvial aquifer that includes an updated summary of the aquifer hydrogeology and results of the simulation of water availability obtained by using a numerical groundwater-flow model. A hydrogeologic framework of the aquifer was developed from available water-use data, recharge and evapotranspiration estimates, streamflow data, lateral groundwater flow estimates, and reservoir storage and levels for the study area. The groundwater transient model was calibrated to observed water-level data, reservoir stage, and stream base-flow and seepage data and was used to compute a mean annual water budget for the study period 1980–2015. This report documents the construction and calibration of this groundwater-flow model. Groundwater-availability scenarios were performed by using the calibrated groundwater model to (1) estimate the EPS pumping rate that could retain a minimum 20-, 40-, and 50-year life of the aquifer, (2) quantify the potential effects of projected well withdrawals on groundwater storage over a 50-year period, and (3) simulate the potential effects of a hypothetical 10-year drought on groundwater storage and lake storage.

Description of Study Area

The Washita River alluvial aquifer is one of several alluvial aquifers along rivers that cross western Oklahoma, including the Canadian River to the north and North Fork Red River to the south (fig. 2), and is a source of water for various uses. The study area begins at the upstream extent of the Washita River where the river and its associated alluvial aquifer cross the Texas–Oklahoma border. The study area extends across west-central Oklahoma from the Texas border for about 65 miles to the southeast part of Custer County, Okla., and includes 131 river miles of the Washita River and about 10 miles of Foss Reservoir. The altitude of the Washita River at the western, upstream end is approximately 2,232 ft above NAVD 88, and where the river leaves the study area downstream from Clinton, Okla., the altitude of the river is 1,437 ft. The mean stream gradient for this 141-mile reach of the Washita River is approximately 5.6 feet per mile.

The Washita River alluvial aquifer is a long, narrow surficial aquifer that underlies the Washita River valley in Oklahoma from the western border with Texas southeast to near Lake Texoma (fig. 1), covering approximately 110 square miles (mi^2) (71,000 acres). The aquifer is made up of alluvium and terrace deposits of the Washita River and several tributaries, and the extent of the hydrologic investigation area includes underlying and adjacent bedrock units of Tertiary and Permian ages. The OWRB has designated the westernmost section of the aquifer in Roger Mills and Custer Counties, Okla. (fig. 1) (reach 1) of the Washita River alluvial and terrace aquifer (OWRB, 2012b) for the MAY and EPS determination. The study area, referred to throughout this report as the Washita River alluvial aquifer, has the same extent as reach 1 of the Washita River alluvial aquifer.

The Washita River is the primary source of inflow to Foss Reservoir, a Bureau of Reclamation reservoir constructed in 1961 for flood control, water supply, and recreation. Foss Reservoir provides 18,000 acre-ft/yr for Clinton, Bessie, New Cordell (fig. 2), and Hobart (south of study area, not shown on fig. 2) in Oklahoma (OWRB, 2012b). For the study period 1980–2015, about half of the annual surface-water inflow to Foss Reservoir was supplied by base flow. Base flow was

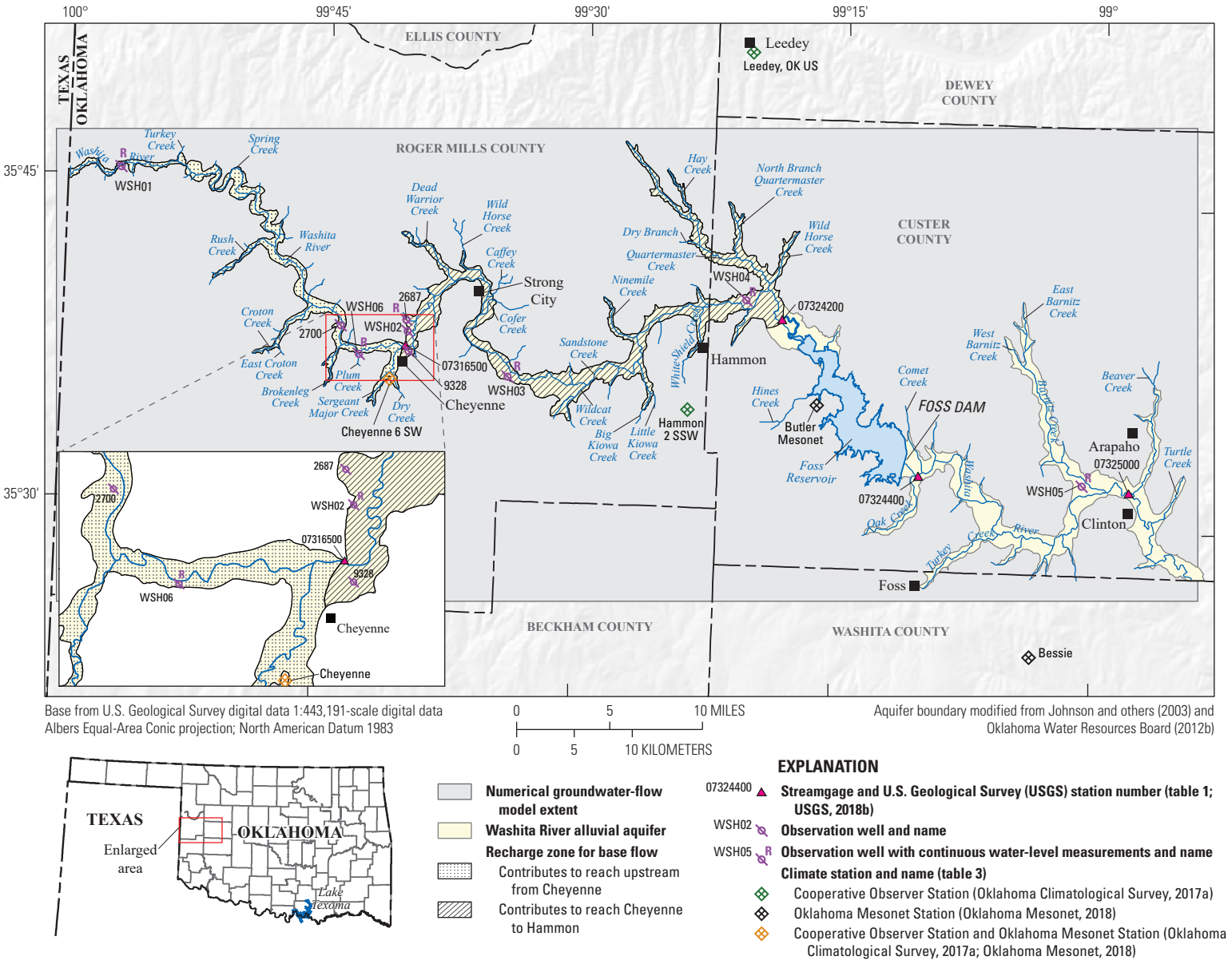

Figure 1. Locations of hydrological features, observation wells, streamgages, climate stations, and cities associated with the study of reach 1 of the Washita River alluvial aquifer, Roger Mills and Custer Counties, western Oklahoma.

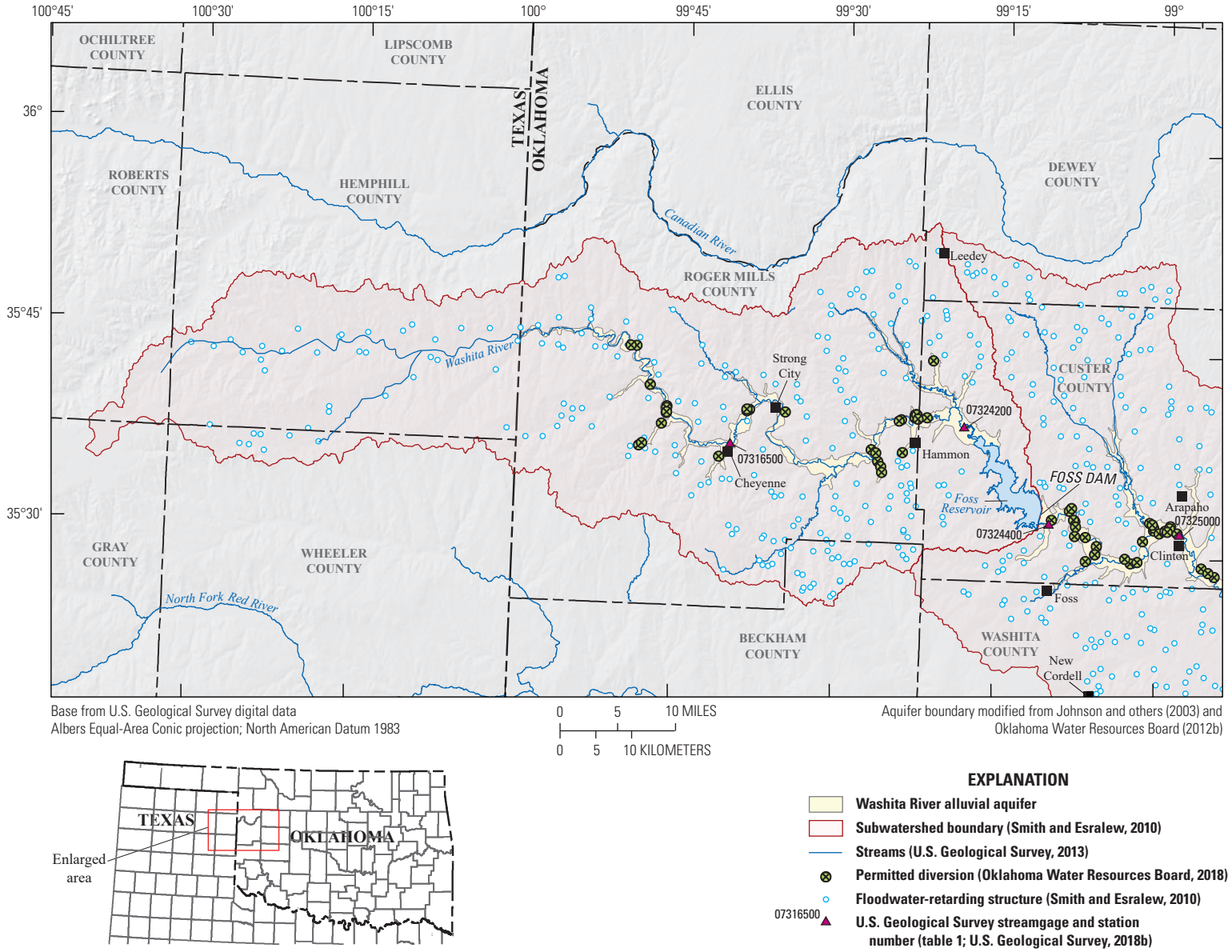

Figure 2. Major geographic and surface-water features, floodwater-retarding structures, and surface-water diversions in and near the Washita River subwatershed, western Oklahoma.

computed at the USGS streamgage 07324200 Washita River near Hammon, Okla. [hereinafter referred to as the Hammon streamgage] (table 1). Base flow, which is the component of streamflow supplied by the discharge of groundwater to streams (Barlow and Leake, 2012) was computed by using the USGS Groundwater Toolbox (Barlow and others, 2015) (table 2); refer to the "Base Flow" section of this report for additional details. The total annual base flow and the base-flow index (the ratio of total annual base flow to the total annual streamflow) at the Hammon streamgage, upstream from Foss Reservoir, generally increased during the study period 1980–2015, but a decrease in base flow occurred during 2012–14 (table 2). The observed increases in base flow are likely attributable to increased precipitation (and recharge), the several hundred impoundments or floodwater-retarding structures that regulate the runoff recession of single storm events (Smith and Esralew, 2010; fig. 2) in the Washita River subwatershed, or changes in agricultural practices that reduced runoff and promoted artificial recharge to the aquifer.

Previous Investigations

A description of the groundwater resources along the Washita River in the study area in Leonard and others (1958) includes descriptions of the alluvial sedimentology, depositional history, and the general characteristics of the groundwater system. The groundwater resources and groundwater use in Custer County (fig. 1) are described in Hart (1978). The bedrock lithology and stratigraphy for Custer County are described in Fay (1978).

Schipper (1983) describes the Washita River alluvial aquifer and includes a groundwater management model for Roger Mills and Custer Counties. Schipper (1983) provides a compilation of hydrologic data for the 1970s and a detailed description of the aquifer hydrogeologic framework. Kent and others (1984) used information provided by Schipper (1983) to estimate the EPS pumping rate for the Washita River alluvial aquifer and built a finite-difference groundwater model following the method of Trescott and others (1976).

The groundwater model in Kent and others (1984) has a uniform grid with 1,320-ft cells and values estimated for depth to water, saturated thickness, transmissivity, and recharge. In many places along the narrow aquifer, only three model cells cover the width of the aquifer. The numerical model was run as a steady-state simulation and was calibrated by using mass balance of inflow and outflow; no hydraulic head or flow targets were used during calibration. Hydraulic and recharge parameters were adjusted to maintain the starting hydraulic head field under steady-state flow conditions. The Washita River was assumed to be gaining streamflow from groundwater throughout Washita River alluvial aquifer, and this gain was assumed to be equal to aquifer recharge. The model was then run as a transient simulation for 20 years, and the pumping at all cells was varied until the number of cells with less than 5 ft of saturated thickness was equal to half of the aquifer area.

Kent and others (1984) divided the Washita River alluvial aquifer into three subareas. The first subarea included the Washita River alluvial aquifer from the Texas-Oklahoma border to about 6 miles (mi) downgradient from Cheyenne (fig. 1). The second subarea included the Washita River alluvial aquifer from 6 mi downgradient from Cheyenne to Foss Reservoir. The third subarea included the Washita River alluvial aquifer downgradient from Foss Dam. Separate EPS pumping rates were determined for each subarea: 2.70 (acre-ft/acre)/yr for the area upgradient from Cheyenne and 1.75 (acre-ft/acre)/yr for the other two subareas. The weighted EPS for the three subareas of the Washita River alluvial aquifer was estimated to be 2.18 (acre-ft/acre)/yr.

Table 1. Information for selected continuous-record streamgages (USGS, 2018b) in the Washita River alluvial aquifer study area, western Oklahoma.

[USGS, U.S. Geological Survey; Dates are in month/year format]

USGS station number (fig. 1)	Station name	Short name	Latitude, in decimal degrees	Longitude, in decimal degrees	Period of record used in this analysis (may contain gaps)	
					Begin	End
07316500	Washita River near Cheyenne, Okla.	Cheyenne streamgage	35.62644	−99.66840	10/1937	12/2015
07324200	Washita River near Hammon, Okla.	Hammon streamgage	35.47310	−100.12095	10/1969	12/2015
07324400	Washita River near Foss, Okla.	Foss streamgage	35.65644	−99.30621	3/1956	12/2015
07325000	Washita River near Clinton, Okla.	Clinton streamgage	35.42227	−99.96928	10/1935	12/2015

Table 2. Annual-mean streamflow and annual-mean base flow for selected USGS streamgages in the Washita River alluvial aquifer study area, 1980–2015.

[USGS, U.S. Geological Survey; ft³/s, cubic foot per second; acre-ft/yr, acre-foot per year; %, percent; BFI, base-flow index; --, data not available or not applicable; Base-flow values computed by using USGS Groundwater Toolbox (Barlow and others, 2015)]

Year	07316500 Washita River near Cheyenne, Okla. (Cheyenne streamgage)			07324200 Washita River near Hammon, Okla. (Hammon streamgage)			07324400 Washita River near Foss, Okla. (Foss streamgage)			07325000 Washita River near Clinton, Okla. (Clinton streamgage)		
	Mean streamflow, in ft³/s	Mean base flow		Mean streamflow, in ft³/s	Mean base flow		Mean streamflow, in ft³/s	Mean base flow		Mean streamflow, in ft³/s	Mean base flow	
		ft³/s	% (BFI)		ft³/s	% (BFI)		ft³/s	% (BFI)		ft³/s	% (BFI)
1980	18.7	11.7	62.7	37.3	14.1	37.7	46.2	9.9	21.3	71.4	31.5	44.1
1981	3.9	2.7	70.3	4.5	1.6	35.3	9.9	7.1	71.6	26.3	14.3	54.5
1982	58.8	13.0	22.0	106.9	19.4	18.2	116.2	49.4	42.5	199.9	103.7	51.9
1983	20.5	13.7	66.9	47.7	29.4	61.6	101.0	57.8	57.3	157.4	89.8	57.1
1984	9.2	7.0	76.2	21.0	13.2	62.9	7.4	6.6	89.1	30.3	24.6	81.1
1985	13.2	7.1	53.6	14.8	8.9	60.1	10.5	9.3	88.8	22.1	16.4	74.2
1986	23.8	11.6	48.8	77.6	32.2	41.4	56.5	12.5	22.0	217.4	60.8	28.0
1987	36.3	23.6	65.1	--	--	--	246.3	121.4	49.3	336.3	181.6	54.0
1988	23.4	16.9	72.3	--	--	--	--	--	--	174.7	127.6	73.1
1989	21.1	11.7	55.4	--	--	--	9.1	8.8	96.7	279.2	177.1	63.4
1990	26.2	11.3	43.2	96.7	44.9	46.5	73.5	32.9	44.7	145.3	100.2	68.9
1991	9.0	5.3	58.6	32.1	20.6	64.0	36.7	11.5	31.3	82.3	44.1	53.6
1992	11.6	8.4	72.2	35.7	26.2	73.3	40.3	12.7	31.5	90.8	53.8	59.2
1993	21.9	15.5	70.9	65.6	46.3	70.6	104.6	53.4	51.0	183.8	123.5	67.2
1994	8.0	4.3	54.0	20.3	13.4	65.8	5.6	4.4	78.8	36.8	20.7	56.3
1995	21.9	8.8	40.4	80.2	31.3	39.0	95.4	40.7	42.6	270.8	119.0	43.9
1996	23.0	12.1	52.5	86.7	49.3	56.9	143.4	60.1	41.9	341.5	173.7	50.9
1997	72.0	42.9	59.6	294.4	184.9	62.8	390.5	188.1	48.2	692.3	471.1	68.0
1998	46.7	32.7	70.0	209.3	153.8	73.5	221.4	106.0	47.9	345.1	222.9	64.6
1999	30.5	19.8	65.0	119.1	88.3	74.1	120.0	53.7	44.7	190.2	114.6	60.3
2000	28.9	17.1	59.1	77.2	51.7	66.9	69.3	24.7	35.6	127.4	71.3	56.0
2001	35.4	26.9	75.9	112.1	68.9	61.5	150.0	73.8	49.2	211.3	150.8	71.4
2002	25.6	15.2	59.5	47.9	28.8	60.1	6.3	5.2	82.4	32.4	21.4	66.0
2003	31.3	19.3	61.7	54.7	32.6	59.6	47.4	14.1	29.7	65.0	35.8	55.0
2004	24.1	15.6	64.7	43.2	26.5	61.3	25.8	11.8	45.7	59.7	29.9	50.1
2005	25.2	17.3	68.5	55.4	37.2	67.2	79.1	29.8	37.6	116.3	70.8	60.8
2006	8.1	4.6	57.0	14.6	9.0	61.6	11.1	10.1	90.7	24.2	19.5	80.4
2007	45.1	24.2	53.6	128.5	57.8	44.9	142.3	52.7	37.1	234.1	101.4	43.3
2008	60.6	30.8	50.8	103.7	55.1	53.1	84.6	18.4	21.7	167.5	80.4	48.0
2009	30.6	24.7	80.8	51.4	38.3	74.5	52.7	13.9	26.4	97.4	46.1	47.4
2010	34.9	22.9	65.6	62.0	35.0	56.4	40.9	18.4	45.0	77.0	46.8	60.8
2011	7.9	6.0	75.9	12.5	10.6	84.6	13.0	12.5	96.0	22.0	19.4	88.0
2012	3.2	1.9	59.1	3.0	0.6	20.0	5.8	5.0	86.2	12.6	8.1	64.0
2013	1.1	0.2	20.0	0.9	0.0	1.1	4.5	3.4	75.8	7.4	4.3	57.8
2014	0.9	0.1	12.2	0.4	0.0	0.0	3.5	2.8	80.0	7.4	3.5	47.7
2015	53.4	23.5	44.0	95.9	34.3	35.7	31.6	4.5	14.2	117.6	28.9	24.6
Mean	**25.4**	**14.7**	**58.0**	**67.1**	**38.3**	**53.1**	**74.4**	**32.8**	**53.0**	**146.5**	**83.6**	**58.2**
Mean, in acre-ft/yr	**18,421**	**10,669**		**48,556**	**27,725**		**53,830**	**23,727**		**106,045**	**60,519**	

Land Cover and Population

Land-use surveys documented in the CropScape database indicate that the land cover for the Washita River alluvial aquifer during 2008–18 was mostly rural, undeveloped land and that most of the land was used for growing crops (National Agricultural Statistics Service, 2019). The CropScape database includes information about land-cover characteristics at a 30-meter (98-foot) resolution for land overlying the Washita River alluvial aquifer from 2008 to 2018. Developed land covered 3 percent of the area, forest covered 2 percent of the area, and water, wetland, or barren land covered 9 percent of the area. The majority of the Washita River alluvial aquifer area was covered by cropland (56 percent), grass/pasture (18 percent), and shrubland (12 percent). Winter wheat (70 percent) and alfalfa (19 percent) accounted for 89 percent of the crop types over the Washita River alluvial aquifer area (fig. 3). Although crop types may change on the basis of economic conditions and hydrologic factors such as flooding or drought conditions, the percentages of total crop land cover and individual crop types only changed by 1–2 percent during 2008–18 (National Agricultural Statistics Service, 2019).

U.S. Census Bureau information was used to determine changes in population in the study area from 2000 to 2015. Oklahoma cities and towns closest to the Washita River alluvial aquifer with more than 500 residents include Hammon, Arapaho, Cheyenne, and Clinton (fig. 1) (U.S. Census Bureau, 2017). During 2000–15, the U.S. Census Bureau (2017) noted that populations of these four cities and towns increased as follows: the population of Hammon increased 19.4 percent from 493 to 589; the population of Arapaho increased 9.6 percent from 751 to 823; the population of Cheyenne increased 9.5 percent from 749 to 820; and the population of Clinton, the most populous city near the Washita River alluvial aquifer, increased 5.9 percent, from 8,886 to 9,410. The combined population of all four cities and towns increased by about 7 percent from 2000 to 2015.

Climate

The Washita River alluvial aquifer straddles the boundary between the humid subtropical climate of the interior lowlands to the east, and the cooler, semiarid midlatitude steppe climate of the Great Plains of North America to the west (Kottek and others, 2006). Long-term precipitation data for the region including the study area were obtained for three Oklahoma Mesonet stations and three National Oceanographic and Atmospheric Administration (NOAA) cooperative observer (COOP) stations (table 3) (Oklahoma Mesonet, 2018; Oklahoma Climatological Survey, 2017a). Years with less than 9 months of rainfall data were not included in this analysis. The long-term mean annual precipitation at these six stations ranged from 23.2 to 27.8 inches (in.) (table 3), which does not represent the extent to which mean annual precipitation varies in the study area. Mean annual precipitation is approximately 10 in. greater in the eastern part of the study area than in the western part of the study area, and precipitation amounts steadily increase from west to east (Oklahoma Climatological Survey, 2017a). Annual precipitation is less in the western part of the study area in part because this area is affected by a regional orographic rain shadow formed by the Rocky Mountains (Tortorelli and others, 1991). May and June are normally the wettest months of the year, whereas January and February are the months with the least amounts of precipitation (fig. 4). During May and June, parts of the study area can receive as much as 4 in. of precipitation. In January and February, precipitation is typically less than 1 in., some of which is snow; annual snow totals typically range from 1 to 10 in. (Oklahoma Climatological Survey, 2017b).

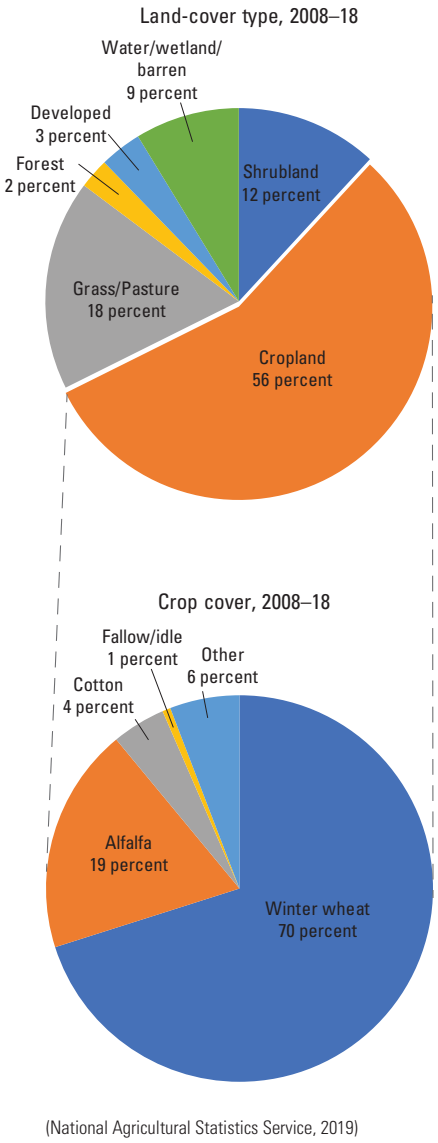

(National Agricultural Statistics Service, 2019)

Figure 3. Land cover and crop cover over the Washita River alluvial aquifer, western Oklahoma, 2008–18.

Mean annual precipitation for the COOP station in Leedey, Okla. (hereinafter referred to as the Leedey COOP station) during 1941–2017 was 24.4 in. (table 3), and total annual precipitation at this station varied from as little as 11.8 in. to as much as 43.7 in. (Oklahoma Climatological Survey, 2017a). Although the Leedey COOP station is about 5 mi north of the northern boundary used in the numerical groundwater model (fig. 1), it is within the Washita River subwatershed boundary (fig. 2) and was used in this analysis because it provided the longest continuous precipitation records among all nearby climate stations that included the years 1980–2015.

A long-term mean annual precipitation amount of 24.6 in. for 1920 to 2017 was determined from data from the six climate stations in or near the study area (fig. 5). A 5-year weighted moving mean was used to delineate wet and dry periods by combining the available long-term precipitation data from the six climate stations. Periods when the 5-year moving average was below the long-term mean annual precipitation were classified as dry, and periods above the long-term mean annual precipitation were classified as wet (fig. 5).

Between 1920 and 2017, a pattern of consecutive wet years followed by consecutive dry years is evident. Some of the more noteworthy features in the long-term record include the extended dry periods during 1930–40, 1943–56, 1961–72, and 2009–14. Wet periods lasting 2–6 years preceded and followed each of these dry periods. From 1969 to 1994 the 5-year moving average was relatively stable, during which time there were 9 years when the annual precipitation was above the long-term mean annual precipitation amount and 17 years when it was below that amount (fig. 5). From 1995 to 2004, annual precipitation mostly remained above the long-term mean, and the greatest annual precipitation total on record occurred in 1997, with 43.7 in. recorded at the Leedey COOP station (Oklahoma Climatological Survey, 2017a) and 50.5 in. at the Butler Mesonet station (Oklahoma Climatological Survey, 2017a). After a few years of near-average precipitation from 2005 to 2008, drought conditions returned during 2009–14, before being alleviated by above-average precipitation during 2015–17 (refer to the “Recharge” section of this report for addition details).

Groundwater Use

Groundwater-use data for Oklahoma are self-reported annually to the OWRB by permitted users. The OWRB staff reviewed groundwater-use data from 1967 to 2015 overlying the Washita River alluvial aquifer for inconsistencies to ensure errors in reported data were corrected (Ellis and others, 2020). Annual groundwater-use categories analyzed for this report include agriculture, irrigation, public supply, mining, and other. Uses that are also required to be reported to the OWRB include thermoelectric power, industrial, commercial, and recreation, fish, and wildlife, but these categories accounted for little to none of the groundwater use in the Washita River alluvial aquifer study area (table 4). Irrigators using more than 5 (acre-ft/acre)/yr must report use parameters to the OWRB so that the volume of groundwater used can be calculated (OWRB, 2017b). The most complete records for this reporting began in 1967; therefore, water-use data in this report start in 1967. Reporting requirements have changed at various times since permitting began. Prior to 1980, irrigators were only required to record crop type, frequency of irrigation, and number of acres irrigated. Since 1980, irrigators have been required to include the number of applications and the inches of water per application (OWRB 2017b), which allows a more precise estimation of the volume of irrigation water used. Since annual groundwater-use reporting began in 1967, reporting has not been required for domestic water wells, agricultural use less than 5 (acre-ft/acre)/yr, or irrigation applied to fewer than 3 acres (OWRB, 2017b).

Table 3. Mean annual precipitation at selected Mesonet and National Oceanographic and Atmospheric Administration (NOAA) cooperative observer (COOP) climate stations used in the analysis of the Washita River alluvial aquifer study area.

[All precipitation values are in inches per year. --, no data available]

Station name (fig. 1)	Period of record	Number of years	Mean annual precipitation			
			Period of record	1930–1988	1989–2008	2009–2014
Bessie (Mesonet)[1]	1994–2017	23	27.8	--	29.8	21.0
Butler (Mesonet)[1]	1994–2017	23	27.3	--	28.7	20.3
Cheyenne (Mesonet)[1]	1994–2017	23	27.0	--	28.8	20.5
LEEDEY (COOP)[2]	1941–2017	76	24.4	23.1	26.9	20.6
HAMMON 2 SSW (COOP)[2]	1920–2004	84	25.7	24.3	29.2	--
CHEYENNE 6 SW (COOP)[2]	1923–1993	70	23.2	22.9	21.7	--

[1]Oklahoma Mesonet, 2018.

[2]Oklahoma Climatological Survey, 2017a.

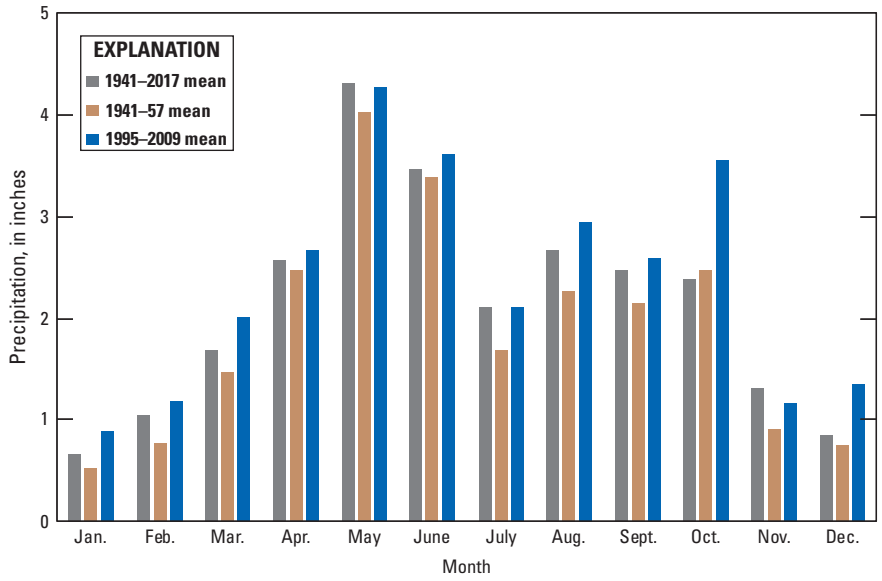

Figure 4. Mean monthly precipitation at the Leedey, Oklahoma, climate station for the period 1941–2017 (Oklahoma Climatological Survey, 2017b), and mean monthly precipitation for the dry period 1941–1957 and the wet period 1995–2009.

Temporary permits are issued by the OWRB for a groundwater user to extract a set volume of groundwater over a 90-day period. Temporary permits started being documented in the OWRB database in 1992. From 1992 to 2017, 145 temporary permits were issued in the study area, with water used predominantly for oil, gas, and mining, with a combined total reported use of 1,427.6 acre-ft/yr (OWRB, 2017b). During 1992–2017, the year with the largest temporarily permitted groundwater use was 2012, with 454.6 acre-ft, all of which was used for oil, gas, and mining.

Data from 245 groundwater-use permits were categorized by type per year from 1967 through 2015 for the Washita River alluvial aquifer study area (Ellis and others, 2020). The mean annual total groundwater use for the period of record, 1967–2015, was 6,079 acre-ft (fig. 6). Nearly 98 percent of the total groundwater use reported was for irrigation. Periods with below-average precipitation (fig. 5) typically correspond to greater reported groundwater use. From 1967 to 1980, the mean annual use of 7,189.5 acre-ft/yr was greater than the mean annual use for the period of record, and precipitation totals for 8 of those 14 years were below the 76-year mean (fig. 5 and fig. 6 and table 4). Annual groundwater use increased from 6,748 acre-ft in 1967 to 9,599 acre-ft in 1972 before declining during the early 1990s to about 2,000 acre-ft, with the exception of 1976 and 1980 when reported groundwater use was greater than 8,000 acre-ft. Some of these variations in water use could be attributed to the differences in reporting requirements for irrigation use. After declining to about 2,000 acre-ft/yr in the early 1990s, groundwater use increased during 1994–1996, with annual use ranging from about 4,000 to 8,000 acre-ft/yr. In 1997 precipitation was well above average, and reported groundwater use declined to 2,030 acre-ft/yr (fig. 6). Subsequently, groundwater use increased over the next 2 years before steadily declining from 1999 to 2003 (fig. 6). Reported groundwater

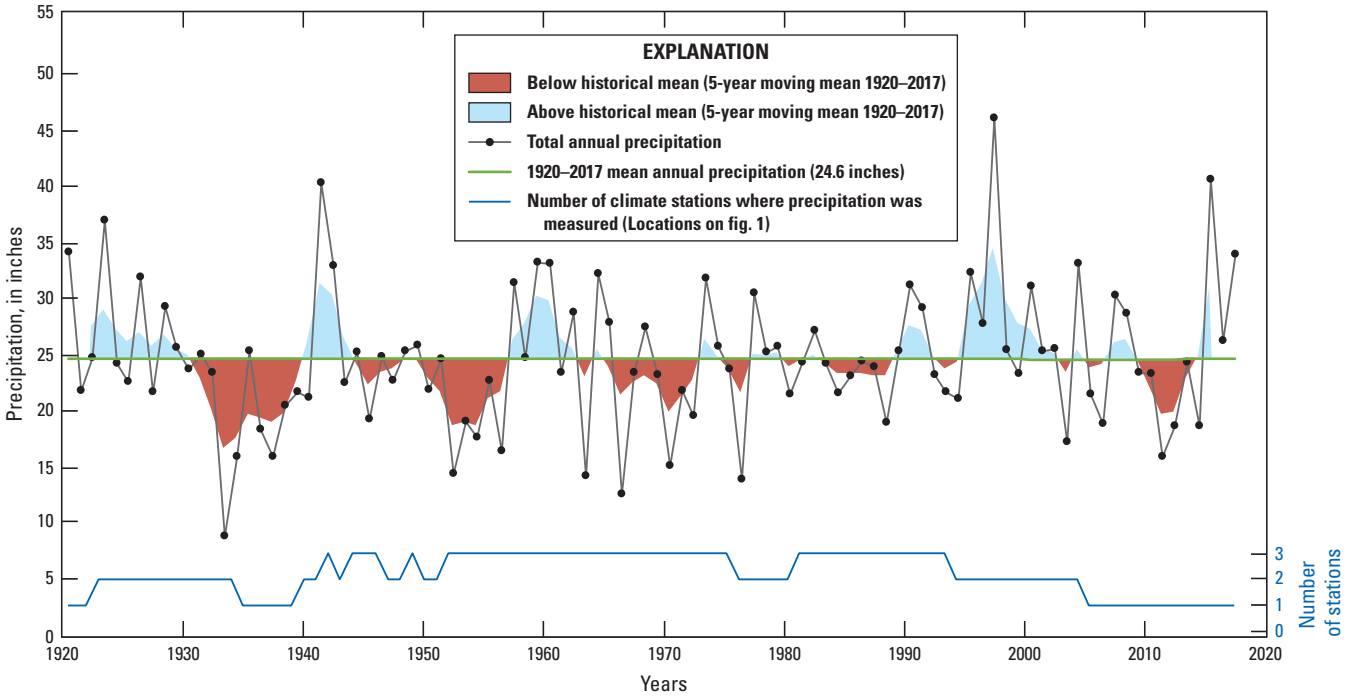

Figure 5. Wet and dry periods defined as departure of the 5-year weighted moving average from the mean annual precipitation, 1920–2017, and the number of climate stations with observations.

Table 4. Mean annual reported groundwater use in the Washita River alluvial aquifer study area, 1967–2015.

[%, percent]

Period	Mean annual reported groundwater use by use type, in acre-feet per year and percentage of use type for period									
	Agriculture	Irrigation	Public supply	Industrial	Thermoelectric power	Mining	Commercial	Recreation, fish, and wildlife	Other	Total
1967–1980	0	7,183	6.0	0	0	0.1	0	0	0	7,189.5
	0.0%	99.9%	0.1%	0.0%	0.0%	0.0%	0.0%	0.0%	0.0%	
1981–1993	0.2	3,980	37	0	0	1.0	0	0	0.1	4,018.4
	0.0%	99.0%	0.9%	0.0%	0.0%	0.0%	0.0%	0.0%	0.0%	
1994–2003	2.1	4,472	196	0	0	4.3	0	0	126	4,800.0
	0.0%	93.2%	4.1%	0.0%	0.0%	0.1%	0.0%	0.0%	2.6%	
2004–2015	2.7	7,322	54	0	0	23	0	0	94	7,496.0
	0.0%	97.7%	0.7%	0.0%	0.0%	0.3%	0.0%	0.0%	1.3%	
1967–2015	1.1	5,814	65	0	0	6.8	0	0	49	5,935.6
	0.0%	98.0%	1.1%	0.0%	0.0%	0.1%	0.0%	0.0%	0.8%	

use steadily increased from 4,716 acre-ft in 2008 to more than 10,000 acre-ft in 2013 and 2014. This pattern of increasing groundwater usage (fig. 6) is likely a result of several consecutive years of drought conditions (fig. 5). In 2015, the study area received more than 40 in. of precipitation, and reported groundwater use decreased more than 5,000 acre-ft from the previous year.

Streamflow Characteristics

In addition to data from the Hammon streamgage, daily streamflow measurements were available for the period 1980–2015 for three more USGS streamgages (fig. 1 and table 2) near the towns of Cheyenne, Foss, and Clinton, Okla. These stations are USGS streamgage 07316500 Washita River near Cheyenne, Okla. (hereinafter referred to as the Cheyenne

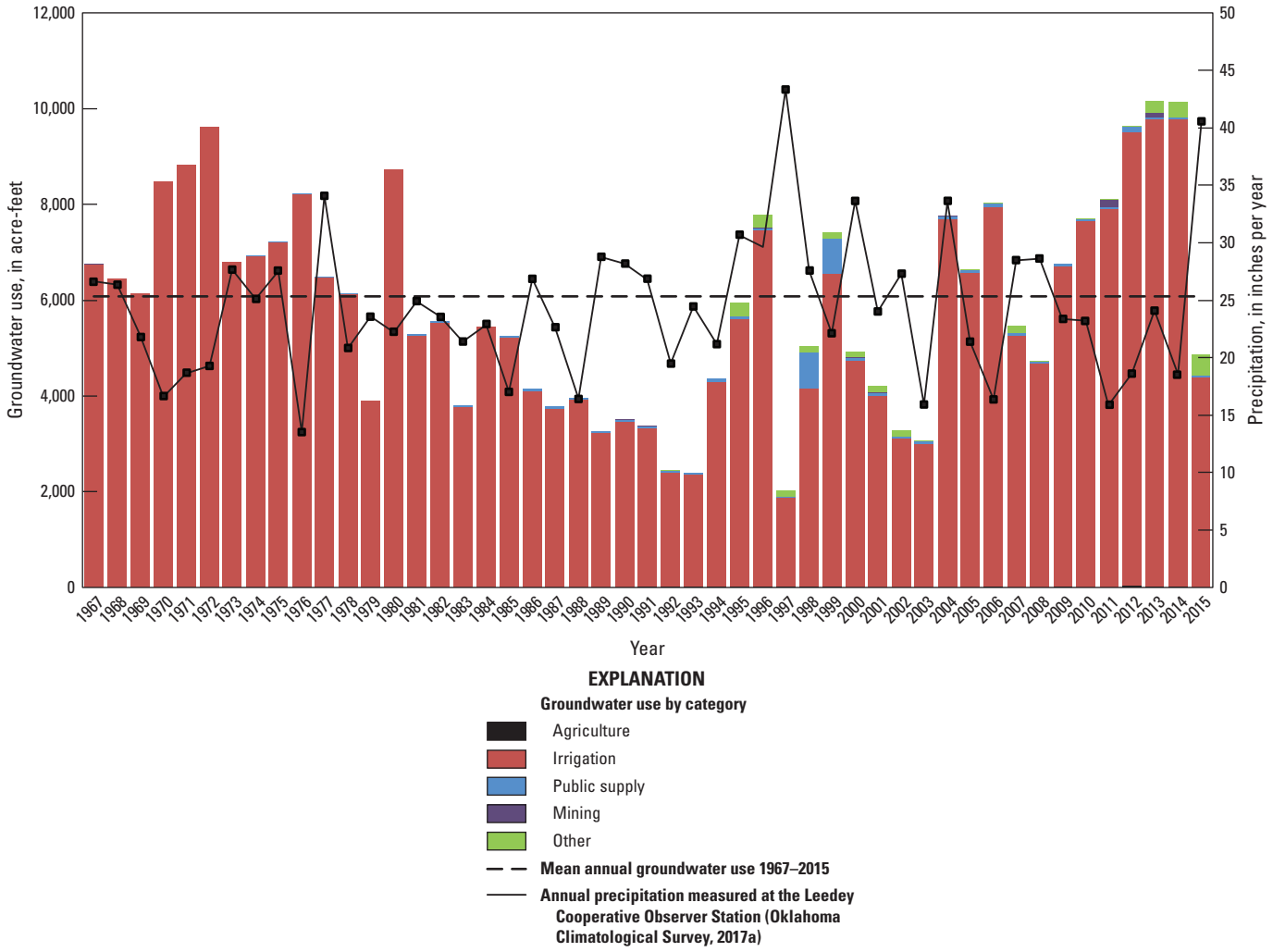

Figure 6. Estimated annual groundwater use and annual precipitation from the Leedey climate station during 1967–2015 by category for the Washita River alluvial aquifer, western Oklahoma.

streamgage), USGS streamgage 07324400 Washita River near Foss, Okla. (hereinafter referred to as the Foss streamgage), and USGS streamgage 07325000 Washita River near Clinton, Okla. (hereinafter referred to as the Clinton streamgage) (fig. 1 and table 2) (USGS, 2018b). Mean annual streamflows at the Cheyenne and Hammon streamgages were greatest during a wet period from 1995 to 2002 (about 72 cubic feet per second [ft³/s] and 294 ft³/s, respectively) and were very low (about 0.9 and 0.4 ft³/s, respectively) during the hydrologic drought from 2011 to 2014 (table 2) (Shivers and Andrews, 2013).

Streamflow downstream from Foss Dam (fig. 1) was controlled by releases from Foss Dam, local precipitation, and groundwater base flow. Mean annual streamflow released from Foss Dam was approximately 41.1 ft³/s during the study period, with greater releases during wet periods and a prolonged period with no releases during dry periods.

Mean annual streamflow (74.4 ft³/s) measured at the Foss streamgage includes flow from Oak Creek (fig. 1) and was similar to that measured at the Hammon streamgage (67.1 ft³/s) (table 2). Streamflow measured at the Clinton streamgage includes the inflows from Turkey Creek and more substantial inflows from Barnitz Creek, neither of which were measured during the period of study. Mean annual streamflow measured at the Clinton streamgage for the study period was 146.5 ft³/s. Washita River streamflow was not measured downstream from the Clinton streamgage in the study area.

Geologic Units and Hydrogeology of the Study Area

The Washita River alluvial aquifer is composed of alluvium and terrace deposits of Quaternary age that unconformably overlie bedrock units of Permian age (fig. 7) (Fay, 2010). At the western edge of Roger Mills County, the Washita River alluvial aquifer is about 0.25 mi wide and increases to an average of 1.5 mi wide at the eastern end of the Washita River

alluvial aquifer at Clinton, Okla. (Leonard and others, 1958). Alluvium underlies the Washita River from the Texas border to near Lake Texoma in south-central Oklahoma. Fay (2010) and Johnson and others (2003) have mapped alluvium adjacent to the Ogallala Formation of the High Plains aquifer near the Texas border; field observations and aerial orthophotography (Microsoft Corporation, 2017), however, indicate that the Ogallala Formation is separated from the Washita River alluvial aquifer by outcrops of the Cloud Chief Formation of Permian age and a part of the Cloud Chief Formation that is covered by a veneer of eroded Ogallala Formation rocks.

The Washita River alluvial aquifer is located on the northern flank of the Anadarko Basin, and beds of Permian age dip from 10 to 80 feet per mile to the south (Fay, 1978). Although there are many faults in the study area (Holland, 2015), no substantial offsets are indicated on the maps in Johnson and others (2003), and these faults likely do not cut across the Washita River alluvial aquifer. The Washita River alluvial aquifer was initially delineated where the alluvial and terrace deposits are indicated on the geologic map by Heran and others (2003). In the "Hydrogeologic Framework of the Washita River Alluvial Aquifer" section of this report, the alluvium and terrace deposits are further delineated for areas that do not have enough saturated thickness to be considered a water source (western part of the study area). In the easternmost part of the study area, the terrace deposits overlie the Rush Springs aquifer and are considered part of the Rush Springs aquifer and not the Washita River alluvial aquifer.

Hydrogeologic Units

A hydrogeologic unit is a continuous unit with consistent hydraulic properties that may or may not coincide with a single stratigraphic unit and is hydraulically distinct from vertically or laterally adjacent hydrogeologic units in the same hydrogeologic system (fig. 8). Each hydrogeologic unit may include zones or distinct vertical intervals that are unique but are discontinuous and not considered to be distinct hydrogeologic units.

Alluvium and Terrace Deposits of Quaternary Age

The hydrogeologic units of the Washita River alluvial aquifer consist of alluvium and terrace deposits of Quaternary age that were transported primarily by water and range from clay to gravel in size (Fay, 2010). The terrace includes windblown deposits of silt-sized material (Wentworth, 1922) and, in some cases, contains sand and gravel laid down at several levels along former courses of present-day rivers. Although Miller and Stanley (2004) and Fay (2010) delineate different units of Quaternary age in the study area, the Washita River alluvial aquifer is defined in this report as one hydrogeologic unit because there is no extensive strata or zone that has distinct hydraulic properties. The alluvium is coarsest in the western part of the study area where it is closer to the Ogallala Formation (fig. 7). Eastward, the amount of coarse sediment decreases because more eroded silt and clay from the Cloud Chief Formation has entered the valley from tributaries. In Custer County, the Rush Springs Formation is adjacent to the Washita River alluvial aquifer in the northern part of the study area. Erosion of the Rush Springs Formation may have introduced more sand to the alluvium downgradient from Foss Dam.

Three deposits of Quaternary age delineated in Leonard and others (1958) compose the Washita River alluvial aquifer; from youngest to oldest, they are alluvium, low terrace deposits, and older terrace deposits. The low terrace deposits are connected to the alluvium and are typically coarser in texture with higher hydraulic conductivity than the alluvium. Leonard and others (1958) described the older terrace deposits as topographically higher and disconnected from the alluvium and low terrace deposits. Conversely, on more recent geological maps (Johnson and others, 2003; Fay, 2010), the alluvium is not differentiated from the terrace deposits. The terrace deposits on more recent maps are equivalent to the older terrace deposits described in Leonard and others (1958).

Ogallala Formation of Tertiary Age

Underlying the alluvium and terrace deposits in the far western part of the study area is the Ogallala Formation of Tertiary age (figs. 7 and 8). The Ogallala Formation consists of brown to light tan sediments eroded from the ancestral Rocky Mountains and deposited by streams, alluvial fans, and wind. The Ogallala Formation is considered a major aquifer in Oklahoma and is composed of a fine- to medium-grained sand with some clay, silt, gravel, volcanic ash, and caliche beds, with some beds locally cemented by calcium carbonate (Carr and Bergman, 1976). The Ogallala Formation subcrop area below the alluvium and terrace is poorly defined because the loosely consolidated materials of the Ogallala Formation resemble those of the overlying alluvium and terrace deposits. The Ogallala Formation thickness towards the westernmost extent in the study area is 320 ft and thins eastward to the erosional extent (fig. 7). Reworked sediments of the Ogallala Formation are the main source for the coarse alluvial sediment in the different alluvial units (Leonard and others, 1958).

Bedrock Units of Permian Age

The units of Quaternary and Tertiary ages are underlain by consolidated bedrock units of Permian age. These bedrock units are reddish-brown and consist of (from youngest to oldest) the Elk City Member of the Quartermaster Formation (referred to locally as the Elk City Sandstone [Fay and Hart, 1978]), the Doxey Shale and Cloud Chief Formations of the Foss Group (Fay and Hart, 1978), and the Rush Springs Formation of the Whitehorse Group (figs. 7 and 8). The Doxey Shale was originally classified as a member of the

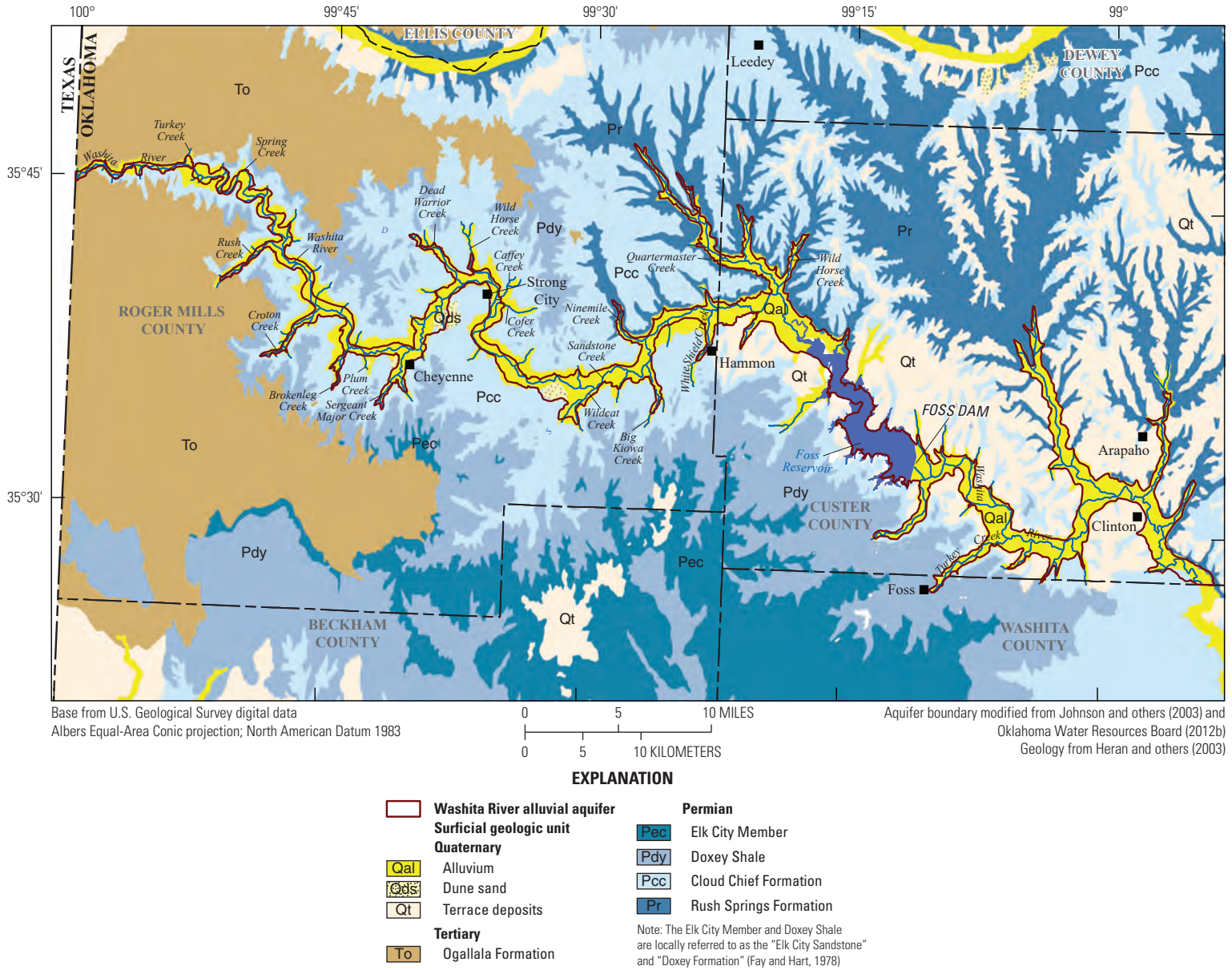

Figure 7. Surficial geologic units in the Washita River alluvial aquifer study area, western Oklahoma.

System	Geologic Unit		Hydrogeologic Unit	Thickness, in feet*	Description*
Quaternary	Alluvium and terrace deposits		Washita River alluvial aquifer	0–230	Alluvium and terrace deposits that were transported primarily by water and range from clay to gravel in size. The terrace includes windblown deposits of silt and sand size and, in some cases, contains gravel laid down at several levels along former courses of present-day rivers
Tertiary	Ogallala Formation		High Plains (Ogallala) aquifer	0–320	Brown to light tan sediments eroded from the ancestral Rocky Mountains deposited by streams, alluvial fans, and wind; fine- to medium-grained sand with some clay, silt, gravel, volcanic ash, and caliche beds, with some beds locally cemented by calcium carbonate
Permian	Quartermaster Formation	Elk City Member[1]	Elk City aquifer	0–50	Reddish-brown fine-grained sandstone with minor amounts of silt and clay; weakly cemented by iron oxide, calcium carbonate, and gypsum
	Foss Group	Doxey Shale[2]	Confining unit	0–195	Reddish-brown silty shale and siltstone
		Cloud Chief Formation	Confining unit	0–175	Reddish-brown to orange-brown shale, interbedded with siltstone and sandstone; some dolomite and much gypsum
	Whitehorse Group	Rush Springs Formation	Rush Springs aquifer	0–300	Orange-brown, fine-grained sandstone with a siltstone component, exhibiting predominantly medium- to large-scale cross-bedding; containing the Weatherford Gypsum bed
		Marlow Formation			Orange-brown, cross-bedded, fine-grained sandstone and siltstone

*Thicknesses and descriptions modified from Carr and Bergman (1976), Fay (1978), and Neel and others (2018).
[1]Referred to locally as the Elk City Sandstone (Fay and Hart, 1978).
[2]The Doxey Shale was originally classified a member of the Quartermaster Formation (Griley, 1933), but Fay and Hart (1978) raised the Doxey Shale to formation rank and included it in the Foss Group. Fay and Hart (1978) also reclassified the Cloud Chief Formation as a member of the Foss Group.

Figure 8. Surficial geologic and hydrogeologic units in the Washita River alluvial aquifer study area, western Oklahoma.

Quartermaster Formation (Griley, 1933), but Fay and Hart (1978) raised the Doxey Shale to formation rank and included it in the Foss Group. Fay and Hart (1978) also reclassified the Cloud Chief Formation as a member of the Foss Group. The Elk City Member consists of fine-grained sandstone with minor amounts of silt and clay and with weak cementation of iron oxide, calcium carbonate, and gypsum (Carr and Bergman, 1976); the Elk City Member is considered a major bedrock aquifer in Oklahoma south of the study area (OWRB, 2012b). The Doxey Shale is a confining unit in the study area. Based on the geologic map (fig. 7), the Doxey Shale and Elk City Member do not appear to subcrop below the Washita River alluvial aquifer but are located at the surface south of the Washita River alluvial aquifer in the study area. The Cloud Chief Formation consists of shale, interbedded with siltstone and sandstone, and has some dolomite and gypsum; the formation underlies much of the Washita River alluvial aquifer in the western part of the study area (Hart, 1978; Fay, 2010). The Cloud Chief Formation is considered relatively impermeable and likely provides minimal water to the Washita River alluvial aquifer. The Rush Springs Formation, part of the Whitehorse Group, underlies the Washita River alluvial aquifer in the eastern part of the study area. The Rush Springs Formation is part of a major bedrock aquifer, the Rush Springs aquifer, in Oklahoma, but is not used as an aquifer in the western part of the study area underlying the Washita River alluvial aquifer, the Ogallala Formation, and the Cloud Chief Formation (Neel and others, 2018). The Rush Springs Formation is a cross-bedded, fine-grained sandstone with a siltstone component and contains the Weatherford Gypsum bed (Carr and Bergman, 1976). The Rush Springs Formation likely subcrops below the Washita River alluvial aquifer, but the extent is difficult to discern from the geologic map (fig. 7). The Rush Springs Formation is possibly in direct hydraulic connection with the Washita River alluvial aquifer in some areas (Hart, 1978), but the quantity of groundwater flowing between the Rush Springs Formation and the Washita River alluvial aquifer has not been measured. The Rush Springs Formation outcrop is exposed on the north side of the Washita River alluvial aquifer starting about 4 mi west of Hammon and extends eastward to about the middle part of Foss Reservoir. Barnitz Creek overlies the Rush Springs Formation and the northern margin of the Washita River alluvial aquifer.

Groundwater Quality

Groundwater samples were collected between July 28 and August 25, 2014, from the Washita River alluvial aquifer as part of the OWRB Groundwater Monitoring and Assessment Program (OWRB, 2017a). Groundwater was sampled from 12 wells along the 116-mi reach 1 of the Washita River alluvial aquifer (fig. 9). Nine of the wells were in Roger Mills County, and 3 were in Custer County. The groundwater samples were analyzed for physical properties (water temperature, dissolved oxygen, pH, and specific conductance), major ions, dissolved solids, nutrients, and trace metals.

Dissolved-solids concentrations in the groundwater samples ranged from 1,760 to 3,650 milligrams per liter (mg/L), with a median concentration of 2,895 mg/L and a mean concentration of 2,832 mg/L (OWRB, 2017a). The U.S. Environmental Protection Agency (2020) has established a secondary drinking water standard of 500 mg/L for dissolved solids; however, the State of Oklahoma considers water with dissolved solids less than 5,000 mg/L to be fresh (OWRB, 2017a). No groundwater samples had dissolved solids concentrations exceeding the 5,000-mg/L threshold (OWRB, 2017a).

Specific conductance ranged from 2,060 to 3,940 microsiemens per centimeter at 25 degrees Celsius (µS/cm), with a median value of 2,925 µS/cm and a mean of 2,988 µS/cm. All groundwater samples were classified as hard water, with hardness values greater than 180 mg/L of calcium carbonate. The hardness ranged from 1,088 to 1,916 mg/L, with a median value of 1,708 mg/L and a mean value of 1,679 mg/L. Of the trace metals and elemental constituents analyzed, only concentrations of iron, manganese, and uranium exceeded the secondary drinking water standards or maximum contaminant levels. Concentrations of iron in samples from 4 of the 12 wells exceeded the secondary drinking water standard (300 micrograms per liter [µg/L]; U.S. Environmental Protection Agency, 2020), and the median iron concentration for all samples was 158 µg/L. Concentrations of manganese in samples from 4 of the 12 wells exceeded the secondary drinking water standard (300 µg/L; U.S. Environmental Protection Agency, 2020), and the median manganese concentration for all samples was 96.5 µg/L. The uranium concentration in 1 of the 12 wells exceeded the maximum contaminant level (30 µg/L; U.S. Environmental Protection Agency, 2020), with a value of 40.7 µg/L. The median concentration of uranium for all samples was 7.9 µg/L.

Major-ion data from the OWRB Groundwater Monitoring and Assessment Program were plotted on a piper diagram (Piper, 1944) to determine the sources of the dissolved constituents in the groundwater (fig. 10). Major-ion concentrations in the groundwater were fairly similar in samples representing different parts of the aquifer, with calcium being the dominant cation in all but four groundwater samples and sulfate being the dominant anion in all groundwater samples (fig. 10). The four groundwater samples in which calcium concentrations were lowest were collected from wells located farthest upgradient (fig. 9). These wells were categorized as having no dominant ion type. The percentages of calcium in samples from these four wells were less than about 75 percent of the total cations, with magnesium and sodium plus potassium each representing about 25 percent of the remaining cations. The concentrations of calcium, magnesium, and sulfate in the groundwater were attributed to the dissolution of gypsum, dolomite, and calcite within the Cloud Chief Formation, which underlies the sampling extent of the Washita River (Becker and Runkle, 1998) (figs. 7 and 9). The concentrations of sodium, chloride, and potassium in the groundwater samples were likely from evaporite deposits in the Rush Springs Formation.

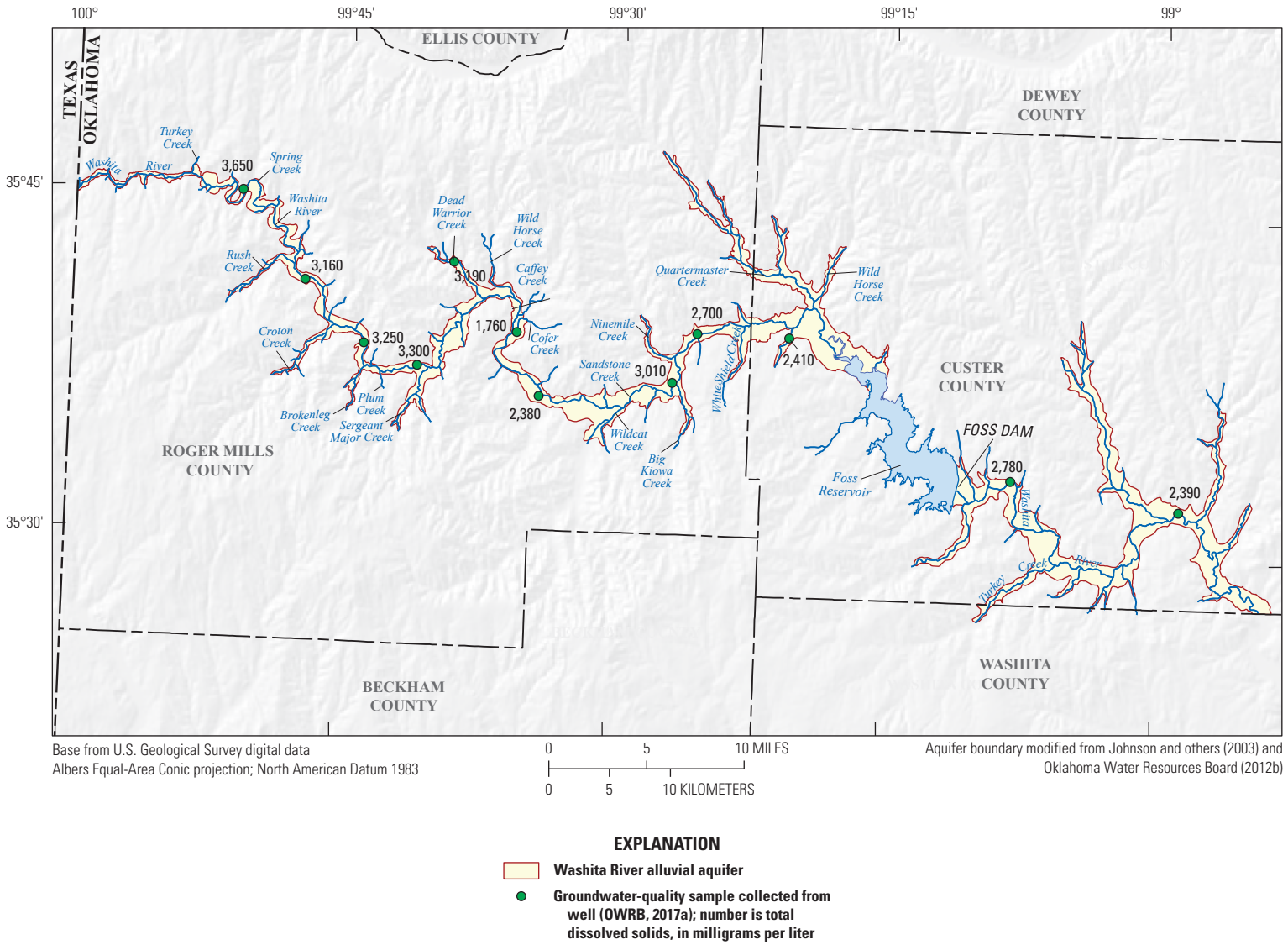

Figure 9. Locations of groundwater-quality samples collected from wells in the Washita River alluvial aquifer, western Oklahoma, and total dissolved solids in groundwater samples collected during July–August 2014.

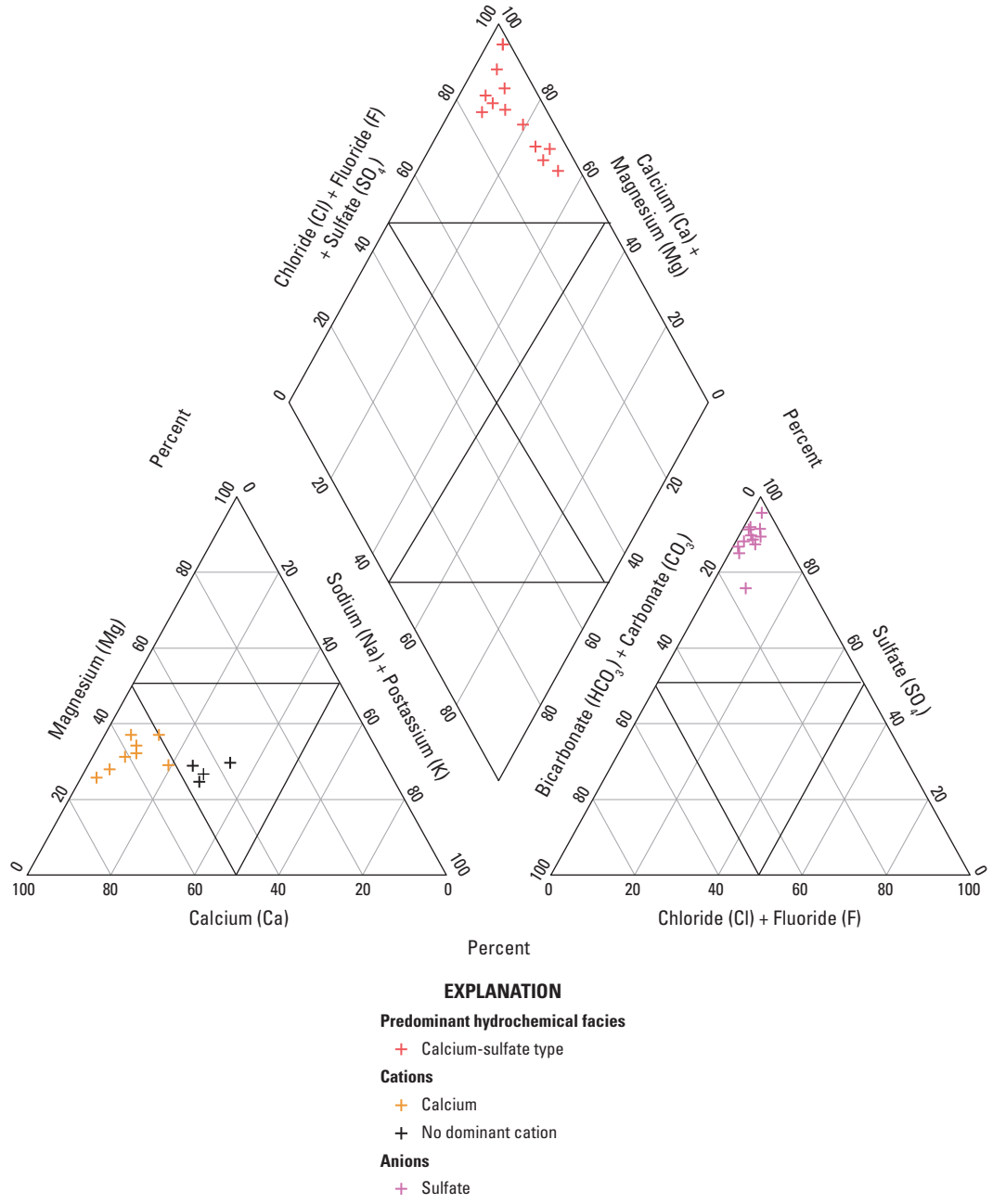

Figure 10. Major cations and anions in groundwater-quality samples of produced water from 12 wells open to the Washita River alluvial aquifer, western Oklahoma, July–August 2014.

Hydrogeologic Framework of the Washita River Alluvial Aquifer

The hydrogeologic framework of the Washita River alluvial aquifer describes the physical characteristics of the aquifer, the characteristics and hydraulic properties of hydrogeologic units, the potentiometric surface, and groundwater-flow directions at a scale that captures the regional controls on groundwater flow. The hydrogeologic framework was used in the construction of numerical groundwater model of the Washita River alluvial aquifer described in this report.

Aquifer Extent

The extent of the Washita River alluvial aquifer was modified for this study from the alluvium extent mapped by Johnson and others (2003) and Fay (2010) by using existing well lithologic logs (OWRB, 2015) and high-resolution orthophotographs (Microsoft Corporation, 2017) to delineate alluvium. In many places, the Washita River alluvial aquifer extent was found to be a smaller area than the mapped alluvium (fig. 7). Bedrock units of Permian age that underlie the Washita River alluvial aquifer were delineated by using mapped outcrops adjacent to the aquifer. Because beds of Permian age dip gently to the south, the Cloud Chief Formation has been removed by erosion to expose the Rush Springs Formation on the north side of the Washita River alluvial aquifer; however, the Cloud Chief Formation covers the south side of the Rush Springs Formation (fig. 7). The alluvium and terrace deposits were not found to have enough saturated thickness to be considered a water source in the western part of the study area, and in the easternmost part of the study area, the terrace deposits overlie the Rush Springs aquifer and are considered part of the Rush Springs aquifer and not part of the Washita River alluvial aquifer.

Lithological borehole logs from the OWRB (OWRB, 2015), and results from ambient seismic soundings collected as part of this study (USGS, 2018b) and available in Ellis and others (2020) were used collectively to define the altitude of the base of the Washita River alluvial aquifer, which is shown in figure 11 as the estimated aquifer thickness. The aquifer thickness was determined by using the 60-meter (197-ft) digital elevation model land surface (USGS, 2018a) and the points of measured depth to the base of the aquifer. The aquifer thickness was interpolated between points of calculated thickness, and the edge of the alluvial aquifer (farthest away from the river) was set to zero thickness for use as a control point.

The ambient seismic method described by Lane and others (2008) was used at 45 locations across the Washita River alluvial aquifer (fig. 11). Many of the ambient seismic points were along lines traversing the Washita River alluvial aquifer to show a cross-sectional profile of the aquifer. All ambient seismic sounding locations were published in the USGS National Water Information System database (USGS, 2018b) and are available in Ellis and others (2020). At each site, a Tromino digital seismometer was oriented to geographic north and pushed into a flat area of bare ground, allowing the stabilizing spikes on the bottom of the unit to firmly anchor into the soil (Tromino, 2012). The Tromino digital seismometer was then leveled and set to record for 10–30 minutes, a timeframe chosen based on the instrumentation guidelines (Bard and SESAME-Team, 2004) and the estimated thickness of the alluvial deposits. During that timeframe, the Tromino digital seismometer gathered ambient seismic shear waves, measuring the frequency and amplitude of shear waves along two horizontal axes and one vertical axis. Unconsolidated alluvial deposits have a slower shear-wave velocity than that of the consolidated bedrock; this contrast in shear-wave velocities causes the horizontal-to-vertical ratio of the velocities to form a peak from which a measurable resonant frequency of the consolidated bedrock is attained by using Grilla, a postprocessing software package provided by the digital seismometer manufacturer (Tromino, 2017). Bedrock depth was estimated from this resonant frequency according to the following equation from Tromino (2012):

$$Z = V_S / (4F_0) \quad (1)$$

where

Z is the depth to bedrock, in feet;
V_S is the shear-wave velocity of the unconsolidated alluvial deposits, in feet per second; and
F_0 is the resonant frequency of the consolidated bedrock, in Hertz.

The Washita River alluvial aquifer likely contains some caliche zones. Caliche zones have shear-wave velocities similar to those of consolidated bedrock; therefore, these zones may have caused a low bias to the depth to bedrock as estimated by horizontal-to-vertical spectral ratio (HVSR) seismic methods. In general, HVSR seismic methods probably are less accurate than more direct methods of estimating the depth to bedrock. Chandler and Lively (2014) collected HVSR seismic measurements at 41 control points of known depth in Minnesota glacial deposits. About 10 percent of those measurements had errors greater than 25 percent, and about 37 percent of those measurements had errors greater than 15 percent. The ambient seismic data for this study indicated a range in thickness of 0 to 200 ft, with an average of 98 ft to the base of the Washita River alluvial aquifer (fig. 11). Many of the ambient seismic points were along lines traversing the Washita River alluvial aquifer to show a cross-sectional profile of the aquifer, and ambient seismic points are published in the USGS National Water Information System database (USGS, 2018b) and are available in Ellis and others (2020).

The aquifer base was interpolated between points of measured base-of-aquifer altitude that indicated an ancestral valley (erosional surface of bedrock) trending to the southeast. Most lithological borehole logs typically noted bedrock that

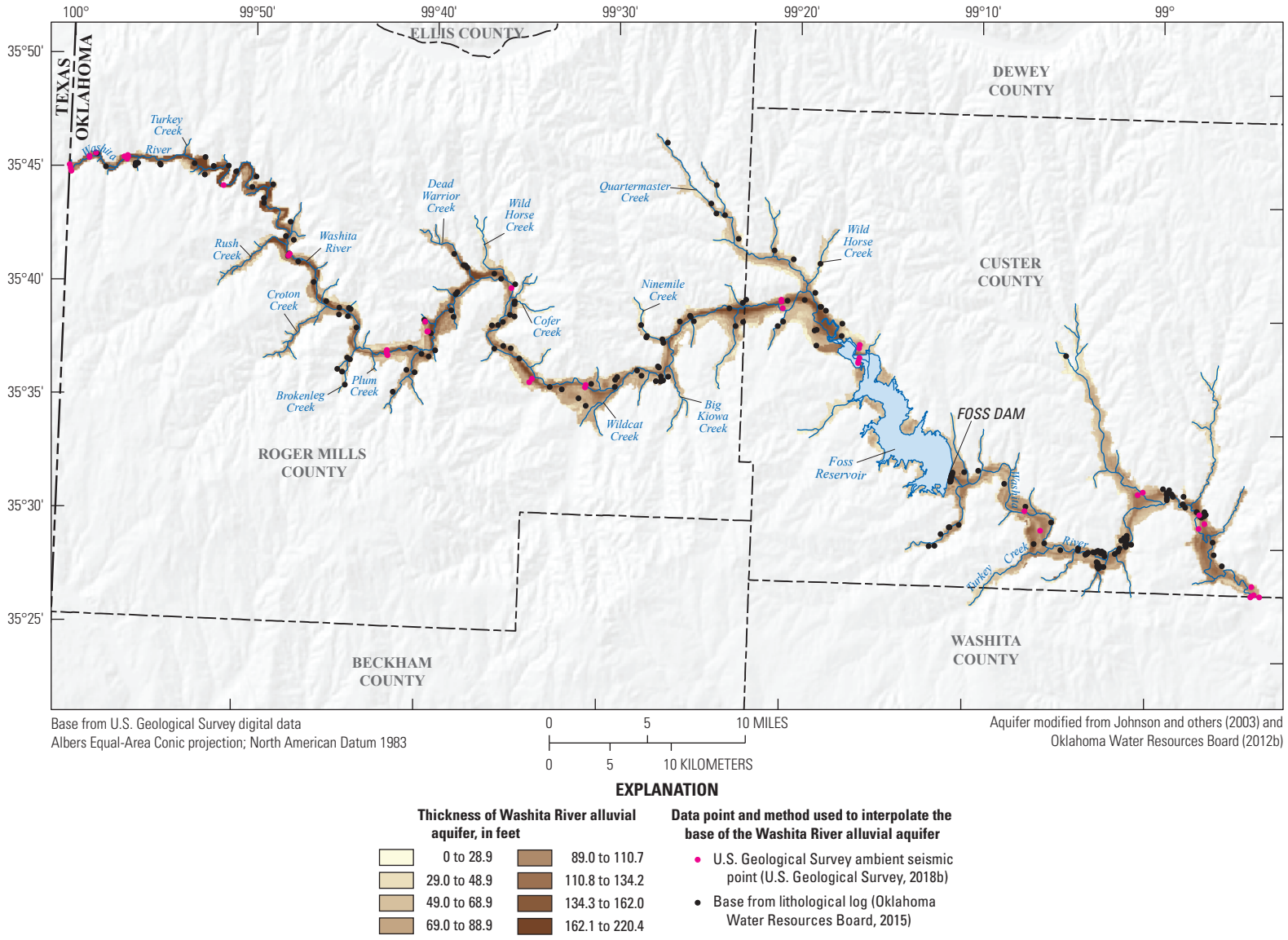

Figure 11. Points and methods used for the interpolation of the aquifer thickness of the Washita River alluvial aquifer, western Oklahoma.

changed from tan to red. The thickness of the Washita River alluvial aquifer as estimated for this report is highly variable, with a mean of 52 ft and a narrow, deep channel that is approximately 220 ft thick near the northern part of Roger Mills County in the western part of the Washita River alluvial aquifer (fig. 11). The mean thickness is biased thin because several tributary valleys have alluvium less than 50 ft thick.

Potentiometric Surface and Groundwater-Level Fluctuations

Potentiometric-surface maps show the altitude at which the groundwater level would have stood in tightly cased wells at a specified time; the potentiometric surface is usually contoured or spatially interpolated from synoptic water-table-altitude measurements in many wells across the aquifer extent. In this report, the water table is the same as the potentiometric surface for the Washita River alluvial aquifer because the aquifer is unconfined. Potentiometric-surface maps are used to indicate the general directions of groundwater flow in the aquifer. Groundwater generally flows perpendicular to potentiometric contours in the direction of decreasing contour altitudes. The potentiometric surface for March 2017 was mapped by using groundwater-level measurements from 20 wells, (USGS, 2018b) and Ellis and others (2020), and the approximate altitude of the Washita River and Foss Reservoir stages (USGS, 2018a and Bureau of Reclamation, 2018) (fig. 12); Foss Reservoir had a mean stage of 1,630.6 ft in 2015 (Bureau of Reclamation, 2018). The potentiometric surface was also approximated and was derived as the difference between the 60-meter digital elevation model land surface (USGS, 2018a) and the measured depth to water.

Methods described in Cunningham and Schalk (2011) were used to obtain groundwater-level measurements from 20 domestic and irrigation wells across the Washita River alluvial aquifer during March 2017 (USGS, 2018b) and Ellis and others (2020). In addition, reports of the depth to which driller's encountered water during drilling, provided on well completion reports (OWRB, 2018), for wells in the Washita River alluvial aquifer were used to fill in areas with few groundwater-level measurements. These two sources of measurements were used to determine the potentiometric surface for the Washita River alluvial aquifer. The potentiometric surface was interpolated between measured wells and contoured using a 20-ft interval (fig. 12). Groundwater in the Washita River alluvial aquifer flows generally downgradient to the southeast and locally flows toward and discharges to the Washita River in most areas. The Washita River is generally a gaining stream except for the western part of the Washita River in Roger Mills County as evidenced by the mapped potentiometric-surface contours that show a "V" pattern that point upstream (fig. 12).

The three observation wells with long-term water-level data (at least 25 measurements spanning at least 10 years) were OWRB wells 2687, 9328, and 2700 (OWRB, 2015) (figs. 1 and 13*C*). All three observation wells were in the Cheyenne area, and nearly all water-level measurements were made during January–March when irrigation water use is minimal.

OWRB observation well 2687 was located approximately 2.5 mi north of the town of Cheyenne on the western margin of the Washita River alluvial aquifer (fig. 1). The general pattern of slightly increasing groundwater-level altitudes is evident from 1987 to 2001 in well 2687 (fig. 13*C*). Groundwater-level altitudes can change markedly during wet and dry periods, particularly the dry period during the early 1980s, the wet period from 1985 to 2002, the erratic wet and dry years of 2003–2010, and the drought of 2011–2016. Most changes in annual-mean precipitation are attenuated; the lag in groundwater-level changes was most likely because the depth to water was more than 25 ft below land surface.

OWRB observation well 9328 is located just north of Cheyenne, Okla., on a low terrace just above the floodplain of the Washita River, and the period of record for groundwater-level measurements was from 1980 to 2002 (figs. 1 and 13*C*). The groundwater-level altitude slightly increased from 1983 to 1988. The groundwater-level record for well 9328 remained approximately static during the wet period of 1985–2002; the pattern for well 2687 was tempered by the subsequent erratic wet and dry years of 2003–2015.

OWRB observation well 2700 is located approximately 3.75 mi west-northwest from Cheyenne (fig. 1). The period of record for groundwater-level measurements was from 1980 to 1994. An overall pattern of decreasing groundwater-levels in well 2700 was evident during the wet period starting in 1985 (fig. 13*C*).

Textural and Hydraulic Properties

The Washita River alluvial aquifer is an unconsolidated alluvium deposited in a fluvial environment; therefore, the horizontal hydraulic conductivity and specific yield of the alluvial aquifer can be highly variable. The hydraulic conductivity of the Washita River alluvial aquifer was estimated from two aquifer tests reported by Burns & McDonnell Engineering Company, Inc. for the City of Clinton, Okla., in the southeast end of the Washita River alluvial aquifer (Burns & McDonnell Engineering Company, Inc., 2015) and from lithological logs for 216 wells registered with the OWRB (fig. 14).

Burns & McDonnell Engineering Company, Inc. conducted two aquifer tests west of Clinton, Okla.; however, the details of how the tests were performed are not provided in the report. One test was located at well DXN-TH7, and one at well M-1 (fig. 14). At both locations, the aquifer was confined or leaky confined, and observation wells near the tests ranged from unconfined to semiconfined and confined. Transmissivity at well M-1 was calculated to be 9,000 gallons per day per foot or 1,069 to 1,230 feet squared per day (ft^2/d), or hydraulic conductivity of 27.3 feet per day (ft/d) over the approximately 44 ft of saturated thickness at the site. At well DXN-TH7, the

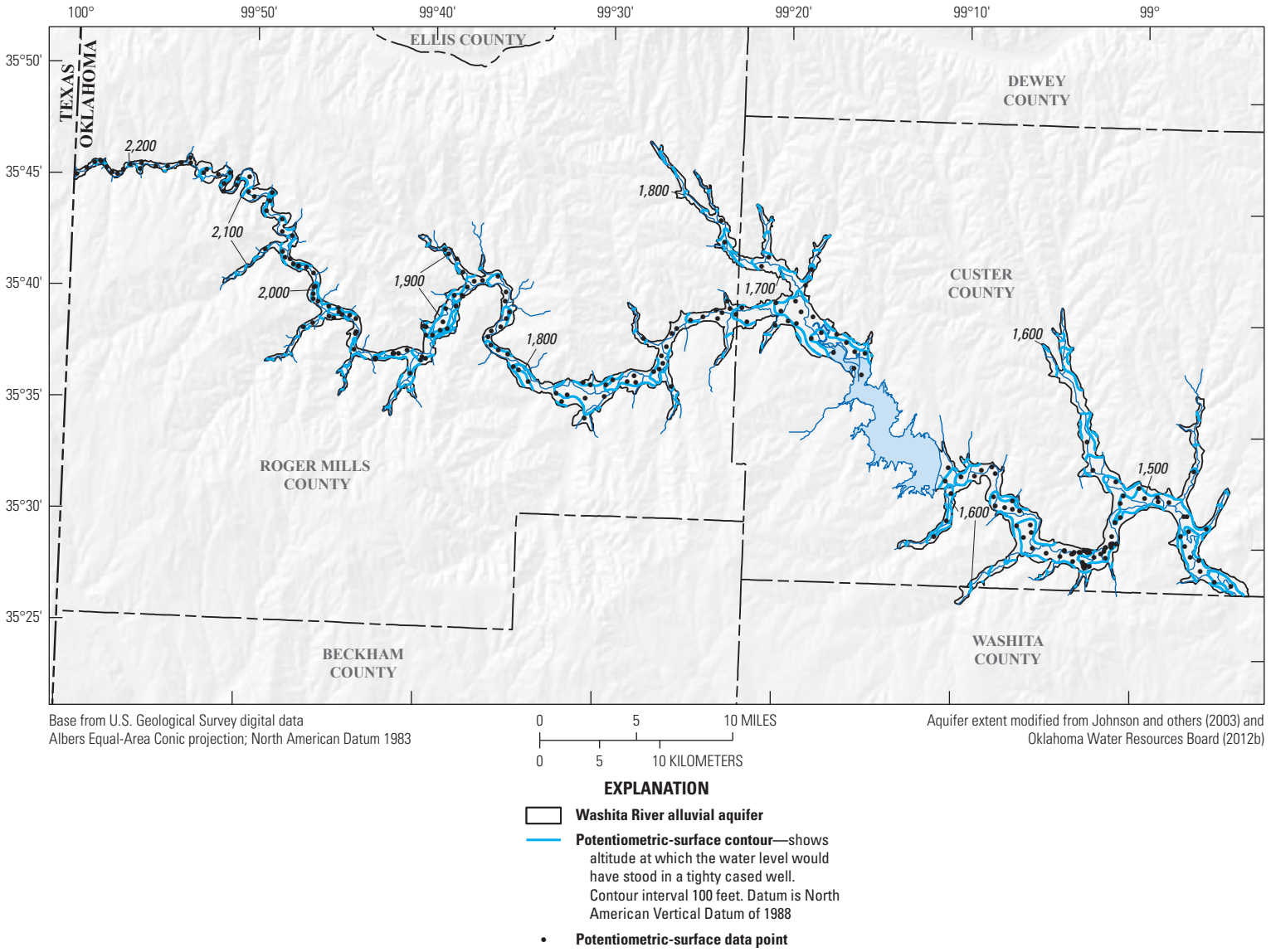

Figure 12. Potentiometric-surface contours for March 2017 based on groundwater-level altitudes measured in wells and first water reported from drillers' logs completed in the Washita River alluvial aquifer, western Oklahoma.

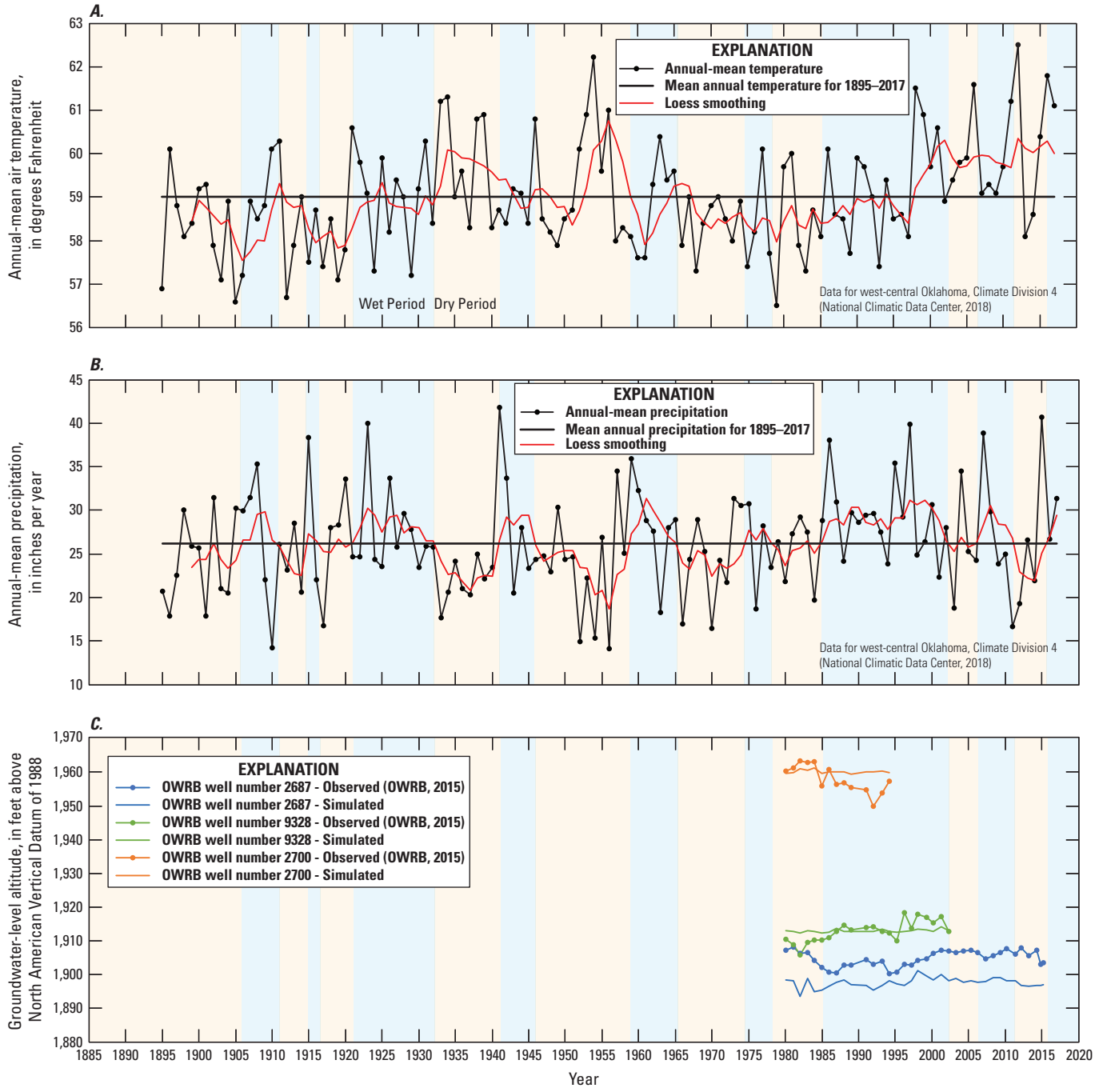

Figure 13. *A*, Annual-mean air temperature, *B*, annual-mean precipitation, and *C*, groundwater-level altitude measured in or near Oklahoma Water Resources Board (OWRB) observation wells 2687, 9328, and 2700 completed in the Washita River alluvial aquifer, western Oklahoma.

aquifer behaved as a leaky confined system during a pumping and recovery test. The transmissivity was calculated to be 30,000 gallons per day per foot (40,104 ft^2/d), or a hydraulic conductivity of 105.5 ft/d over 38 ft of saturated thickness.

For various locations where subsurface information was available, the mean hydraulic conductivity for the total aquifer thickness was estimated from lithological borehole logs (OWRB, 2015). Mean horizontal hydraulic conductivity was then interpolated across the aquifer to provide an initial distribution of horizontal hydraulic conductivity by using the inverse-distance-weighted interpolation method (Esri, Inc., 2015), where values nearest the interpolated location have the greatest influence on the interpolated value at that location. The mean horizontal hydraulic conductivity was estimated by assigning a published horizontal hydraulic conductivity value to intervals listed in borehole logs and calculating the

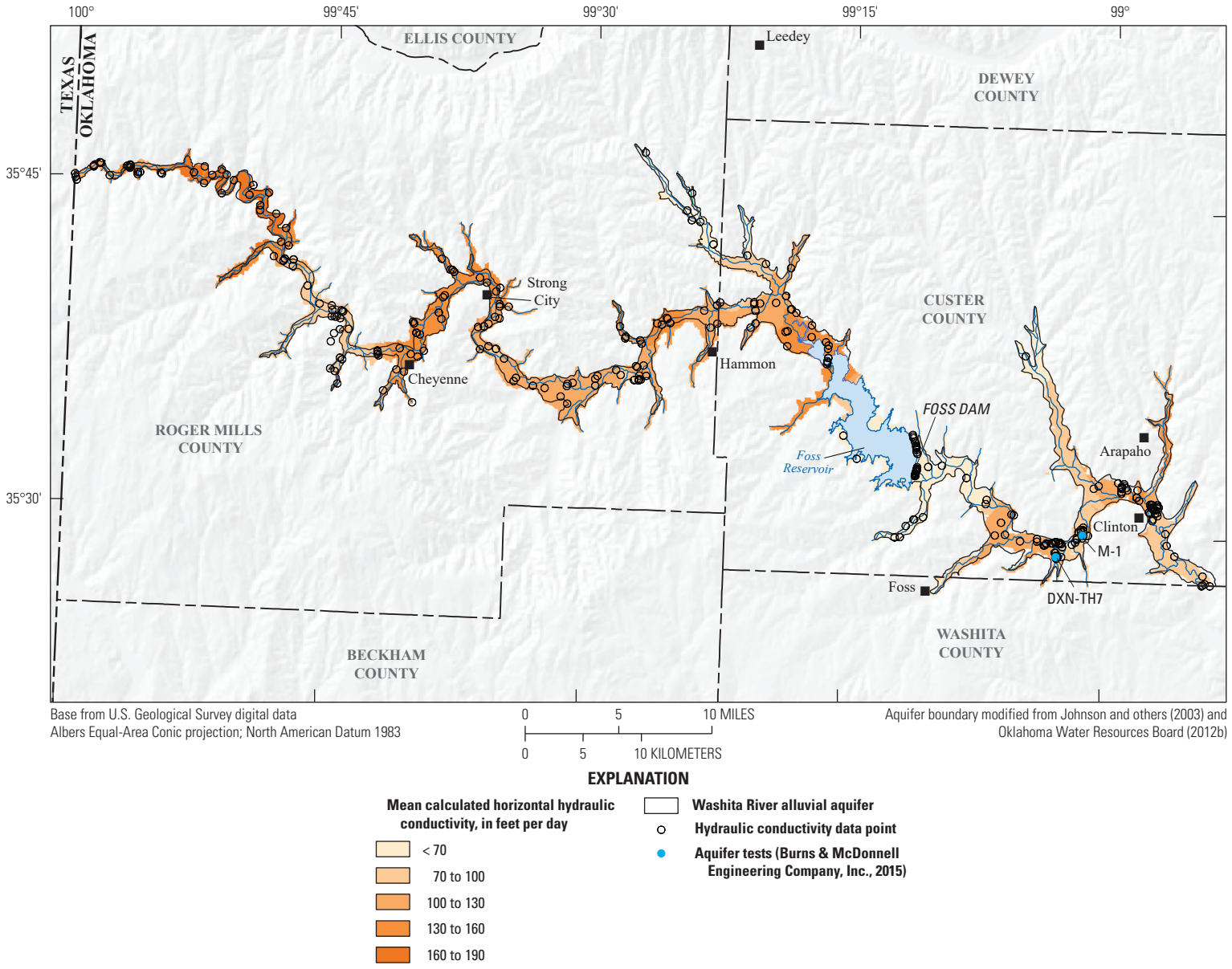

Figure 14. Locations of mean horizontal hydraulic conductivity based on lithologic descriptions reported in borehole logs (OWRB, 2015) and from aquifer tests (Burns & McDonnell Engineering Company, Inc., 2015), Washita River alluvial aquifer, western Oklahoma.

mean, weighted by the thickness of each interval. To estimate horizontal hydraulic conductivity values for intervals described in logs, the standard texture class that best matched the log texture was assigned to the intervals. The horizontal hydraulic conductivity for the texture classification published by the U.S. Environmental Protection Agency (1986) was then assigned to that interval, and the mean horizontal hydraulic conductivity was determined by weighting each interval by the interval thickness (fig. 14). The horizontal hydraulic conductivity derived by using lithologic borehole logs is typically less than that derived from aquifer tests by approximately 5–10 percent. No information was available on specific yield from published aquifer tests in the Washita River alluvial aquifer, so that parameter was estimated as described in the "Calibration Parameters" and "Using the Water-Table-Fluctuation Method to Estimate Recharge" sections of this report.

Conceptual Flow Model

A conceptual flow model is a simplified description of the aquifer system that includes the hydrologic boundaries, the major inflow and outflow sources of the groundwater-flow system, and a conceptual water budget with the estimated mean flows between those hydrologic boundaries. The conceptual flow model and hydrogeologic framework were used to conceptualize, design, and build the numerical groundwater-flow model. The conceptual water budget (table 5) includes estimated mean annual inflows to and outflows from the Washita River alluvial aquifer for the period 1980–2015 and includes a sub-accounting of mean annual inflows and outflows for the parts of the aquifer that were upgradient and downgradient from Foss Reservoir. The starting date of 1980 was chosen because water-use data were sparse prior to 1980.

Water Use

During the period 1980–2015, groundwater use was estimated for 156 irrigation, mining, and public supply active and temporary permits (OWRB, 2018) (fig. 15). Of the 156 permits, 121 were upgradient from Foss Reservoir, and 35 were downgradient from Foss Reservoir. Mean annual groundwater use for the study period totaled 5,502 acre-ft/yr, or about 14 percent of aquifer outflows (table 5). Mean annual groundwater use for the study period included 4,923 acre-ft/yr and 579 acre-ft/yr upgradient and downgradient from Foss Reservoir, respectively (table 5). Total groundwater use includes 5,319 acre-ft/yr for irrigation (97 percent), 179 acre-ft/yr for public supply (3.3 percent), and 4 acre-ft/yr for all other use types (greater than 1 percent) (OWRB, 2018).

Reported surface-water use in the Washita River alluvial aquifer consists of 69 permitted diversions along the Washita River and associated tributaries (fig. 2). The mean annual withdrawal rate for all surface-water permitted diversions during the study period was 1,523 acre-ft/yr (OWRB, 2018), including 919 acre-ft/yr and 604 acre-ft/yr of permitted use upgradient and downgradient from Foss Reservoir, respectively. During the study period, 27 permitted diversions had mean annual withdrawal rates between 2 and 298 acre-ft/yr. This total withdrawal includes all active and temporary permits in the boundaries of the Washita River alluvial aquifer for the study period.

Recharge

For this report, groundwater recharge is defined as the amount of water that originates as precipitation and infiltrates from the land surface through the unsaturated zone and to the top of the water table. Other processes that may be included in a broader definition of recharge are stream seepage, lateral

Table 5. Conceptual water budget for the Washita River alluvial aquifer, western Oklahoma, 1980–2015.

[All units in acre-feet per year unless otherwise specified; %, percent; --, not quantified]

Water-budget category	Upgradient from Foss Reservoir	Downgradient from Foss Reservoir	Total	Percentage of water budget
Inflow				
Recharge	15,370	6,799	22,169	56%
Lateral flow[1]	2,308	14,849	17,157	44%
Lakebed seepage[1]	--	--	--	--
Total inflow	17,678	21,648	39,326	
Outflow				
Stream seepage[1]	4,676	17,320	21,996	56%
Saturated-zone evapotranspiration	8,079	3,749	11,828	30%
Groundwater use	4,923	579	5,502	14%
Net change in groundwater storage	--	--	--	--
Total outflow	17,678	21,648	39,326	

[1]Lakebed seepage, stream seepage, and lateral flow represent net terms.

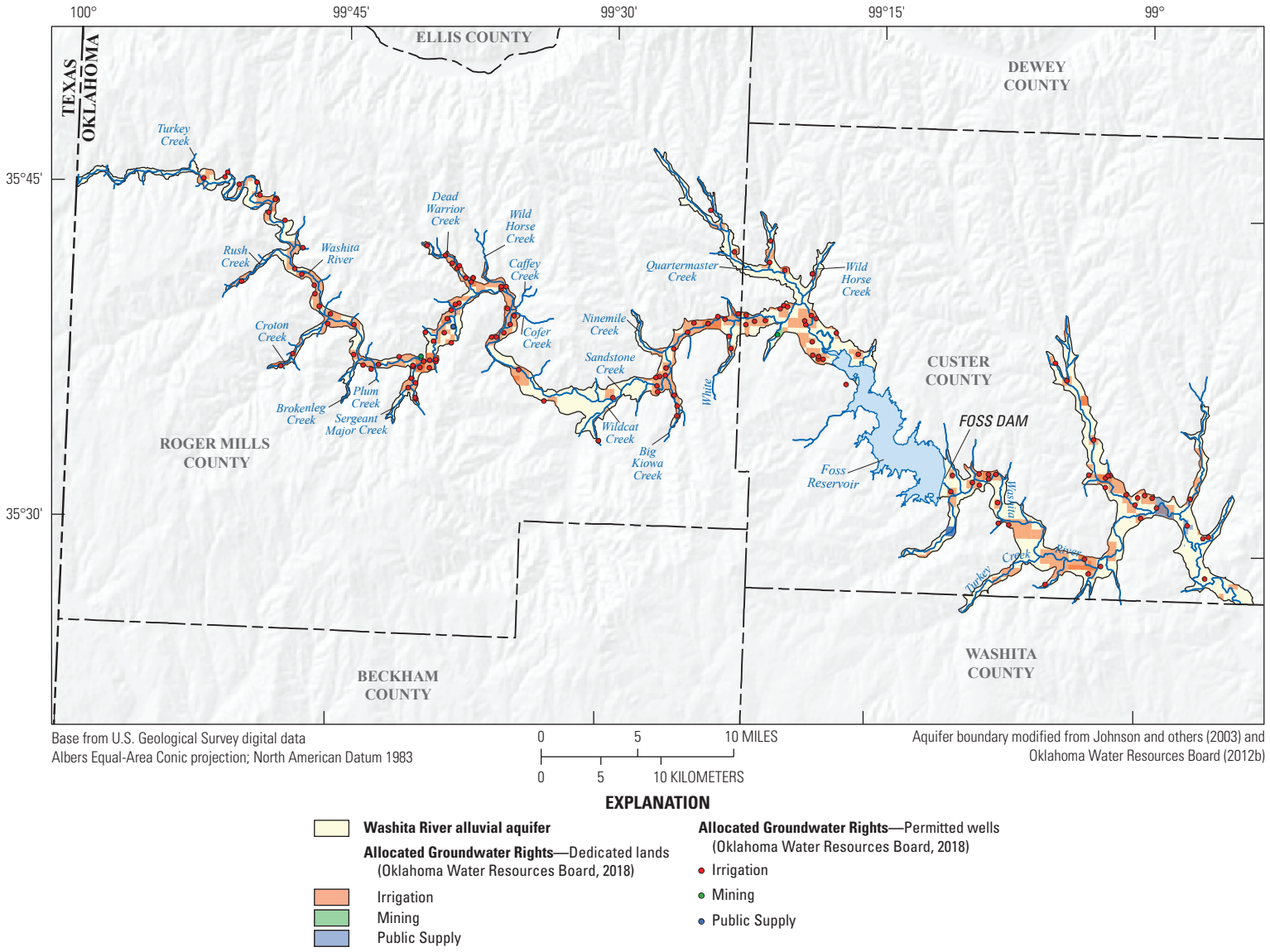

Figure 15. Locations of permitted groundwater wells and usage categories in the Washita River alluvial aquifer, western Oklahoma, 1980–2015.

groundwater flow from adjacent hydrogeologic units, or lakebed seepage, which are accounted for separately in the Washita River alluvial aquifer conceptual water budget.

Recharge rates are controlled by several factors, including precipitation rates, evapotranspiration (ET) rates, unsaturated-zone permeability and moisture capacity, and slope of the land surface (Keese and others, 2005). Although recharge rates are difficult to measure because of high spatial and temporal variability, methods using a mass-balance approach, streamflow-hydrograph techniques, environmental tracers, physical measurements, and computer code have been used to estimate recharge rates. Estimates of recharge for the study area were obtained by using the Soil-Water-Balance (SWB) code (Westenbroek and others, 2010) and a water-table-fluctuation method (Healy and Cook, 2002).

Using the Soil-Water-Balance Code to Estimate Recharge

Spatially distributed recharge resulting from precipitation and infiltration to the Washita River alluvial aquifer was computed for each month of the study period by using the SWB code (Westenbroek and others, 2010). The SWB code is based on a modified Thornthwaite-Mather method (Thornthwaite and Mather, 1957) and uses grids of landscape and climate data to provide estimates of spatially distributed deep percolation through the soil profile, which is referred to as recharge for the purposes of this report. The SWB code uses a mass-balance approach to compute gridded recharge as the difference between sources and sinks for each grid cell, while accounting for the cumulative effects of the change in soil moisture. All values in the mass-balance equation (modified from Westenbroek and others, 2010) are reported in inches:

$$R = (P + S + R_i) - (Int + R_o + P_{et}) - \Delta Sm \qquad (2)$$

where

R is recharge,
P is precipitation,
S is snowmelt,
R_i is surface runoff inflow,
Int is plant interception,
R_o is surface runoff outflow,
P_{et} is potential evapotranspiration, and
ΔSm is the change in soil moisture.

Daily climate data for 21 climate stations (table 6), including precipitation and minimum and maximum air temperature, were obtained (National Climatic Data Center, 2018; Oklahoma Mesonet, 2018) and interpolated to a grid by using a 350-ft uniform spacing. Soil properties (soil-water storage capacity and hydrologic soil group) and land cover were derived from the Digital General Soil Map database (Natural Resources Conservation Service [NRCS], 2018), which is an inventory of generalized soil characteristics at a scale between 1:12,000 and 1:63,360. Some precipitation was accounted for as snowmelt, based on the daily minimum and maximum air temperatures. Surface runoff inflow—whereby runoff is routed between cells moving downhill—was calculated by using a flow-direction grid derived from a digital elevation model (DEM) (USGS, 2018a) and a runoff curve number. For the flow-direction grid, this study used a light detection and ranging (lidar) dataset (USGS, 2016) upscaled to the model grid. To ensure correct routing of surface runoff and to eliminate areas of internal drainage that can result in unrealistic amounts of recharge, depressions in the DEM were filled. Plant interception occurs when precipitation is captured by vegetation prior to reaching the top of the soil profile and was specified for each land-cover type during the growing season. Surface runoff outflow was calculated by using NRCS curve numbers related to the relation between rainfall and runoff (Westenbroek and others, 2010). Potential evapotranspiration in the SWB code was calculated by using methods from Hargreaves and Samani (1985), discussed further in the "Saturated-Zone Evapotranspiration" section of this report.

Root-zone depths represent the maximum depth to which various types of vegetation will grow and are classified based on land-cover and soil type. Greater plant root-zone depths result in the increased uptake of water by roots in the soil-moisture zone, thus decreasing recharge, whereas less root-zone depth results in less soil water uptake and more water going to recharge. Winter wheat, the dominant crop type overlying the Washita River alluvial aquifer (National Agricultural Statistics Service, 2019; fig. 3), has mean and maximum rooting depths of about 1.0 and 4.6 ft, respectively, in Oklahoma (Patrignani and others, 2012; David Marburger, Oklahoma State University, written commun., 2018). To account for this root-zone depth range, 50 percent of the default values of Westenbroek and others (2010) for each land-cover type were selected, which resulted in root-zone depths for crops between 1.0 and 1.7 ft.

An important assumption of the SWB code is that standing water does not persist from day to day and is not available to provide recharge to groundwater. Another assumption of the SWB code is that if the water on the surface is not snow, then it evaporates or runs off after 1 day. The root zone is presumed to be above the water table so that the only source of water for the soil profile is water percolating from the land surface. In parts of the Washita River alluvial aquifer, particularly near lakes and streams, plant roots reach the water table, and the SWB code overestimates recharge for wet periods during the growing season because it calculates actual plant uptake according to available soil water and does not include plant uptake directly from groundwater. Thus, there is an additional loss through ET that is not accounted for, comparable to the difference between the actual and potential ET calculated by the SWB code. This topic is discussed further in the "Simulation of Groundwater Flow" section of this report.

The SWB code estimated the mean annual recharge for the study period as about 2.5 in. or about 11 percent of the mean annual precipitation of 23 in. (fig. 16). The SWB code inputs and outputs are available in Ellis and others (2020).

Table 6. Selected climate stations used for assessing the soil-water balance in and near the Washita River alluvial aquifer, western Oklahoma.

[SWB, Soil-Water-Balance; dates are in month/day/year format]

Station identifier	Station name	Latitude, in decimal degrees	Longitude, in decimal degrees	Station period of record (may contain gaps) or single measurement date	
				Begin	End
Oklahoma Mesonet climate stations (Oklahoma Mesonet, 2018) used for running the SWB code					
ARNE	Arnett	36.07204	−99.90308	2/1/2009	12/31/2017
BESS	Bessie	35.40185	−99.05847	1/1/1994	12/31/2017
BUTL	Butler	35.59150	−99.27059	1/1/1994	12/31/2017
CHEY	Cheyenne	35.54615	−99.72790	2/1/2009	12/31/2017
PUTN	Putnam	35.89904	−98.96038	1/1/1994	12/31/2017
WEAT	Weatherford	35.50830	−98.77509	1/1/1994	12/31/2017
National Oceanic and Atmospheric Administration climate stations (National Climatic Data Center, 2018) used for running the SWB code					
USC00410157	ALLISON	35.61030	−100.10220	8/1/2001	12/31/2017
USC00340684	BESSIE 4 WNW MESONET, OK US	35.40167	−99.05833	2/1/2009	12/31/2017
USC00411408	CANADIAN 22 SE	35.64670	−100.06570	3/1/2003	2/1/2015
USC00341738	CHEYENNE	35.60000	−99.68330	7/1/1980	12/31/1994
US1OKRM0002	CHEYENNE 18.1 SW	35.86130	−99.78200	2/3/2007	12/31/2017
USC00341909	CLINTON	35.50139	−98.97722	7/31/1936	8/15/2005
USW00003932	CLINTON SHERMAN AIRPORT	35.61030	−100.10220	8/16/1958	12/31/2017
USC00342849	ELK CITY 4 W	35.39250	−99.50639	5/1/1904	12/31/2017
USC00345090	LEEDEY	35.86290	−99.34280	8/1/1941	12/31/2017
USC00345648	MAYFIELD	35.33920	−99.87690	10/4/2010	2/29/2012
USC00347343	PUTNAM 3 N MESONET, OK US	35.89889	−98.96028	2/1/2009	12/31/2017
USC00347579	REYDON	35.62560	−99.91060	1/1/1980	8/18/2005
USC00347952	SAYRE	35.30620	−99.62750	5/31/1936	12/31/2017
USC00348652	SWEETWATER	35.42190	−99.90530	9/17/1982	4/30/2008
USC00349422	WEATHERFORD	35.02580	−99.10580	12/31/1904	12/31/2017

The SWB code estimated the minimum and maximum mean annual recharge values for the study period as about 0.38 in/yr (2014) and 6.8 in/yr (2015), respectively. Monthly mean recharge tended to be greatest from March to June and in October (fig. 17*B*). Recharge in these months corresponds to between 8 and 16 percent of the monthly mean precipitation for those months (fig. 17*A*). July and February were the months with the least amounts of recharge. Recharge amounts in July and February correspond to between 4 and 15 percent of monthly mean precipitation for those months.

Even though more precipitation falls on the eastern part of the aquifer, landscape characteristics affect recharge enough that mean annual recharge for the study period was greatest in the western part of the aquifer—generally defined as the area west of Cheyenne—where the Washita River alluvial aquifer incises the Ogallala Formation (fig. 18). The hydrologic soils group assigned to the Washita River alluvial aquifer alluvium incising the Ogallala Formation (fig. 7) had a high infiltration capacity, and a low overland flow capacity. The available water (holding) capacity for the alluvium west of Rush Creek was also smaller than in other areas, indicating a sandier soil texture (as opposed to clay), and consequently a greater potential for infiltration. Additionally, runoff from the Ogallala Formation to the incised Washita River alluvial aquifer alluvium increased recharge. Using the Soil-Water-Balance code, runoff from one cell in the model is assumed to infiltrate into nearby cells. Hence, recharge may be shifted from the Ogallala Formation to the thin area of Washita River alluvial aquifer alluvium, rather than simulating overland flow to surface-water storage (Stanton and others, 2012). Additionally, fewer temporal climate data (precipitation and minimum and maximum air temperature) were available for the western part of the Washita River alluvial aquifer—generally defined as the part of the aquifer between the Texas–Oklahoma

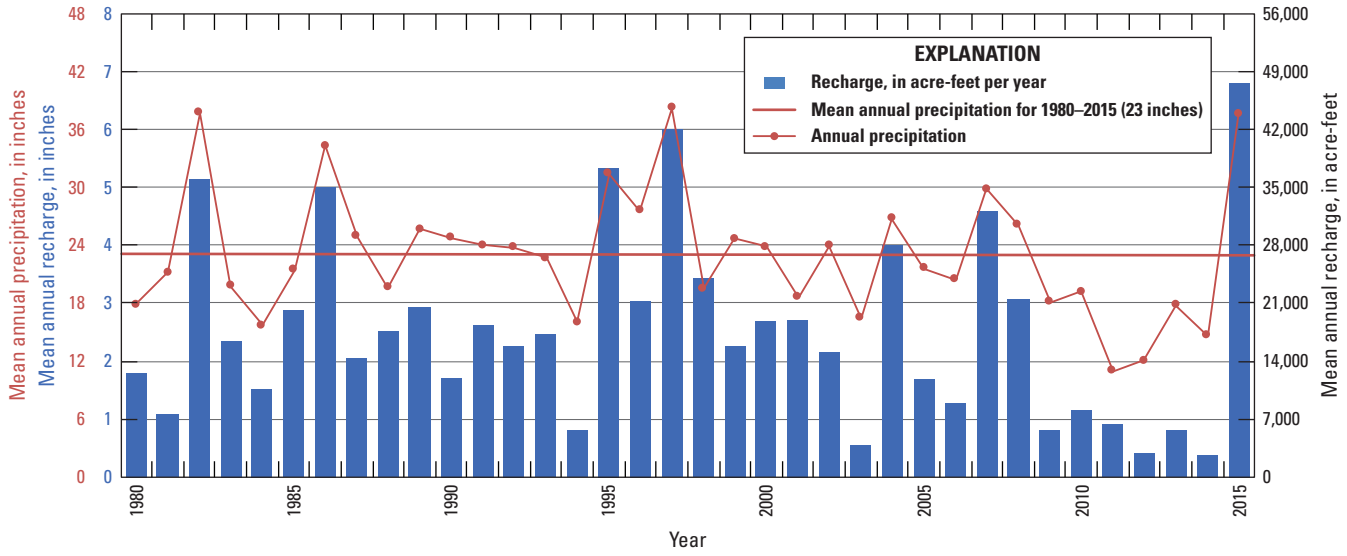

Figure 16. Mean annual precipitation and recharge computed by using the Soil-Water-Balance code (Westenbroek and others, 2010) for the Washita River alluvial aquifer, western Oklahoma, 1980–2015.

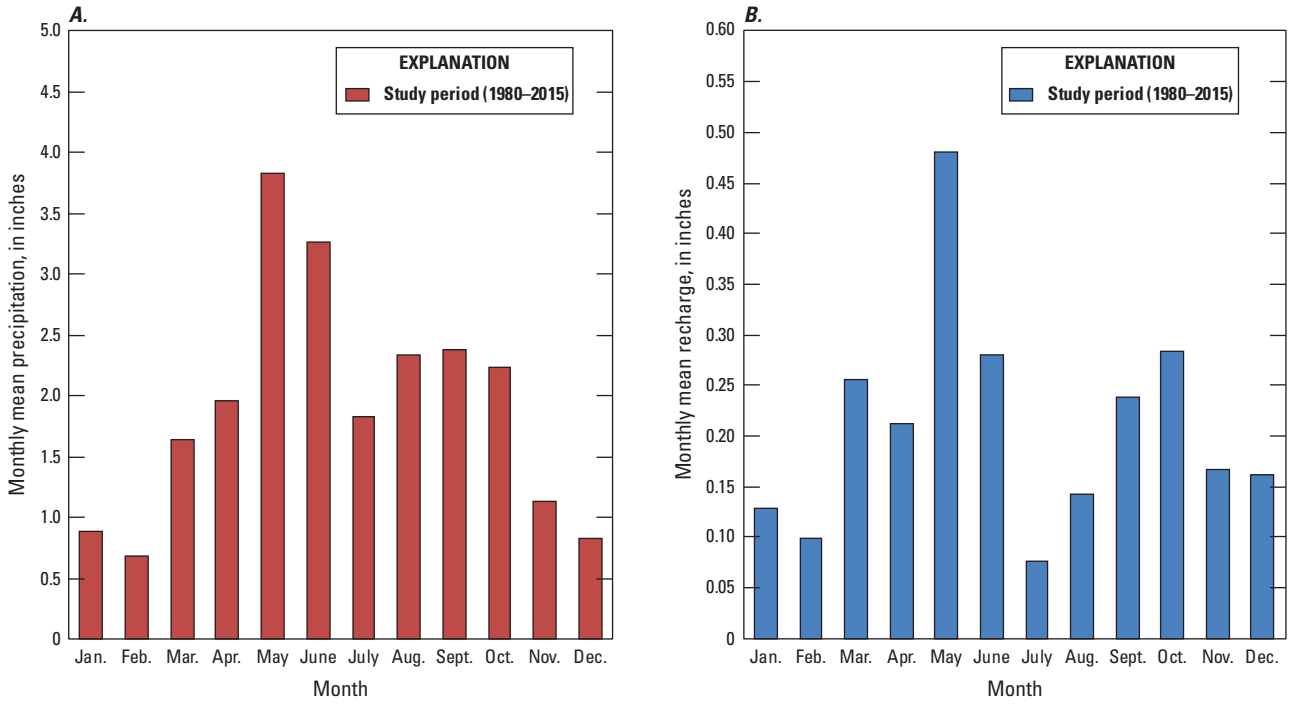

Figure 17. Monthly mean *A*, precipitation and *B*, recharge computed by using the Soil-Water-Balance code (Westenbroek and others, 2010) for the Washita River alluvial aquifer, western Oklahoma, 1980–2015.

border and the Cheyenne streamgage—than for the part of the aquifer downgradient from Foss Reservoir. SWB code calculations indicated greater recharge in the terrace deposits than in the alluvium deposits because of a sandier soil type in the terrace deposits that had a lower available water capacity (Westenbroek and others, 2010; fig. 18).

Mean annual recharge rates estimated by the SWB code were compared to published estimates of mean annual recharge. Kent and others (1984) estimated a recharge of 3.72 in/yr, or about 12 percent of a mean precipitation of 32.2 in/yr, across the Washita River alluvial aquifer that covers the extent of Oklahoma and includes other reaches not discussed in this report. Schipper (1983) estimated a recharge

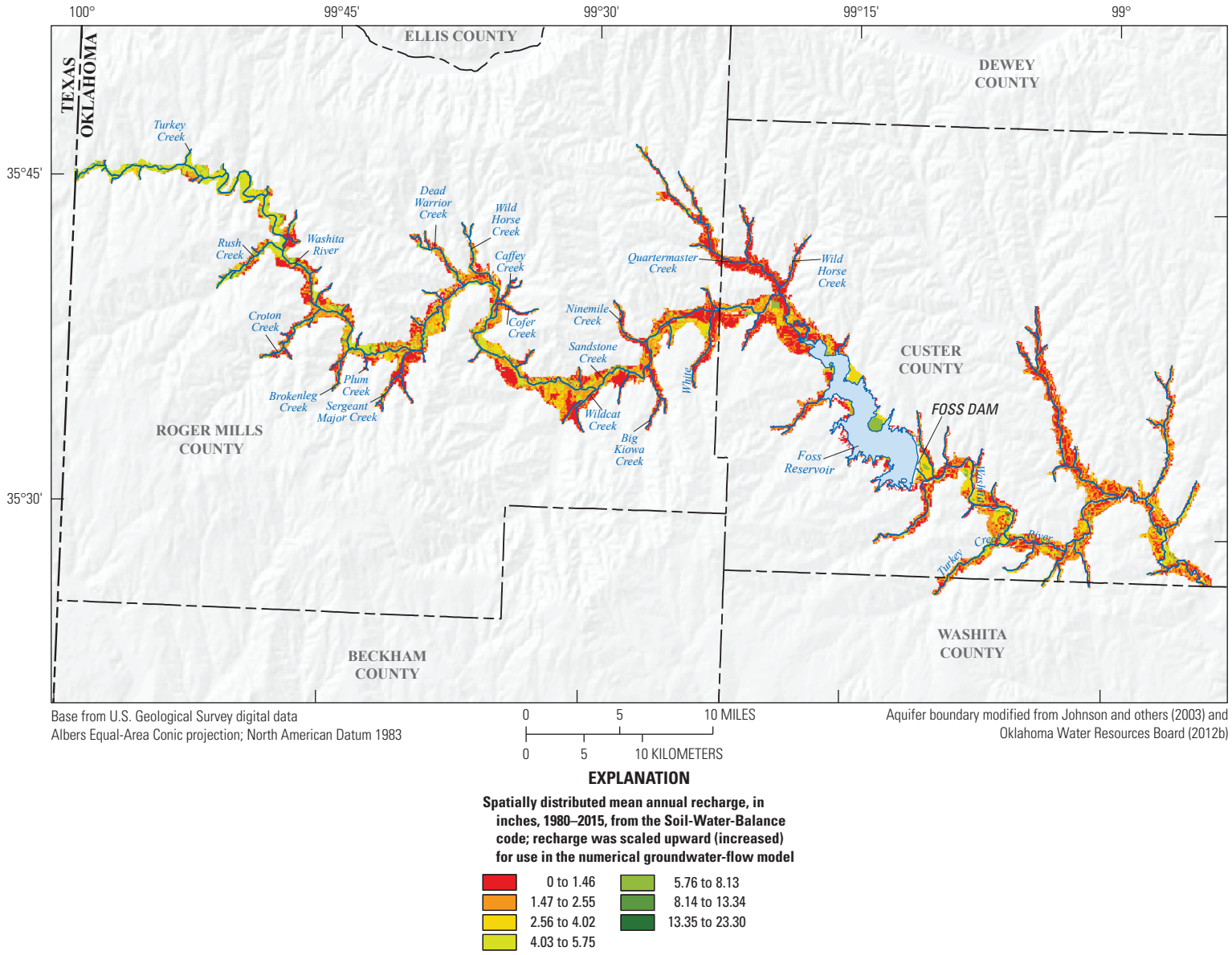

Figure 18. Mean annual groundwater recharge computed by using the Soil-Water-Balance code (Westenbroek and others, 2010) for the Washita River alluvial aquifer, western Oklahoma, 1980–2015.

of 3.17 in/yr, or 13 percent of precipitation, through calibration of a groundwater model. The Schipper (1983) model simulated the Washita River from the Texas–Oklahoma border to the southern boundary of Custer County, which is approximately the same downgradient extent as the study area in this report. The mean annual recharge rate estimated by using the SWB code for the Washita River alluvial aquifer for this study (2.5 in/yr) is lower than these published estimates of recharge for the Washita River alluvial aquifer. The reason recharge is lower than published estimates may be attributable to recharge from crop irrigation that was included in the published estimates but not included in the mean annual recharge rate estimated by using the SWB code. Recharge from crop irrigation (commonly referred to as irrigation return flows) likely infiltrates through the unsaturated zone down to the water table. Schipper (1983) estimated recharge from crop irrigation at 15 to 25 percent of pumping based on a water-budget analysis and ET estimates. Other studies have found that irrigation increases groundwater recharge (Roark and Healy, 1998; McMahon and others, 2011), and recharge rates are greater in irrigated cropland areas compared to natural rangeland or non-irrigated cropland (Scanlon and others, 2005). Annual recharge in irrigated cropland in Nebraska was 0.13–0.30 in/yr greater than annual recharge in non-irrigated cropland and was 1.3–1.6 in/yr greater than in rangeland (Dugan and Zelt, 2000; McMahon and others, 2007; Stanton and others, 2010). To account for possible recharge from crop irrigation and to more closely match published recharge estimates for the Washita River alluvial aquifer, recharge for this aquifer for this study was estimated as 3.15 in/yr, or about 14 percent of precipitation, which is a 25-percent increase from the initial estimates from the SWB code. Estimates of recharge as a percentage of precipitation can vary for different periods analyzed. When applied across the 132-square-mile (mi^2) aquifer area used for modeling purposes (84,366 acres) (modified from Neel and others, 2018), the mean annual recharge of 3.15 in/yr corresponds to a mean annual recharge volume of about 22,169 acre-ft/yr, or about 56 percent of aquifer inflows in the conceptual water budget (table 5). Following Neel and others (2018), the aquifer area for modeling purposes was 132 square miles rather than the 110 square-mile land surface area of the Washita River alluvial aquifer. The aquifer area for modeling purposes was larger than the land-surface area of the alluvial aquifer in order to establish the boundary conditions representing locations in the model where water flows into or out of the model region.

Using the Water-Table-Fluctuation Method to Estimate Recharge

The water-table-fluctuation (WTF) method (Healy and Cook, 2002) was used to estimate recharge to the Washita River alluvial aquifer (fig. 19). The SWB code method estimates spatial recharge via gridded cells across an area, and the WTF method estimates recharge at a specific location over a period of time. The WTF method was used as an additional method to estimate recharge for this study. The WTF method is based on the premise that short-term (hours to 2–3 days) rises in continuously recorded groundwater levels in unconfined aquifers are caused by recharge arriving at the saturated zone following a period of precipitation. The method is best applied to aquifers with shallow water tables that display rapid groundwater-level rises and declines in response to precipitation. The method cannot distinguish between recharge from precipitation and recharge from other sources such as irrigation return flow or streambed seepage. Using the WTF method, recharge (R) was calculated as the sum of individual groundwater-level rises in response to precipitation:

$$R = Sy \times \Delta h/\Delta t \quad (3)$$

where

Sy is the specific yield (dimensionless),
Δh is the change in groundwater-level altitude, in feet, and
Δt is the change in time, in hours.

Groundwater recharge was estimated at two observation wells upgradient from Foss Reservoir: WSH01 and WSH02 (fig. 1). Continuous readings were collected from two additional observation wells, WSH04 and WSH05, but groundwater-level readings at these observation wells did not react to precipitation, indicating that the water table at those locations is not directly connected to landscape hydrological processes. Well screens in WSH04 and WSH05 could be located below a local confining unit with recharge occurring in an upper sand unit, or the water table could be deep enough that plant roots do not intersect the water table and recharge from rainfall events is so attenuated that groundwater-level changes for discrete events cannot be detected.

The WTF method for recharge uses groundwater-level change related to a precipitation event in shallow, unconfined aquifers, multiplied by the specific yield of the aquifer to calculate the amount of water from that precipitation event that became groundwater recharge (eq. 2). If the groundwater level was increasing or decreasing before the precipitation event, that pattern is extrapolated below the groundwater-level peak to remove the effects of these increases or decreases in groundwater levels. Optimally, each well site would also be instrumented to collect precipitation deposition so that rainfall events could be correlated to recharge peaks and the percentage of precipitation that becomes recharge could be estimated. None of the well sites in this study area were equipped with precipitation gages, and none of the climate stations in the area (fig. 1) were close enough to well sites for use in estimating precipitation related to recharge peaks.

The WTF method is approximate and relies on infiltration of precipitation reaching the water table within days of the rainfall event so that it forms a hydrograph peak. The WTF method also requires the groundwater level to not be affected by other processes such as pumping wells, surface runoff, or

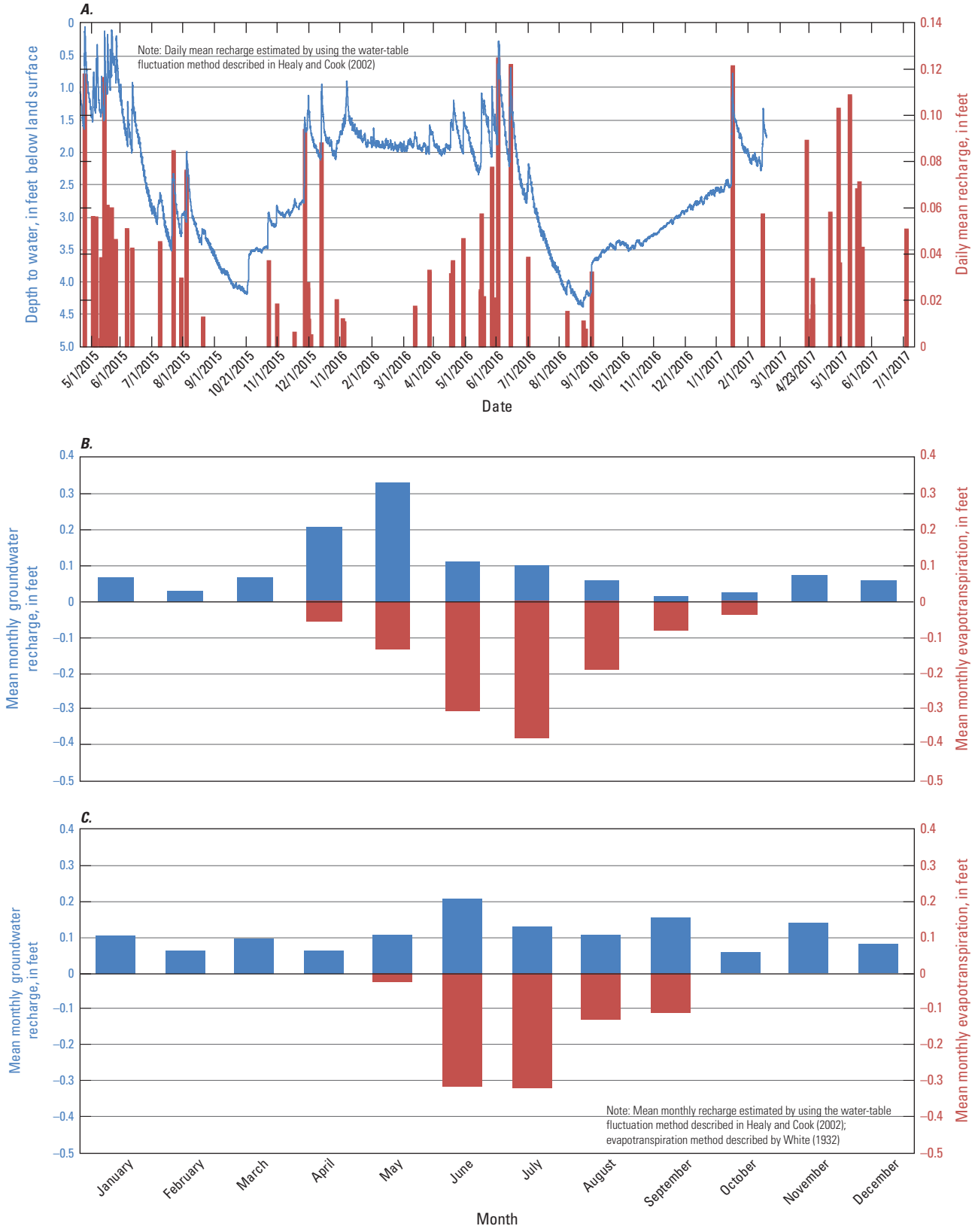

Figure 19. *A*, Daily mean groundwater recharge and depth to water at USGS observation well WSH01 (U.S. Geological Survey, 2018b) from April 23, 2015, to March 1, 2017; *B*, mean monthly changes in groundwater recharge and evapotranspiration at observation well WSH01 during 2015–17; and *C*, mean monthly groundwater recharge and evapotranspiration at observation well WSH02 during 2015–17, Washita River alluvial aquifer, western Oklahoma.

infiltration from surface water. The groundwater level then decreases only as groundwater is redistributed or removed from the aquifer by other processes. Thus, the aquifer must be unconfined, the water table must be close enough to the land surface so that the capillary fringe intersects the root zone, and the topsoil and aquifer material must be permeable enough so that the infiltration flow rate is greater than the rate at which the groundwater dissipates or flows to groundwater sinks. The WTF method is used to estimate the groundwater-level change, and this change is multiplied by the estimated specific yield, which increases the error. For example, observation well WSH01 (USGS site number 354529099565501) is an existing well registered with the OWRB (OWRB well 90854). The groundwater-levels were measured continuously at 30-minute intervals with a pressure transducer. The well is located approximately 480 ft south of the Washita River and approximately 3 mi east of the Texas–Oklahoma border (fig. 1). The period of groundwater-level records for well WSH01 is just over 2 years, from April 23, 2015, to March 1, 2017 (fig. 19*A*). The altitude of the land surface at well WSH01 is 2,197 ft. Local land use at the well WSH01 site in 2006 was classified as shrubland and grassland/herbaceous (Fry and others, 2011), and the well site is located on the valley bottom with little slope and silty, sandy soil. During the period of data collection, the water table was between 0.1 and 4.4 ft below land surface (fig. 19*A*).

Numerous recharge peaks were identified in April and May 2015, and large, but more isolated, recharge peaks occurred during June to August. No recharge took place in September 2015, but one recharge peak was identified in October followed by several large peaks in November and December.

The specific yield of the aquifer at WSH01 was not measured but was estimated based on the general soil characteristics from soil survey geospatial data (NRCS, 2018). The soil on the western half of the Washita River alluvial aquifer is mapped as being silty and has an available water capacity of 0.86 in. of water per foot of soil. Converting this to a percentage results in a specific yield of 0.071. Assuming a 10-percent error results in a range of specific yield of 0.065–0.079. The NRCS soils data are only relevant to approximately the uppermost 5 ft of the soil profile, not the entire aquifer thickness. Given the mixture of alluvium and eroded bedrock from adjacent units at the surface, it is not unsurprising that the surficial specific yield of the aquifer at WSH01 was lower than the specific yield of 0.12 that was determined in the "Calibration Parameters" section of this report to best represent the alluvium of the majority of the aquifer. A groundwater-level time series graph for WSH01 (fig. 19*A*) shows a decrease of approximately 3 ft from June to September 2015, most likely from plant uptake and little precipitation. All 61 precipitation events during the period of data collection were used to calculate recharge, and many of these events lasted more than 1 day.

Mean monthly recharge was estimated for WSH01 and WSH02 by using the WTF method. For WSH01, recharge was estimated to be greatest during April and May and lowest during September and October (fig. 19*B*). For WSH02, recharge was estimated to be greatest during June and September and lowest during February and October (fig. 19*C*). ET in the shallow alluvium likely takes up the potential precipitation that would become recharge; therefore, when ET is high, recharge is likely to be low, unless the precipitation exceeds the plant uptake capacity. Once precipitation exceeds the plant uptake capacity, the precipitation is available for recharging the groundwater. Mean monthly ET, described in the "Saturated-Zone Evapotranspiration" section of this report, is shown on figures 19*B* and 19*C* to illustrate the relation between ET uptake of precipitation and groundwater recharge in the Washita River alluvial aquifer.

Saturated-Zone Evapotranspiration

Evapotranspiration is the process by which water is transferred to the atmosphere directly by evaporation or indirectly by plant transpiration. This process occurs in the saturated and soil-moisture (unsaturated) zones, typically in areas where the water table is at or near land surface, such as lakes or wetlands. The soil-moisture-zone component of evapotranspiration was not considered to be a part of the conceptual water budget because it occurs before infiltrating precipitation has become groundwater recharge. For this investigation, evapotranspiration by plants from the saturated zone—or saturated-zone evapotranspiration (ETg)—was quantified in the water budget.

Rates of ETg are difficult to estimate over a large area, but should be roughly proportional to (1) the area where the saturated zone intersects the plant root zone, (2) the mean depth to groundwater in that area during the growing season, and (3) the mean rate of transpiration associated with the assemblage of plants in that area. The area where the saturated zone intersects the plant root zone probably is small (compared to the Washita River alluvial aquifer area) and confined to the 73,584-acre area of active alluvium (Qal, fig. 7) along perennial or near-perennial streams. About 16 percent (11,828 acres) of the active alluvium area was classified as wetland (land area with frequently saturated or flooded soils) by the National Wetlands Inventory (U.S. Fish and Wildlife Service, 2018). ETg also was assumed to be proportional to and no greater than the P_{et} minus the A_{et} computed by using the Hargreaves and Samani (1985) method as described by Westenbroek and others (2010). This assumption resulted in the summed components of ETg not exceeding the P_{et}. ETg was assumed to be active for about half the year (182.5 days), greatest annually in wet and hot years, and greatest monthly in early summer (Scholl and others, 2005) when precipitation and temperature are above average.

By using the assumptions previously listed, groundwater outflow by ETg could be estimated from daily groundwater-level fluctuation data at wells with shallow depths to water according to methods of White (1932). This method estimated annual ETg rates by using specific yield from soil columns

and hourly groundwater-level measurements from a continuous well. This method was applied for undisturbed salt grass cover in southwest Utah with a mean depth to water of 12–24 in. Because ETg rates in the high desert of Utah are likely to be greater than those in Oklahoma, an annual ETg rate of about 12 in/yr was assumed to be appropriate for the Washita River alluvial aquifer, similar to the rate for the North Fork Red River alluvial aquifer (Smith and others, 2017). If about 16 percent (11,828 acres) of the active alluvium area (73,584 acres) had similar cover and depths to water—based on the National Wetlands Inventory—this rate would correspond to an annual ETg outflow of 11,828 acre-ft/yr for the Washita River alluvial aquifer (table 5).

Streamflow

Daily streamflow data from the Cheyenne, Hammon, Foss, and Clinton streamgages (fig. 1; table 2) were used to estimate base flow and seepage calibration targets for the groundwater model. The Washita River alluvial aquifer is also hydraulically connected to the surface water in several smaller tributaries, such as Barnitz and Quartermaster Creeks, for which streamgaging data were not available during the study period.

From the Texas–Oklahoma border to Foss Reservoir, there are no permanent flow controls on the Washita River. However, 69 surface-water diversions were permitted by the OWRB for irrigation upstream from Foss Reservoir (fig. 2). Streamflow downstream from Foss Dam (fig. 1) is controlled by releases from Foss Reservoir. Mean streamflow released from Foss Reservoir was approximately 41.1 ft^3/s during the study period (Bureau of Reclamation, 2018), with greater releases during wet periods and a prolonged period with no releases during dry periods such as the hydrologic drought from 2011 to 2015 except for October 2013. Additionally, 31 surface-water diversions are permitted by the OWRB downgradient from Foss Reservoir on tributaries of the Washita River.

Mean monthly streamflow measured at the Cheyenne and Hammon streamgages (fig. 1) is highly variable, and the mean daily streamflow was nearly two and a half times greater at the Hammon streamgage (67.1 ft^3/s) than at the Cheyenne streamgage (25.4 ft^3/s) for 1980–2015 (table 2). Mean daily streamflow values at the Cheyenne and Hammon streamgages were greater during a wet period from 1995 to 2002 (about 36 ft^3/s and 128 ft^3/s, respectively) and very low during the hydrologic drought from 2011 to 2014 (about 3 and 4 ft^3/s respectively) (fig. 5; table 2). The greatest instantaneous streamflow recorded at the Cheyenne streamgage was 7,050 ft^3/s on May 23, 1941 (USGS, 2018b).

Mean annual streamflow measured at the Foss streamgage included minor flow from Oak Creek (fig. 1), and the mean annual streamflow for the study period was 74.4 ft^3/s, which is similar to that measured at the Hammon streamgage. Streamflow measured at the Clinton streamgage included the tributary of Turkey Creek and substantial streamflow from Barnitz Creek that was not continuously measured during the period of study. Mean annual streamflow measured at the Clinton streamgage for the 1980–2015 period was approximately 146.5 ft^3/s (table 2). The Washita River streamflow was not continuously measured in the study area downstream from the Clinton streamgage.

Seepage Runs

Synoptic streamflow measurements (also known as seepage-run measurements) (USGS, 2018b) were collected by using the methods of Rantz and others (1982) during a period of minimal runoff on February 29 and March 1, 2016, and February 9, 2017. A positive difference between the inflow and outflow is considered seepage into the stream from an underlying aquifer or aquifer system and is indicative of a gaining stream. A negative difference between the inflow and outflow is considered seepage into the underlying aquifer from the stream and is indicative of a losing stream. Both efforts measured streamflow at various locations along the Washita River and several tributaries during times preceded by periods of no recent precipitation. During February and March, riparian vegetation ET is also assumed to be minimal. During the 2016 seepage-run measurements, diversions for irrigation were visually observed between the Cheyenne streamgage and White Shield Creek (fig. 1), which potentially affects the interpretation of streamflow gains and losses between these two measured sites. Thus, a second seepage run was conducted on February 9, 2017, focusing on the Washita River upstream from Foss Reservoir. Streamflow measurements were augmented with streamflow data from each USGS streamgage on the Washita River in the study area.

Generally, streamflow in the Washita River increased from upstream to downstream in the areas upgradient and downgradient from Foss Reservoir (figs. 20 and 21). Downstream increases in base flow could be caused by increased inflows to the stream from the alluvium and terrace and from adjoining bedrock aquifers. Average base flow from 22 named and 24 unnamed tributaries (20 unnamed tributaries downstream from site SR1) to the Washita River was estimated based on available data from nearby streamgages and by using estimated streamflows from StreamStats (Smith and Esralew, 2010).

StreamStats was used during the seepage run on February 9, 2017, on the Washita River at the Texas–Oklahoma border to obtain an estimated streamflow of 7.4 ft^3/s. Streamflow at site SR1, approximately 4 river miles east and downstream from the Texas–Oklahoma border, was recorded as 11.9 ft^3/s (figs. 20 and 21). Streamflow at site SR3, approximately 6 mi downstream from site SR1, was 17.6 ft^3/s; however, 3.0 ft^3/s of the streamflow at SR3 is from the Rush Creek tributary. Additionally, Turkey Creek in Roger Mills county and nine unnamed tributaries may contribute streamflow to the Washita River. Streamflow between site SR3 and the Cheyenne streamgage increased from 17.6 to 27.8 ft^3/s.

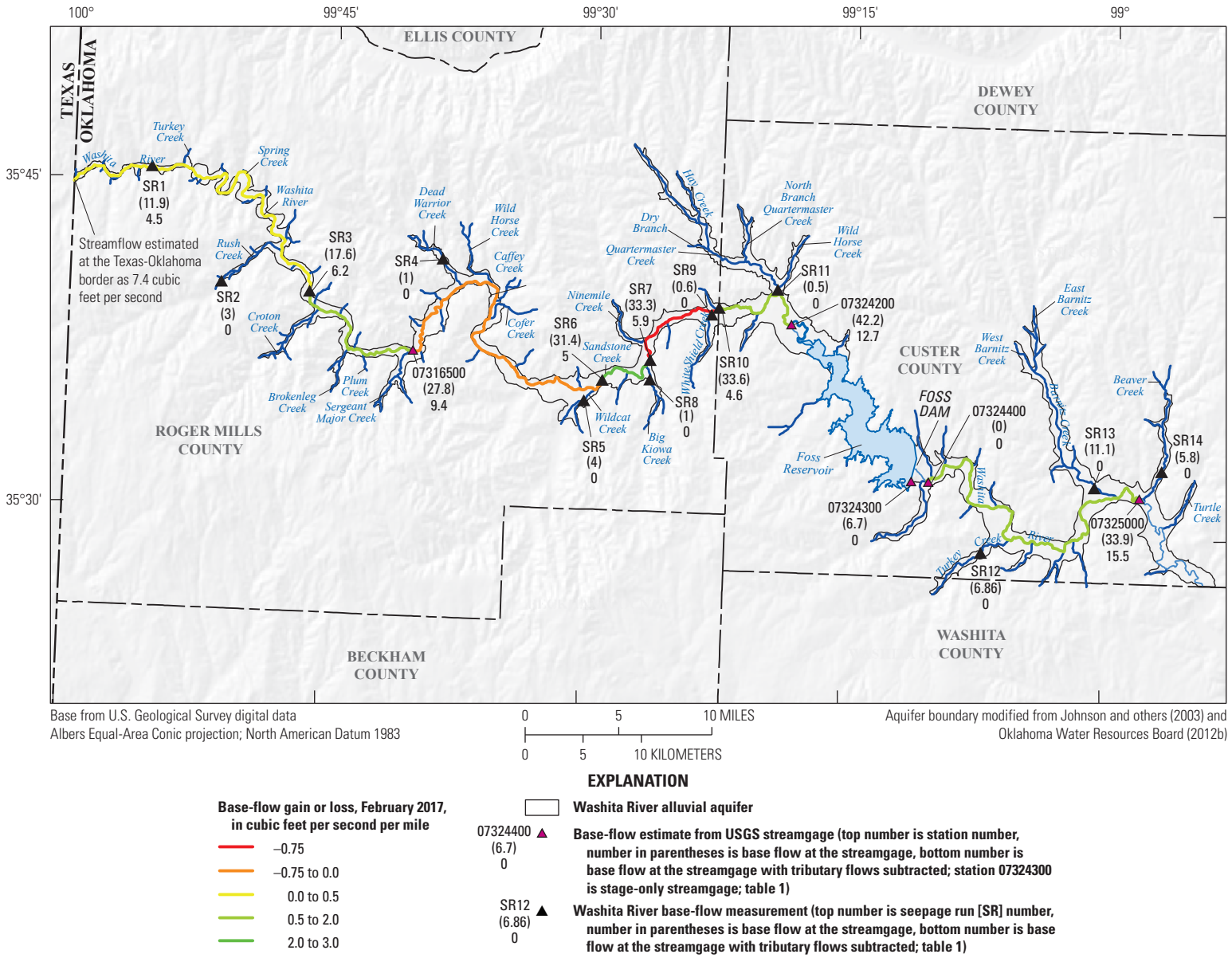

Figure 20. Streamflow measurements and gaining and losing reaches from calculated base-flow gain or loss from the 2017 seepage runs for the Washita River alluvial aquifer, western Oklahoma.

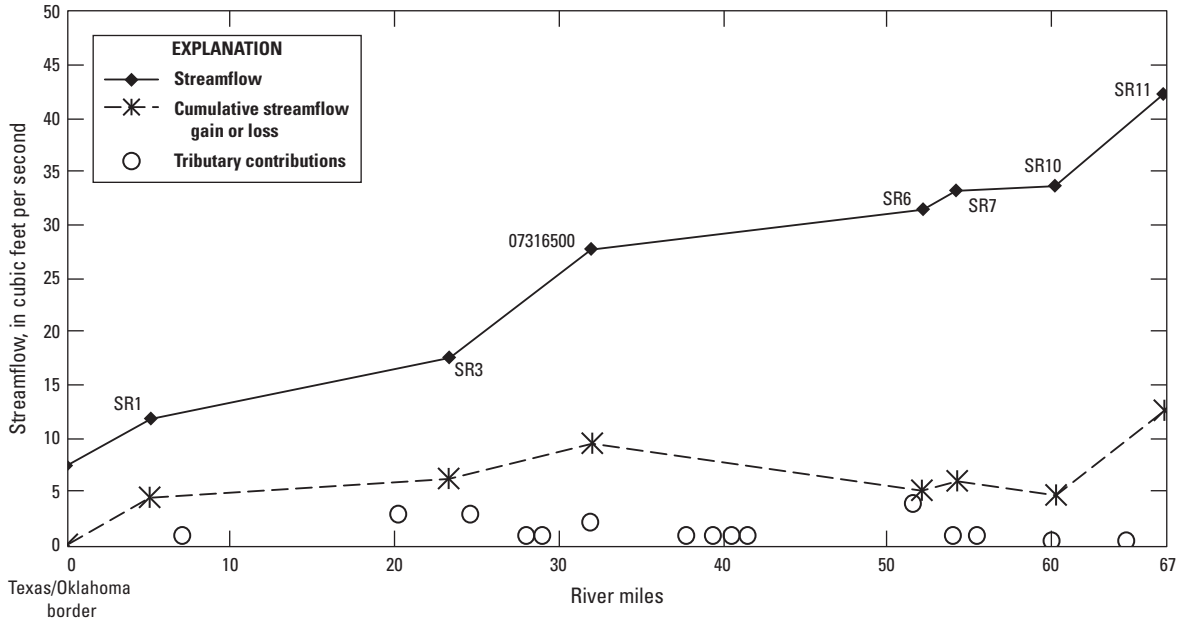

Figure 21. Total and cumulative streamflow gain or loss (measured February 9, 2017) for the Washita River and includes tributary contributions to the Washita River. [See table 1 and fig. 20; SR, seepage run]

Some of this increase is probably from streamflow from four named tributaries (Croton, Brokenleg, Plum, and Sergeant Major Creeks) and three unnamed tributaries located between SR3 and the Cheyenne streamgage. Streamflow increased from 27.8 to 31.4 ft^3/s between the Cheyenne streamgage and site SR6. This streamflow includes streamflow measured at the Dead Warrior Creek (1.0 ft^3/s) and Sandstone Creek (4.0 ft^3/s) tributaries. Additionally, three named tributaries (Wild Horse, Caffey, and Cofer Creeks) and seven unnamed tributaries may contribute streamflow to the Washita River. After accounting for measured or estimated streamflow from these tributaries, cumulative streamflow decreased between the Cheyenne streamgage and SR6. Streamflow increased from 31.4 to 33.3 ft^3/s between sites SR6 and SR7. This increase includes streamflow measured at Big Kiowa Creek (0.1 ft^3/s). Additionally, one unnamed tributary may contribute streamflow to the Washita River in this area. Streamflow increased from 33.3 to 33.6 ft^3/s between sites SR7 and SR10. This increase includes streamflow measured at White Shield Creek (0.6 ft^3/s). Additionally, Ninemile Creek and two unnamed tributaries, located between SR7 and SR10, may contribute streamflow to the Washita River. After accounting for measured or estimated streamflow from the White Shield and Ninemile Creeks and the two unnamed tributaries, estimated base flow was decreased between SR7 and SR10. Streamflow increased from 33.6 to 42.2 ft^3/s between sites SR10 and the Hammon streamgage. This increase includes streamflow measured at Quartermaster Creek (5.9 ft^3/s). Additionally, one unnamed tributary may contribute streamflow to the Washita River between SR10 and the Hammon streamgage.

During the 2016 seepage run, Foss Reservoir was not releasing streamflow into the Washita River, and the streamgage downstream from the Foss Dam streamgage (07324300) recorded streamflow of 6.7 ft^3/s (fig. 20). This streamflow amount represents the cumulative streamflow along Oak Creek and the short Washita River segment between Foss Dam and the streamgage, a channel length of approximately 1 mi. Between the Foss and Clinton streamgages, streamflow in the Washita River increased 27.2 ft^3/s, from 6.7 to 33.9 ft^3/s. After subtracting the measured 6.86 ft^3/s from Turkey Creek and 11.1 ft^3/s from Barnitz Creek (fig. 20), the total base flow was approximately 15.5 ft^3/s along 29.4 river miles (between 07324300 and 07325000 streamgages), or approximately 0.5 ft^3/s per mi. Base-flow amounts per mile for Turkey, Beaver, and Turtle Creeks were estimated, although the channel lengths contributing to the base flows are approximate. Turkey Creek streamflow was measured about 2 mi upstream from the confluence with the Washita River, which is 1.2 ft^3/s per mi over approximately 6 mi of channel. A streamflow of 5.8 ft^3/s was measured in Beaver Creek about 3 mi upstream from the confluence with the Washita River.

Base Flow

Base flow is the component of streamflow supplied by the discharge of groundwater to streams (Barlow and Leake, 2012) that was quantified over the study period 1980–2015 for the study-area streamgages (tables 1 and 2) by using a base-flow index (BFI) computer code to identify the base-flow component of streamflow (Wahl and Wahl, 1995). The BFI code is integrated into the USGS Groundwater Toolbox (Barlow and

others, 2015). The BFI code is used to calculate the minimum streamflow for user-specified *n*-day moving increments in order to compare this streamflow to adjacent minimums to determine turning points on a base-flow hydrograph. The ratio of base flow to the total streamflow is the base-flow index. A base-flow index of 1 indicates that all streamflow is from groundwater, and a base-flow index of 0 indicates that none of the streamflow is from groundwater.

Several releases from Foss Reservoir to the Washita River were recorded during the study period. Base-flow computation at regulated streamgages can be complicated by releases from large reservoirs and floodwater-retarding structures because these releases (and the subsequent bank storage releases associated with these releases) are usually indistinguishable from natural base flows. Thus, the BFI code may overestimate base flows at regulated streamgages on the Washita River (fig. 1), and long-term patterns in base flows may be masked by reservoir releases that are indistinguishable from base flows.

Annual stream seepage during 1980–2015 from the Washita River alluvial aquifer into the reach of the Washita River upstream from Foss Reservoir was estimated as 4,676 acre-ft/yr (table 5). This stream seepage estimate was based on (1) the difference between base flow at the river's confluence with Foss Reservoir and base flow at the Texas–Oklahoma border, (2) estimated base flow in tributaries to the Washita River, and (3) surface-water diversions. Flow in the Washita River at the confluence of Foss Reservoir (29,943 acre-ft/yr) was used to determine the flow at the Hammon streamgage by adjusting upward by 8 percent for the 3.9-mi distance downstream to Foss Reservoir. Flow at the Texas–Oklahoma border (5,334 acre-ft/yr) was determined as 50 percent of flow at the Cheyenne streamgage based on seepage-run data discussed in the "Seepage Runs" section of this report. Tributary stream seepage upgradient from Foss Reservoir was estimated for 16 named tributaries (fig. 1) for a total of 16,072 acre-ft/yr and 12 unnamed tributaries for a total of 4,344 acre-ft/yr based on seepage-run data (fig. 20). Surface-water diversions totaled 919 acre-ft/yr and are discussed in the "Water Use" section of the report.

For the Washita River downstream from Foss Reservoir, the mean annual stream seepage was 17,320 acre-ft/yr (table 5). This mean annual stream seepage was based on (1) the difference between the base flow at the Custer County border and the base flow at the Foss streamgage, (2) releases from Foss Reservoir, (3) estimated base flow in tributaries to the Washita River, and (4) surface-water diversions. The flow at the Custer County border (66,658 acre-ft/yr) was used to determine the flow at the Clinton streamgage, adjusting upward by 10 percent for the distance downstream to the Custer County boundary. Mean annual stream seepage at the Foss streamgage (34,015 acre-ft/yr) was determined as the sum of the base flow at this streamgage and releases from Foss Reservoir. Tributary stream seepage downgradient from Foss Reservoir was estimated for six named tributaries (fig. 1) for a total of 13,031 acre-ft/yr and eight unnamed tributaries for a total of 2,896 acre-ft/yr based on seepage-run data (fig. 20). Surface-water diversions totaled 604 acre-ft/yr and are discussed in the "Water Use" section of the report.

Lateral Groundwater Flows

Estimates of lateral groundwater flow from the Ogallala Formation to the Washita River alluvial aquifer are not available in published literature; however, based on the configuration of the potentiometric-surface contours from this investigation (fig. 12) and available groundwater-level measurements (USGS, 2018b), some lateral groundwater flow from the Ogallala Formation to the Washita River alluvial aquifer may occur. For this study, lateral flow was not estimated in this area (lateral flow equals zero) because (1) additional groundwater-level observations in the Ogallala Formation are needed, (2) the Ogallala Formation is likely drained by a few tributaries to the Washita River upstream from Wild Horse Creek (figs. 1 and 7) that are estimated as a part of streamflow in the conceptual flow model, and (3) lateral flow between the Washita River alluvial aquifer and the Ogallala Formation may be impeded by the presence of the intervening Cloud Chief Formation and Doxey Shale, which predominantly contain shale and siltstone (fig. 7).

West of the Rush Springs aquifer extent (Ellis, 2018) and east of the Ogallala Formation, the surrounding Cloud Chief Formation and Doxey Shale bedrock units are predominantly composed of shale and siltstone (figs. 7 and 8) (Schipper, 1983). Concentrations of calcium, magnesium, and sulfate in the groundwater in the Cloud Chief Formation come from the dissolution of gypsum, dolomite, and calcite (Becker and Runkle, 1998). The calcium-magnesium-sulfate-chloride-type water in the Washita River alluvial aquifer (Kent and others, 1984) west of the Rush Springs aquifer is most likely caused by the inflow of groundwater from the Cloud Chief Formation, which is adjacent to the Washita River alluvial aquifer. However, because of the fine-grained texture of the Cloud Chief Formation and Doxey Shale, the bedrock in these units were regarded as impermeable, as done in other investigations (Leonard and others, 1958; Schipper, 1983; Kent and others, 1984).

The Washita River alluvial aquifer may drain groundwater in the Rush Springs aquifer (Rush Springs Formation, fig. 7), as indicated by potentiometric-surface contours for the Rush Springs aquifer that are parallel to the Washita River alluvial aquifer, or perpendicular to the direction of lateral groundwater flow, in figure 15 of Neel and others (2018). Additionally, groundwater-flow simulations of the Rush Springs aquifer resulted in a mean annual seepage of about 151,000 acre-ft/yr from the Rush Springs aquifer to the Washita River in the Rush Springs aquifer model domain—accounting for just 46 percent of total simulated seepage to all streams (Ellis, 2018, fig. 38). Much of this seepage occurs downstream from Foss Reservoir between the Clinton streamgage and the Washita River at Carnegie, Okla.,

streamgage (07325500) (located east of the study area; not shown on map); however, the remaining seepage between Foss Reservoir and the Clinton streamgage indicates that lateral flow in this area may be a substantial source of inflow to the Washita River alluvial aquifer. The seepage-run data from 2017 indicates an increase in streamflow of approximately 8.9 ft^3/s between site SR7 and the Hammon streamgage—an area that approximately corresponds with the areal extent of the Rush Springs aquifer where it underlies (or lies adjacent to) the Washita River alluvial aquifer upgradient from Foss Reservoir. However, most of this increase in streamflow is estimated to originate from the four named (Ninemile, White Shield, Quartermaster, and Wild Horse) and two unnamed creeks between SR7 and the Hammon streamgage. Thus, only minimal lateral flow likely occurs from the Rush Springs aquifer to the Washita River alluvial aquifer upstream from Foss Reservoir.

Lakebed Seepage

Streamflow from the Washita River is the primary source of surface-water inflow to Foss Reservoir (fig. 1). The active conservation pool (normal pool) storage of Foss Reservoir is 168,732 acre-ft (Bureau of Reclamation, 2018), and the reservoir has mean annual permitted surface-water withdrawals of about 18,000 acre-ft/yr (OWRB, 2012b). The active conservation pool stage is the maximum altitude of a reservoir's conservation pool (the usable stored water above the dead-pool stage). The dead-pool stage is the altitude of the water surface below which the water stored in a reservoir will not drain by gravity through the outlet of the dam; water in the dead pool is not part of the active conservation pool (Water Data for Texas, 2020).

Flow to and from Foss Reservoir and the Washita River alluvial aquifer (termed "lakebed seepage") varies seasonally with changes in precipitation and water use. Stage in Foss Reservoir is generally highest in the early summer after spring rainfall and lowest in the fall after the cumulative effects of increased evaporation and permitted surface-water withdrawals during summer months (Bureau of Reclamation, 2018). Thus, lakebed seepage may occur as an inflow to or an outflow from the Washita River alluvial aquifer during various times of the year, but it is likely a small amount in terms of an aquifer budget and was not quantified for this study.

Conceptual Water Budget

A conceptual water budget for the Washita River alluvial aquifer (table 5) was developed to quantify the amount of water that moves between each boundary of the aquifer and to guide the construction and calibration of the numerical groundwater-flow model. This water budget provides a generalized estimate of mean annual inflows and outflows for the Washita River alluvial aquifer during the study period 1980–2015. Water that flows to the Washita River alluvial aquifer from the study area streams is considered an aquifer inflow, whereas the reverse constitutes an outflow from the aquifer.

Approximately 56 percent of inflows to the Washita River alluvial aquifer occurred as recharge during the study period, and net lateral flow was estimated to be 44 percent of the aquifer inflow (table 5). Net lakebed seepage at Foss Reservoir is likely a relatively small component of the water budget (less than 1 percent); thus, this term was not quantified in table 5. The largest aquifer outflow (56 percent) was net stream seepage. The remaining aquifer outflows were ETg (30 percent) and groundwater use (14 percent).

Simulation of Groundwater Flow

A groundwater model of the Washita River alluvial aquifer was constructed by using MODFLOW-2005 (Harbaugh, 2005) with the Newton solver (MODFLOW-NWT; Niswonger and others, 2011). MODFLOW-NWT uses finite-difference methods to solve the three-dimensional groundwater-flow equation and includes more advanced capabilities to solve nonlinear simulations compared to MODFLOW-2005. In the modular design of MODFLOW, each hydrologic boundary, such as stream seepage, recharge, or groundwater use, is included as a package that, when activated, adds new inflow and outflow terms to the groundwater-flow equation being solved. Model space is discretized into orthogonal cells, and the cell size is the finest resolution at which spatially varying properties may be represented and varied. Model time is discretized into time steps within stress periods. The stress period length is the finest resolution at which temporally varying inflows and outflows may be represented and varied, and the time step length is the finest length of time for which model outputs may be written. The groundwater-model inputs and outputs are available in Ellis and others (2020).

Spatial and Temporal Discretization

The Washita River alluvial aquifer groundwater-model grid was spatially discretized into 384 rows and 927 columns containing 350-ft cells without rotation. Two layers and 30,000 active cells were used to represent geologic units in the study area, and the model area, shown in figure 22, was defined by the hydrologic boundaries discussed in the "Hydrologic Boundaries" section of this report. The top layer (layer 1) represented the undifferentiated alluvium and terrace deposits of Quaternary age with variable thickness determined from the hydrogeologic framework, and the bottom layer (layer 2) represented the bedrock of Permian age which was given a uniform nominal thickness of 100 ft. Areas of the terrace deposits outside of the Washita River alluvial aquifer extent shown on figure 7 were determined to be unsaturated based on an analysis of available well logs and were not included in the model extent. All model layers were assigned

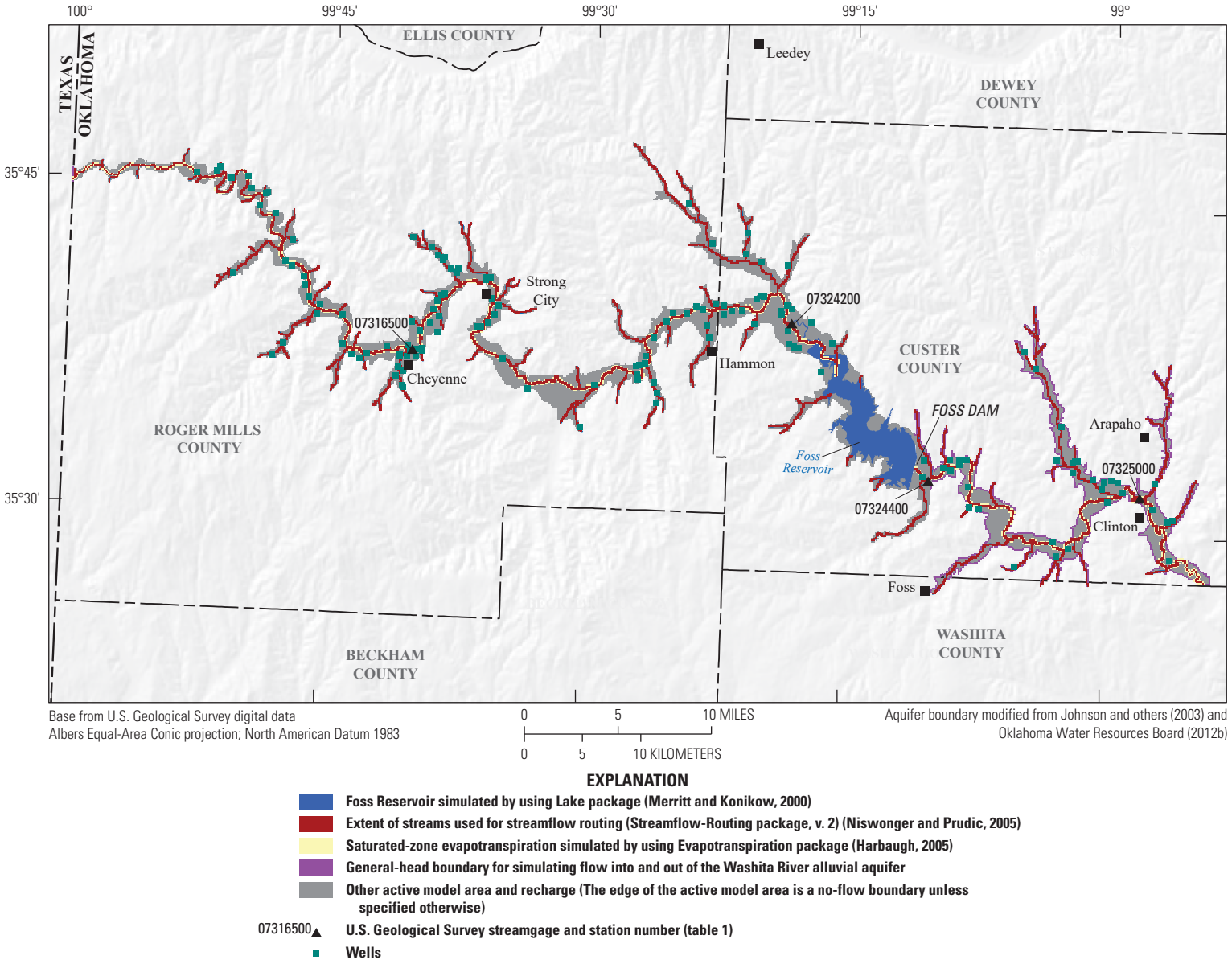

Figure 22. Active model area and boundary conditions for the numerical groundwater-flow model of the Washita River alluvial aquifer, western Oklahoma.

as a convertible-type layer, whereby each layer can convert between confined and unconfined conditions. The model grid was oriented approximately parallel to the hydraulic gradient of the aquifer, and the model active area was expanded in some areas to ensure that each active cell was in connection with at least one other active cell. Conceptually, the aquifer could be divided into two models, one each for the areas upgradient and downgradient from Foss Reservoir; however, the groundwater model described in this report included both areas in a single model.

The groundwater-simulation period was temporally discretized into 433 monthly transient stress periods with one time step each, representing the period of January 1980 to December 2015. The monthly transient stress periods were used to capture seasonally variable processes such as recharge, ETg, and groundwater use. A lack of sufficient water data prior to the mid-1970s precluded the establishment of predevelopment groundwater levels and flow conditions; therefore, an initial 365-day steady-state stress period was configured to represent mean annual inflows and outflows from the Washita River alluvial aquifer for the study period.

Hydrologic Boundaries

Hydrologic boundaries in the groundwater model represent the locations where the inflow or outflow of water may occur (fig. 22) and include specified-flux and head-dependent boundaries. For a specified-flux boundary, a user-specified flow rate governs groundwater exchange at that boundary. Simulated specified-flux boundaries include groundwater use and recharge, as well as the no-flow boundary established at the bottom of layer 2. A no-flow boundary was also established at some locations in each layer where adjoining hydrogeologic units do not yield water to the Washita River alluvial aquifer, mostly in areas west of the Rush Springs aquifer boundary (fig. 13 in Ellis, 2018) (fig. 22). A head-dependent boundary simulates flow based on the difference between a user-specified groundwater level and the groundwater level in model cells. Simulated head-dependent boundaries include ETg, lateral groundwater flow, seeps and springs, stream seepage, and lakebed seepage at Foss Reservoir.

Recharge

Areally distributed recharge from the SWB code was simulated as a specified-flux boundary by using the Recharge package for MODFLOW groundwater-flow models (Harbaugh, 2005). The steady-state simulation used a mean recharge value calculated for the simulation period, and the transient simulation used recharge values calculated for each month of the simulation period. Temporal adjustment of recharge occurred during the calibration phase to obtain better matches between simulated and observed calibration targets for 172 monthly stress periods where recharge occurred. Recharge was applied to the highest active cell, or layer 1 in the model. Where the Washita River alluvial aquifer is missing and bedrock is exposed, no recharge was assumed to occur.

Lateral Groundwater Flow

Possible lateral groundwater flows between the Washita River alluvial aquifer and the Rush Springs aquifer were simulated as head-dependent boundaries by using the General-Head Boundary (GHB) package for MODFLOW groundwater-flow models (Harbaugh, 2005) (fig. 22). The GHB package uses a linear relation between flux and the water-table altitude (or water head), and a user-specified reference groundwater level and hydraulic conductivity simulated for the aquifer. For the purpose of this report, the term “conductance” is defined as the product of hydraulic conductivity of the model cell and the cross-sectional area perpendicular to flow, divided by the distance between the GHB cell and the model cell. When the simulated groundwater level is lower than the reference groundwater level, water flows into the groundwater model. When the simulated groundwater level is higher than the reference groundwater level, water flows out of the groundwater model.

Few groundwater-level observations are available in the Rush Springs aquifer adjacent to the Washita River alluvial aquifer (fig. 25 in Ellis, 2018). Therefore, the reference groundwater level for each GHB cell simulating flow between the Washita River alluvial aquifer and the Rush Springs aquifer was determined from the mean of the nearest simulated groundwater levels from Ellis (2018) during the simulation period for the Washita River alluvial aquifer.

Streams

The major streams and associated tributaries in the study area (fig. 1) were simulated as a head-dependent boundary by using the Streamflow-Routing package, version 2 (SFR2) designed for use with MODFLOW groundwater-flow models (Niswonger and Prudic, 2005). The SFR2 exchanges flow between the aquifer and the stream according to Darcy’s Law; stream seepage is the product of the streambed conductance and the difference between the groundwater level and the stream stage. The streambed conductance is the product of the hydraulic conductivity of the streambed sediments and the area of the stream channel divided by the streambed thickness. Stream stage is calculated by using Manning’s equation, in which stream stage is a function of flow based on the geometry of the stream channel. Where groundwater levels are lower than stream stage, inflow to the aquifer from the stream occurs (termed “seepage from streams”). Where groundwater levels are higher than stream stage, outflow from the aquifer to the stream occurs at a specified streambed conductance rate from the aquifer (termed “seepage to streams”).

Streamflows are calculated for each part of the stream, known as reaches, and they are contained in a model cell until the end of a segment, or group of reaches with uniform or linear hydraulic properties, is reached during each time step. A stream-water balance is used to compute the amount of water available in each stream reach and the amount of water exchanged between the stream and the aquifer in groundwater-flow simulations. Calculation of water exchanges between the stream and aquifer repeats downstream in this manner until water is routed out of the model active area. Inflows (Q_{in}) to each stream reach are calculated by using the following equation (all units are in acre-feet per day):

$$\sum Q_{in} = Q_{sp} + Q_{tr} + Q_{ro} + Q_{pr} - Q_{gwi} \quad (4)$$

where

Q_{sp} is the specified inflow at the beginning of the first reach of a segment,
Q_{tr} is the sum of tributary inflow,
Q_{ro} is direct overland runoff,
Q_{pr} is direct precipitation, and
Q_{gwi} is seepage to streams.

Specified inflows (Q_{sp}) at the beginning of each stream reach include the estimated base flows at the model boundary (Texas–Oklahoma border) from upstream as well as releases from Foss Reservoir (Bureau of Reclamation, 2018) to the first downstream segment. Tributary inflows (Q_{tr}) are based on flow routed from upstream segments, which include the small tributaries associated with the alluvium and terrace of the Washita River. Tributary inflow rates were set for the following tributaries: Rush and Croton Creeks (3.0 ft^3/s), Sergeant Major Creek (2.0 ft^3/s), Dead Indian Creek (1.0 ft^3/s), Sandstone Creek (4.0 ft^3/s), Big Kiowa Creek (0.1 ft^3/s), and White Shield and Quartermaster Creeks (0.5 ft^3/s) (fig. 1). All other tributaries at the model boundary were either assumed to be intermittent or ephemeral, with no specified inflows. Tributaries originating in the model active area were assumed to drain the Washita River alluvial aquifer and were simulated primarily to route groundwater flow to the Washita River. The model is simulated under base-flow conditions; therefore, direct overland runoff (Q_{ro}) and precipitation (Q_{pr}) were not applied to the stream channel. Groundwater discharge from the aquifer simulated by using MODFLOW is a negative value; thus, the seepage to streams or groundwater inflow (Q_{gwi}) is subtracted from the other inflow components. Outflows (Q_{out}) from each stream reach are calculated in the following equation (all units are in acre-feet per day):

$$\sum Q_{out} = Q_{str} + Q_{div} + Q_{et} + Q_{gwo} \quad (5)$$

where

Q_{str} is streamflow out of a reach,
Q_{div} is simulated diversions,
Q_{et} is evapotranspiration, and
Q_{gwo} is seepage from streams.

Streamflow out of each reach (Q_{str}) was routed downstream in all areas except for the stream segments directly above Foss Reservoir, where streamflow was routed into this reservoir, and stream segments located at the boundary of the model. During the simulation period, the 69 permitted surface-water diversions were grouped into 27 simulated diversions (Q_{div}). Diversions can be simulated only from the last reach in any segment; thus, this location may differ somewhat from the actual diversion location. The discrepancies between the actual and simulated diversion locations were not substantial, however, and the diversion rates represented only a small percentage of flow in the SFR2 cells. Surface-water diversions located on unnamed streams—which were considered intermittent or ephemeral streams, and thus supplied from surface runoff—were not simulated in the groundwater model. No evaporative processes (Q_{et}) were applied by using the SFR2 package, although ETg is simulated by using the Evapotranspiration package (Harbaugh, 2005) for alluvium cells that include stream segments.

The extent of the streams used for streamflow routing (fig. 22) was modified from the National Hydrography Dataset Plus (NHDPlus; Horizon Systems Corporation, 2015), a 1:100,000-scale geospatial dataset of surface-water features. Streams having a stream order (Strahler, 1952) of one—defined as headwater streams that are dominated by runoff—were excluded from the stream extent. Differences in stream channel location occurred between the DEM (USGS, 2018a) and the NHDPlus streamline because of the averaging of DEM cells and migration of the stream channel in the alluvial valleys over time. To ensure correct surface-water routing in the stream, the stream location was adjusted to ensure that the stream channel altitude decreased in a downstream direction in each segment. For segments where the streambed slope was zero, either the upstream altitude was slightly increased, or the downstream altitude was slightly decreased.

The SFR2 streambed thickness was set to 2 ft, and a rectangular channel was used to define the stream geometry in all segments of the model. The streambed altitude was derived from a 10-meter (33-ft) DEM, and stream segments were incised between 1 and 5 ft in relation to the DEM altitude. Stream channel widths were estimated from 2013 aerial photographs (NRCS, 2018) and ranged from 7 to 55 ft for the Washita River, and from 5 to 40 ft for the tributaries. Although the streambed conductivity varies based on location and discharge rates, the streambed conductivity was set at 5 feet per day (ft/d) based on Ellis and others (2017) and Ellis (2018).

Reservoir

Foss Reservoir was simulated as a head-dependent boundary by using the Lake package for MODFLOW groundwater-flow models (Merritt and Konikow, 2000; Niswonger and Prudic, 2005). Lake package cells exchange water with adjacent and underlying active model cells based on the lakebed leakance and simulated groundwater levels for the reservoir and surrounding active model cells. The Lake

package computes a water budget independent of MODFLOW during each time step for the simulated lake, in units of cubic feet and days, but presented in this report in acre-feet and days or years, described as

$$h_l^n = h_l^{n-1} + \Delta t \frac{p - e + rnf - w - sp + Q_{si} - Q_{so}}{A_s} \quad (6)$$

where

$h_l^n = h_l^{n-1}$ are lake (reservoir) stage from the current and previous time steps, respectively, in feet;

Δt is the time step length, in days;

p is the rate of precipitation applied to the lake, in cubic feet per day;

e is the rate of evaporation from the lake, in cubic feet per day;

rnf is the rate of surface runoff to the lake, in cubic feet per day;

w is the rate of water withdrawals from the lake, in cubic feet per day;

sp is the net rate of lakebed seepage between the lake (reservoir) and the aquifer, in cubic feet per day;

Q_{si} is the rate of stream inflow to the lake, in acre-feet per day;

Q_{so} is the rate of stream outflow from the lake, in acre-feet per day; and

A_s is the surface area of the lake, in square feet.

Foss Reservoir bathymetry and stage-storage relation data were digitized from a 2007 sedimentation survey (Ferrari, 2011) and were used by the Lake package to determine reservoir volume and surface area for a given stage (fig. 23). Only minor differences between the volume and area relation from the sedimentation study and the relation used in the Lake package occurred; thus, the simulated curves are not shown in figure 23. Foss Reservoir was simulated by using 2,216 cells in layer 1; those cells exchange water laterally with other cells in layer 1 and vertically with cells in layer 2 that are directly under the lakebed. These 2,216 cells correspond to a surface area of 6,232 acres (A_s), which is smaller than the active conservation pool surface area of 6,801 acres (Bureau of Reclamation, 2018), caused by the discretization caused by using square cells. The rate of lakebed seepage (sp)—or the quotient of the hydraulic conductivity and thickness between the aquifer and lake—was set at 0.5 day^{-1}, similar to the rate used in previous models near the study area (Ellis, 2018). This leakance rate governs the lakebed seepage between the aquifer and simulated reservoir.

The rates of precipitation (p), evaporation (e), and withdrawals (w; which include permitted use and flood-control releases) during the simulation period were obtained from the Bureau of Reclamation (2018). The mean annual precipitation at Foss Reservoir for the simulation period was 27.4 in/yr, estimated at Bureau of Reclamation climate stations in the reservoir area. The mean annual precipitation, when applied over the area of the Lake package cells, was about 14,199 acre-ft/yr. The mean annual evaporation for the simulation period was 74.0 in/yr, measured at an evaporation pan (Bureau of Reclamation, 2018). The mean annual evaporation, when applied over the area of the Lake package cells, was about 26,825 acre-ft/yr. Mean annual withdrawals (w) during the simulation period totaled 35,718 acre-ft/yr (Bureau of Reclamation, 2018), including permitted use of

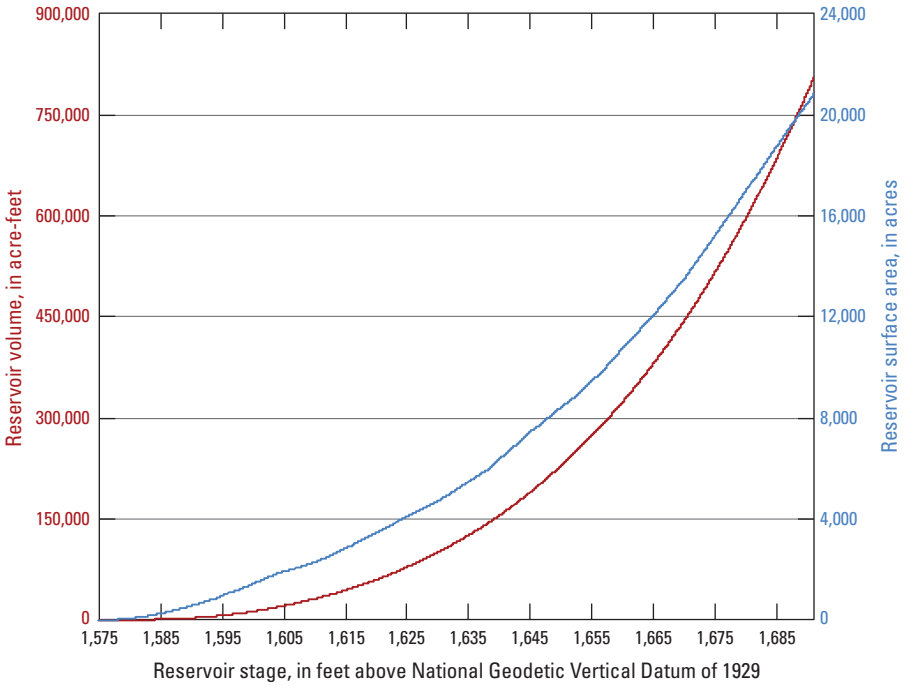

Figure 23. Volume, stage, and surface area for Foss Reservoir in western Oklahoma.

5,974 acre-ft/yr and releases of 29,744 acre-ft/yr. Some estimated releases were greater than the flow recorded at the Foss streamgage (fig. 1; table 1) about 1 mi downstream from the reservoir; thus, the reported releases were reduced to the flow recorded at this streamgage during these months. Releases from Foss Reservoir may occur when the reservoir stage is at the top of the active conservation pool (1,642 ft above the National Geodetic Vertical Datum of 1929 [NGVD 29]).

Surface runoff (*rnf*) was estimated as 20,831 acre-ft/yr and included BFI code-estimated runoff and overland flows entering Foss Reservoir that were not captured by the BFI code method (streamflow minus BFI baseflow equals runoff). The BFI code-estimated runoff was calculated by using streamflow data from the Hammon streamgage (fig. 1; table 2). Stream inflow rates (Q_{si}) to Foss Reservoir were from SFR2 stream segments representing the Washita River and from three tributaries that did not have specified inflows. Mean annual surface-water inflows to Foss Reservoir during the simulation period were estimated at 27,725 acre-ft between 1980 and 2015. Because the reservoir is managed, releases are passed to stream segments downstream from the reservoir; therefore, the stream outflow term (Q_{so}) is zero.

Saturated-Zone Evapotranspiration

ETg was simulated as a head-dependent boundary by using the Evapotranspiration package for MODFLOW groundwater-flow models (Harbaugh, 2005). In this package, saturated-zone evapotranspiration decreases linearly with decreases in the simulated groundwater level, and no saturated-zone evapotranspiration occurs when the simulated groundwater level is below a user-specified root-zone depth. The root-zone depth for the groundwater model was set equal to the SWB code root-zone depth for each land-cover type. Saturated-zone evapotranspiration is unlikely to occur outside of the alluvium because depths to groundwater in the terrace commonly exceed 15 ft; therefore, the Evapotranspiration package was limited to the saturated-zone evapotranspiration area defined by wetlands (U.S. Fish and Wildlife Service, 2018), which are included in the layer 1 alluvium and terrace.

Saturated-zone evapotranspiration rates in the groundwater model were assumed to be proportional to the difference between P_{et} and A_{et} computed by using the SWB code. The variable P_{et} was calculated by using the method in Hargreaves and Samani (1985) and represents the maximum rate at which groundwater could be evapotranspired with unlimited soil-moisture availability. The SWB code computes the change in soil moisture whereby P_{et} is subtracted from daily precipitation. If the resulting value is positive, A_{et} equals P_{et}. If the resulting value is negative, A_{et} is limited to the change in soil moisture and is less than P_{et}. Because the SWB code computes soil-moisture-zone evapotranspiration without regard to the location of groundwater levels in relation to land surface, the difference between P_{et} and A_{et} can be used to approximate saturated-zone evapotranspiration in the groundwater model.

Groundwater Use

Well withdrawals were simulated as a specified-flux boundary by using the Well package for MODFLOW groundwater-flow models (Harbaugh, 2005). Annual reported groundwater use for each permit was divided equally among each of the wells attached to a permit (figs. 6 and 15). These annual well withdrawals were then distributed into monthly well withdrawals by using monthly demand distributions (fig. 24) from the Oklahoma Comprehensive Water Plan (OWRB, 2012b) and spatially discretized into the model cells. Annual irrigation well withdrawals were multiplied by the monthly irrigation demand (as a percentage of annual groundwater use), and annual public-supply well withdrawals were multiplied by the monthly public-supply demand. Annual well withdrawals for other purposes were distributed evenly to all months of the year. Domestic withdrawals, which are not regulated or reported by the OWRB, were not simulated; these withdrawals are likely a minor component of total withdrawals.

Groups of wells attached to a single permit were not allowed to exceed the permitted annual withdrawal amount. Reported annual well withdrawals for 33 irrigation wells (21 percent of all simulated wells) were greater than 645 acre-ft/yr (400 gal/min), but were reduced to 645 acre-ft/yr to avoid the simulation of unrealistic pumping rates. Steady-state well withdrawals were determined as the mean of withdrawals during the simulation period.

Model Calibration

Model calibration is the process of systematically adjusting initial model input values to improve the fit between model-simulated outputs and observed or estimated data (calibration targets). During model calibration, the inputs to be adjusted are updated to new values that reduce the discrepancy, or residual, between the observed and simulated data. Calibration outcomes were evaluated based on the reduction of this residual and the fit of the calibrated groundwater-model water-budget components to those components of the conceptual water budget. The calibration process for the Washita River alluvial aquifer model included (1) manual adjustment of model inputs by trial and error, followed by (2) automated adjustment of model inputs (parameters) by using the nonlinear regression code PEST++ (Welter and others, 2015).

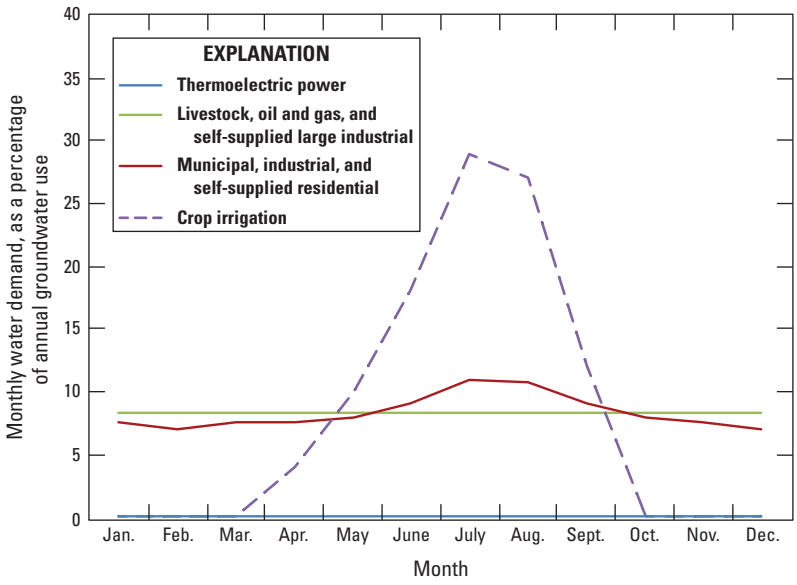

Figure 24. Estimated monthly water demand by groundwater-use type for the Washita River alluvial aquifer, western Oklahoma. Modified from Oklahoma Water Resources Board (2012b).

The PEST++ code uses the Gauss-Marquardt-Levenberg algorithm to adjust user-specified parameters to minimize a sum of squared weighted residuals, or objective function (table 7). The objective function (Φ) is expressed as

$$\Phi = \sum_{i=1}^{n} \left[\omega_i \left(s_i - o_i \right) \right]^2 \qquad (7)$$

where

n is the number of observations,
ω_i is the observation weight,
s_i is the simulated value, and
o_i is the observed or estimated value.

PEST++ automates calibration by running the model as many times as needed to determine the best parameter values while automatically updating the parameter values during each step of the process. This iterative approach allows for the optimal values of many parameters to be estimated together with greater speed than that of a traditional manual calibration approach. Prior to automated calibration, the calibration targets were weighted to account for error in each type of observation.

The automated calibration approach concurrently applied subspace regularization techniques by using singular value decomposition (SVD; Tonkin and Doherty, 2005) in conjunction with singular value decomposition-assist (SVDA; Tonkin and Doherty, 2005) to reduce automated calibration run time and ensure calibration stability. SVD was implemented with PEST++ to identify combinations of parameters that are most responsive to the dataset, thus separating parameters that may be useful for calibration from those parameters that are actually useful and have an effect on modeled outputs. To decrease the run time associated with a large number of parameters, SVDA was also implemented with PEST++. SVDA computes a user-specified combination of parameters, or "super parameters," that enables a reduction in the number of parameters used during calibration. PEST++ requires that the model be run one to two times for either each adjustable parameter or super parameter used in the calibration process multiplied by typically five to seven parameter optimization iterations. Thus, the reduction in the number of parameters by using super parameters resulted in substantial time savings during the Washita River alluvial aquifer model calibration. To further reduce the run time associated with the calibration process,

Table 7. Observation group contribution to the objective function for the automated calibration of the Washita River alluvial aquifer model, 1980–2015.

[USGS; U.S. Geological Survey, OWRB; Oklahoma Water Resources Board]

Observation group	Source	Number of observations	Group contribution (in percent)	Objective function components
Groundwater-level observations	Groundwater-level observations (USGS, 2018b; OWRB, 2018)	168	30	10,874
Reservoir-stage observations	Foss Reservoir stage observations (Bureau of Reclamation, 2018)	433	21	7,514
Base-flow estimates	Cheyenne streamgage (table 1; fig. 1; USGS, 2018b)	433	40	14,250
	Hammon streamgage (table 1; fig. 1; USGS, 2018b)	409		
	Foss streamgage (table 1; fig. 1; USGS, 2018b)	409		
	Clinton streamgage (table 1; fig. 1; USGS, 2018b)	433		
Stream seepage estimates	Conceptual water budget (table 5)	1	9	3,128
Totals		2,286	100	35,766

model runs were performed in parallel on a high-performance computing cluster by using the HTCondor run management software (Condor Team, 2012).

Calibration Parameters

For the Washita River alluvial aquifer model, 8 parameter groups representing 1,535 parameters were defined for the automated calibration (Ellis and others, 2020). These parameter groups are GHB conductance, recharge-rate multipliers, ETg rate and ETg root-zone depth multipliers (1 group), streambed conductance, lakebed leakance and surface runoff, specific yield, horizontal hydraulic conductivity and vertical anisotropy pilot points (1 group), and specific storage.

The GHB cells were grouped into parameter zones for the adjustment of conductance values. The 25 GHB parameter zones (Ellis and others, 2020) were created to account for variations in hydraulic properties of bedrock units adjacent to the Rush Springs aquifer. The recharge parameter group consisted of temporal recharge-rate multipliers for SWB-code-determined recharge in 172 of the 433 stress periods; recharge was negligible in the remaining stress periods. Recharge-rate multiplier parameters were applied uniformly across each stress period to adjust recharge. Entire-array multiplier parameters were used to adjust the ETg rate and ETg root-zone depth uniformly in each transient stress period. A single streambed conductivity parameter was set for all stream segments. A single lakebed leakance parameter was adjusted within a range of values that improved model stability of the reservoir while reducing the stage residual.

Specific yield, horizontal hydraulic conductivity, and vertical anisotropy, or the ratio of horizontal-to-vertical hydraulic conductivity, were represented by using pilot point interpolation in the groundwater model in layer 1 spaced at 3,500-ft intervals (fig. 25) and directly adjusted during calibration. Pilot points provide a balance between the manipulation of values by parameter zones, often defined where values are relatively constant, and the manipulation of values in individual model cells, which may require more detailed data than are typically available. Specific yield, horizontal hydraulic conductivity, and vertical anisotropy values at each pilot point were interpolated independently by using exponentially weighted kriging.

An initial specific yield of 0.12 was obtained from Ellis (2018) and used for the pilot points in layer 1 representing the Washita River alluvial aquifer. The specific yield was adjusted during calibration to values ranging from 0.07–0.18. It was determined the specific yield value of 0.12 provided the best calibration results, hence this value was used in the model to represent the specific yield value in layer 1 across its entire extent. An initial horizontal hydraulic conductivity value of 30 ft/d was set for pilot points in layer 1, similar to the value used for the Washita River alluvial aquifer tributary alluvium and terrace in Ellis (2018). The minimum and maximum horizontal hydraulic conductivity values for all pilot points were set at 6×10^{-4} and 100 ft/d, respectively. The value of 6×10^{-4} ft/d represents the mean of siltstone and claystone values from Morris and Johnson (1967). The maximum horizontal hydraulic conductivity of 100 ft/d represents the fine-gravel horizontal hydraulic conductivity value (100 ft/d) used in Ellis and others (2017). Pilot point vertical anisotropy values for the interpolation zones in both layers were set to an initial value of 10, indicating a horizontal-to-vertical hydraulic conductivity ratio of 10:1.

Values for horizontal hydraulic conductivity in layer 2 were set based on likely values for adjacent and underlying hydrogeologic units based on lithology of these units. A horizontal hydraulic conductivity value of 0.08 ft/d was set where the Washita River alluvial aquifer overlies the Cloud Chief Formation. A horizontal hydraulic conductivity value of 6.6 ft/d from Ellis (2018) was set where the Washita River alluvial aquifer overlies the Rush Springs aquifer. Horizontal hydraulic conductivity values for the Washita River alluvial aquifer in the transition zone between these two hydrogeologic units were graded between 0.08 and 6.6 ft/d. The specific storage values for both layers were set as a static value of 1×10^{-5}, which was comparable to values used by Ryter and Correll (2016) and Ellis and others (2017) for Permian bedrock units in Oklahoma. To improve model stability, a horizontal hydraulic conductivity value of 0.5 ft/d was set under Foss Reservoir in layer 2 of the model. Because no observations or boundary controls represented the bedrock in layer 2 and because calibration targets in layer 1 were not sensitive to parameter changes in layer 2, parameters in layer 2 were not adjusted during model calibration.

Calibration Targets

Calibration targets for the Washita River alluvial aquifer model included groundwater-level (OWRB, 2018; USGS, 2018b) and reservoir-stage (Bureau of Reclamation, 2018) observations, as well as base-flow (table 2) and stream-seepage estimates. For the automated calibration, these targets were weighted and placed into observation groups of the same name (table 7). The observation group contributions to the objective function (table 7) were adjusted prior to the start of the calibration process to ensure a balance between each group so that no single observation group dominated the calibration process. The base-flow estimate group was assigned the greatest contribution to the objective function (40 percent) because those measurements were more accurate and were collected throughout the simulation period. The water-table-altitude observation group was assigned the second greatest contribution to the objective function (30 percent) because those measurements were distributed spatially throughout the study area.

Groundwater-Level Observations

The groundwater model was calibrated to 168 groundwater-level observations at 20 wells in the study area; this total included 20 groundwater-level observations for the steady-state simulation and 147 groundwater-level

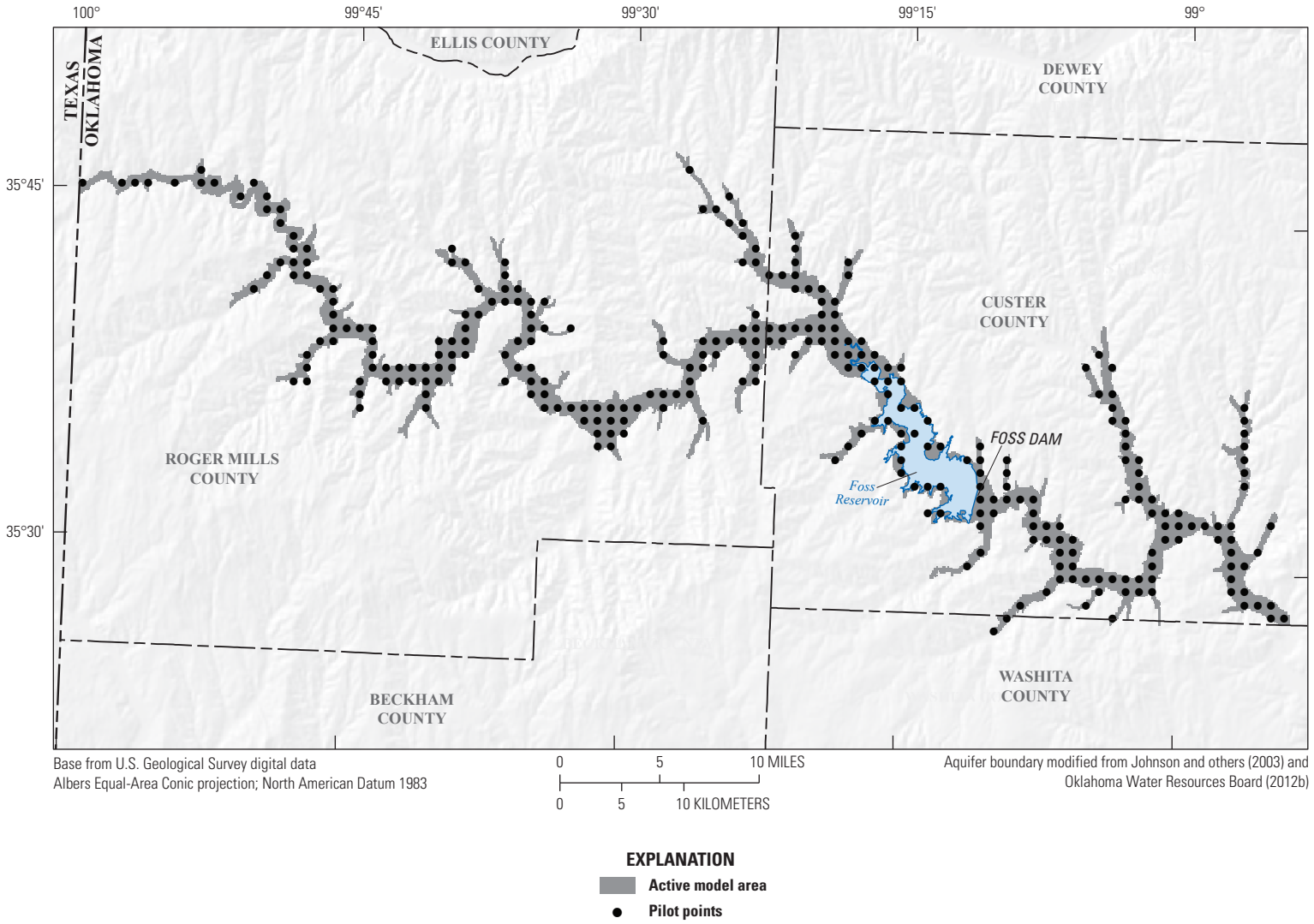

Figure 25. Spatial distribution of pilot points for the Washita River alluvial aquifer model, western Oklahoma, 1980–2015.

observations for the transient simulation (table 8). Of the 147 groundwater-level observations for the transient simulation, about half of the observations occurred after 2003; therefore, a bias toward this period was incurred during model calibration. About 66 percent of the observations were during January–March of each year (fig. 26); thus, most observations were minimally affected by local groundwater withdrawals for irrigation that typically occur between April and September (fig. 24). Two-thirds of the wells had less than five observations during the simulation period (fig. 27), and the three wells located downgradient from Foss Reservoir had less than four groundwater-level observations each. Additionally, the four wells with the greatest number of groundwater-level observations (more than 13 observations) were located nearby or upgradient from the Hammon streamgage. Therefore, with respect to groundwater-level observations, the groundwater model had a greater uncertainty from upgradient to downgradient, particularly in the area downgradient from Foss Reservoir.

When available, screened-interval data were analyzed to ensure that observation wells were completed in the Washita River alluvial aquifer. All groundwater-level observations were originally collected as depth-to-water measurements; groundwater altitudes were calculated by subtracting the measured depth to water from the land-surface altitude specified in the National Water Information System (NWIS) (USGS, 2018b) or OWRB (2018) databases. The land-surface altitude specified in the NWIS database was compared to the altitude obtained from a DEM, and observations with large land-surface altitude discrepancies were discarded.

Table 8. Selected groundwater-level observation wells in and near the Washita River alluvial aquifer, western Oklahoma.

[OWRB ID, the well identifier used by the Oklahoma Water Resources Board (OWRB); USGS, U.S. Geological Survey; --, not available. Dates are in month/day/year format. Groundwater-level observations are available for the long-term groundwater-level recorder wells in the Oklahoma Water Resources Board well database beyond 2010. The number of groundwater-level observations does not include the period-of-record averaged observation used in the steady-state groundwater flow model]

OWRB ID or USGS station number (15-digit number)	Station name	Latitude, in decimal degrees	Longitude, in decimal degrees	Period of record used in this analysis (may contain gaps)		Well or hole depth, in feet	Number of groundwater-level observations during study period
				Begin	End		
Groundwater-level observation wells from the Mass Measurement Program (Oklahoma Water Resources Board, 2017a)							
2675	14N-23W-10-SW-SW-SW	35.69702	−99.64002	5/6/2014	1/21/2015	141	3
2687	14N-23W-32-SW-SW-SW	35.64623	−99.66896	3/26/1980	1/6/2015	86	36
2809	15N-25W-27-SE-NE-NW	35.75101	−99.84745	7/14/2014	1/6/2015	163	3
20600	14N-20W-28-NW-SW-SW	35.65605	−99.34112	12/15/2011	9/30/2015	100	8
78093	14N-24W-34-SE-SE-SE	35.64007	−99.73162	3/8/2004	1/21/2015	190	13
99059	13N-21W-3-NW-NE-NE	35.63862	−99.42110	5/6/2014	5/13/2015	55	4
107564	14N-23W-9-NE-NE-NE	35.70352	−99.65150	7/14/2014	5/26/2015	70	4
118873	14N-24W-32-NE-SW-SW	35.64200	−99.78078	8/13/2014	9/30/2015	160	4
149263	12N-17W-10-NW-NE-NE	35.53676	−98.97921	8/12/2014	1/13/2015	123	2
149664	12N-18W-8-NW-SE-SW	35.52662	−99.13006	3/7/2013	5/7/2013	126	2
Groundwater-level observation wells (U.S. Geological Survey, 2018b)							
353215099004101	12N-17W-09 BBB 1 WSH05	35.53746111	−99.01130556	4/23/2015	11/20/2015	124	3
353626099340901	13N-22W-17 BBD 1 WSH03	35.60734722	−99.56929167	7/14/2014	11/20/2015	50	8
353713099265001	13N-21W-09 BBC 1	35.62051667	−99.44733611	8/6/2014	1/6/2015	--	2
353715099394501	13N-23W-08 ABD 1	35.62088154	−99.66288278	3/26/1980	3/26/1980	--	1
353722099400801	13N-23W-08 ABB 1	35.62282596	−99.66927186	3/26/1980	3/20/2002	--	22
353821099395901	14N-23W-32 DCC 1 WSH02	35.63926389	−99.66654722	3/18/1971	8/23/1995	75	8
353840099435301	14N-24W-34 DDA 2	35.64449233	−99.73177381	3/12/1996	1/27/2010	185	14
353913099352901	14N-24W-18 DDC 1	35.65373333	−99.59156111	7/14/2014	1/6/2015	--	3
354022099202701	14N-21W-21 CDC 1 WSH04	35.6728	−99.34091389	4/23/2015	11/20/2015	75	2
354518099511601	15N-25W-21 DDD 1	35.75507222	−99.85463889	5/20/2014	5/20/2014	--	1
354529099565501	15N-26W-22 DCA 1 WSH01	35.75821389	−99.94877222	5/20/2014	11/19/2015	60	4

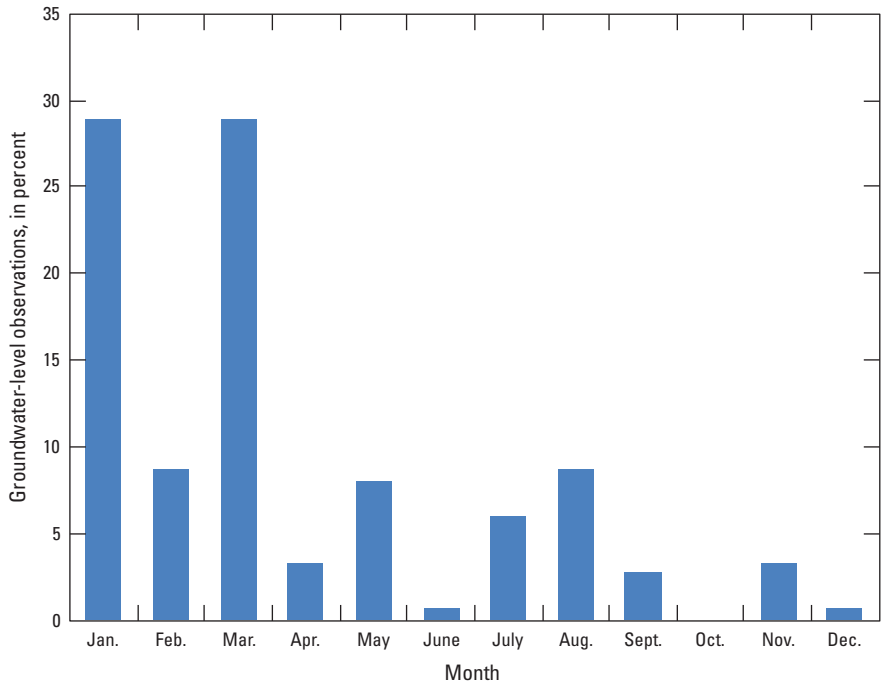

Figure 26. Monthly groundwater-level observations as a percentage of the total number of groundwater-level observations used for the Washita River alluvial aquifer model, western Oklahoma, 1980–2015.

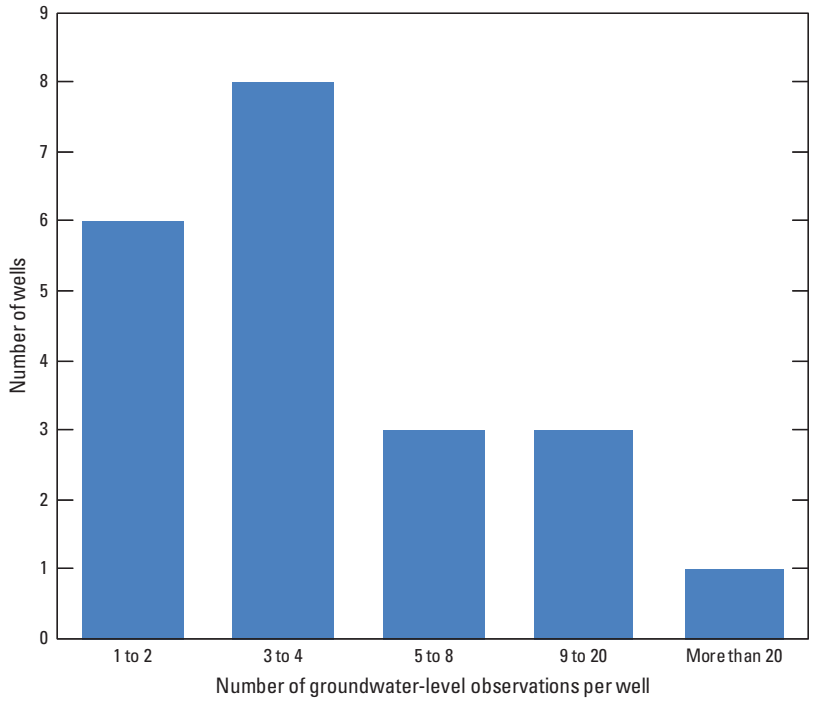

Figure 27. Number of groundwater-level observations per well for wells used in the Washita River alluvial aquifer model, western Oklahoma, 1980–2015.

Foss Reservoir Stage Observations

The groundwater model was calibrated to 433 Foss Reservoir stage observations (table 7), which included 432 monthly stage observations (Bureau of Reclamation, 2018) and 1 steady-state (averaged) stage observation. At active conservation pool stage (1,642 ft above NGVD 29), Foss Reservoir storage was about 168,732 acre-ft; at dead-pool stage (1,597 ft above NGVD 29), storage was about 8,868 acre-ft. Because the dead-pool storage was relatively small, it was not removed from estimates of Foss Reservoir storage used in this report.

Base-Flow and Stream-Seepage Estimates

The groundwater model was calibrated to 1,684 base-flow estimates at 4 streamgages (table 7), including 1,680 monthly estimates and 4 steady-state (averaged) estimates. Base-flow estimates were available during each stress period for the Cheyenne and Clinton streamgages. Base-flow estimates were available for the Foss and Hammon streamgages between January 1980 and September 1987 and between October 1989 and December 2015, respectively.

The groundwater model was calibrated to one stream-seepage estimate (table 7). The simulated stream seepage was determined as the sum of the "Flow to Aquifer" column in the SFR2 secondary output file divided by the 433 monthly transient stress periods used for simulation purposes. Therefore, this value represents the mean stream seepage across the simulation period.

Calibrated Model Fit

The calibrated model fit was evaluated based on the reduction of calibration-target residuals and the fit of the calibrated water-budget components to the components of the conceptual water budget. Residuals were calculated as observed minus simulated values; positive residuals indicate lower simulated than observed values (underpredicted), and negative

residuals indicate higher simulated than observed values (overpredicted). The root-mean-square error (RMSE) of residuals was calculated by using the following equation:

$$RMSE = \sqrt{\frac{1}{n}\sum_{i=1}^{n}\left(o_i - s_i\right)^2} \quad (8)$$

where

n is the number of observations,
o_i is the observed (or estimated) value, and
s_i is the simulated value.

Groundwater Levels

A good agreement between the observed and simulated groundwater-level altitudes (also known as hydraulic heads) was indicated as shown on a 1:1 plot, where the values generally fall along a straight line (fig. 28*A*). The combined groundwater-level mean residual for steady-state and transient simulations was 0.8 ft, indicating that simulated groundwater levels were slightly underpredicted (table 9). The combined groundwater-level RMSE was 7.5 ft, and 75 percent of residuals were within ±7.9 ft (table 9; fig. 28*B*). The simulated groundwater-level relief was 708 ft (highest groundwater-level altitude minus lowest groundwater-level altitude), and the combined RMSE as a percentage of this water-table relief was 1.1 percent (table 9). These results are comparable to those for the Canadian River alluvial aquifer (Ellis and others, 2017), which has a similar geologic setting.

The overall distribution of groundwater-level residuals was reasonable, if not entirely random; wells in some parts of the model exhibited positive or negative bias in residuals (fig. 29). Groundwater levels generally were underpredicted in the alluvium and terrace in areas closer to the surrounding bedrock, whereas groundwater levels were overpredicted near the stream channel because of the inability to simulate the full amount of ETg estimated from the SWB code (refer to the "Using the Soil-Water-Balance Code to Estimate Recharge" section of this report for additional details). Overpredicted groundwater levels also typically occurred in wells downgradient from Foss Reservoir (fig. 29).

The two wells with the greatest residuals (fig. 29) (overpredicted or underpredicted groundwater levels) had only four measured groundwater levels each. Groundwater-level observations were measured at these wells during 2014 and 2015; therefore, temporal uncertainty may account for these large residuals. Additionally, these wells were located at or near a model boundary; thus, structural error may also account for these residuals. Because of model structural error, the model residual may exhibit temporal and spatial correlation structures (Doherty and Hunt, 2010). Simulated groundwater-level altitudes were similar to observed groundwater-level altitudes for three wells monitored by OWRB, shown in figure 13 hydrographs, but the magnitude of the simulated groundwater-level changes was typically less than the observed changes.

Base Flow

The pattern of simulated base flows was similar to that of observed base flows at the four streamgages used in the calibration, but mean simulated base flows were generally lower than mean estimated base flows (fig. 30). The mean base-flow residual was between 16.3 and −1.4 ft^3/s for each streamgage (table 10). For the four streamgages, the RMSE was less than or equal to 9.1 percent of the range in observed base flow, and the mean base flow was slightly underpredicted for the Hammon, Foss, and Clinton streamgages (table 10).

Base flows were somewhat overpredicted during periods of lower base flows (winter and summer months) and underpredicted during periods of higher base flows (fall and spring months). Overpredicted base flows were likely the result of undersimulated ETg because increases in ETg in the model reduced summer low-flow residuals. Underpredicted base flows at the Clinton streamgage during high-flow periods indicate that observed base flows probably were overestimated by BFI because of reservoir releases from Foss Reservoir that could not easily be removed from the base-flow estimates. Reservoir releases from Foss Reservoir did not occur for

Table 9. Statistical summary of groundwater-level residuals for the numerical groundwater-flow model of the Washita River alluvial aquifer, western Oklahoma, 1980–2015.

[RMSE, root-mean-square error; ±, plus or minus]

Statistic	Steady-state simulation	Transient simulation	Combined value (steady state plus transient)
Number of groundwater-level observations	21	147	168
Mean residual, in feet	−3.1	1.3	0.8
75th-percentile residual range, in feet	±8.5	±7.9	±7.9
RMSE, in feet	7.2	7.6	7.5
RMSE percentage of water-table relief (708 feet)	1.0	1.1	1.1

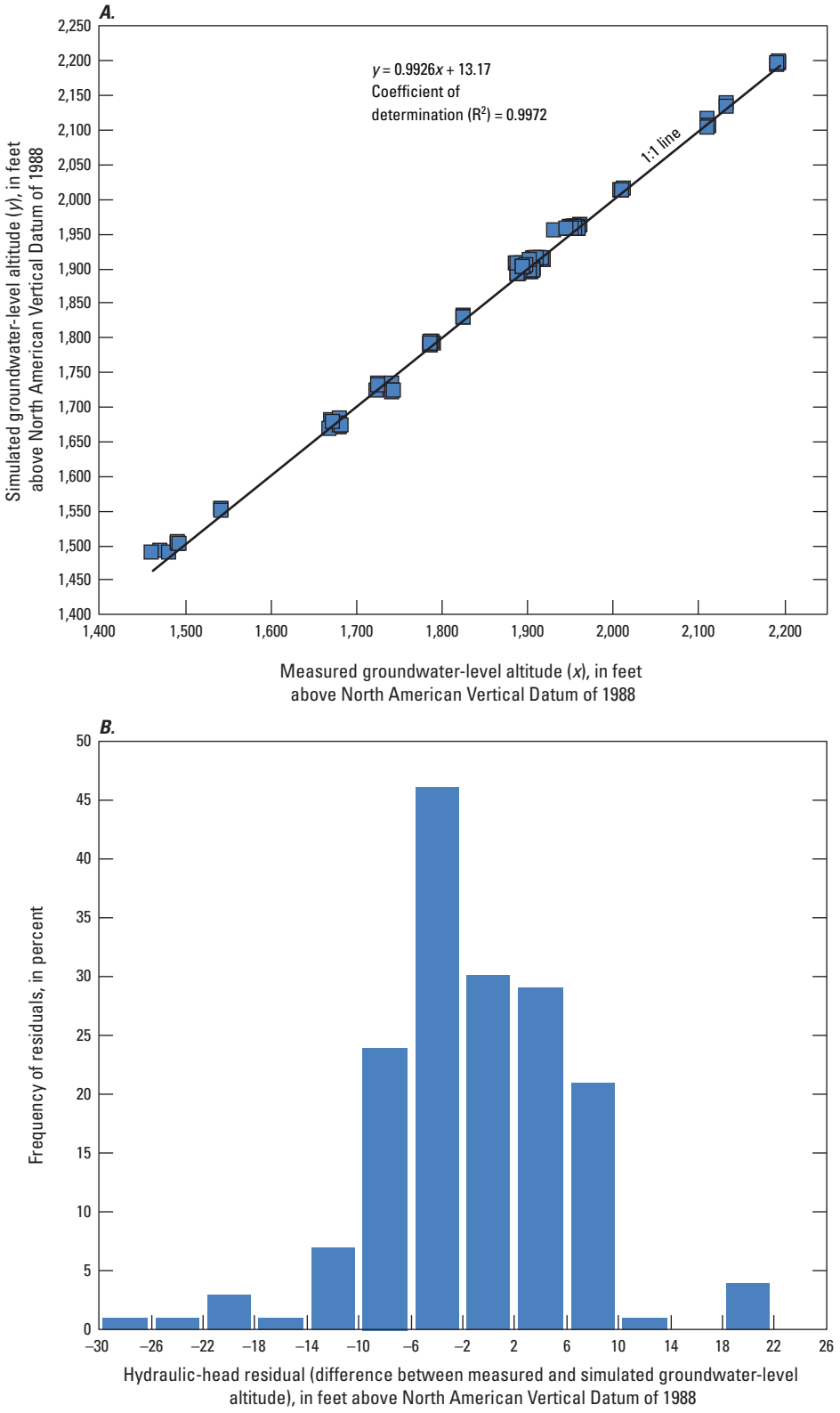

Figure 28. *A*, Simulated and measured groundwater-level altitude, and *B*, frequency of hydraulic-head residuals obtained from the numerical groundwater-flow model of the Washita River alluvial aquifer, western Oklahoma, 1980–2015.

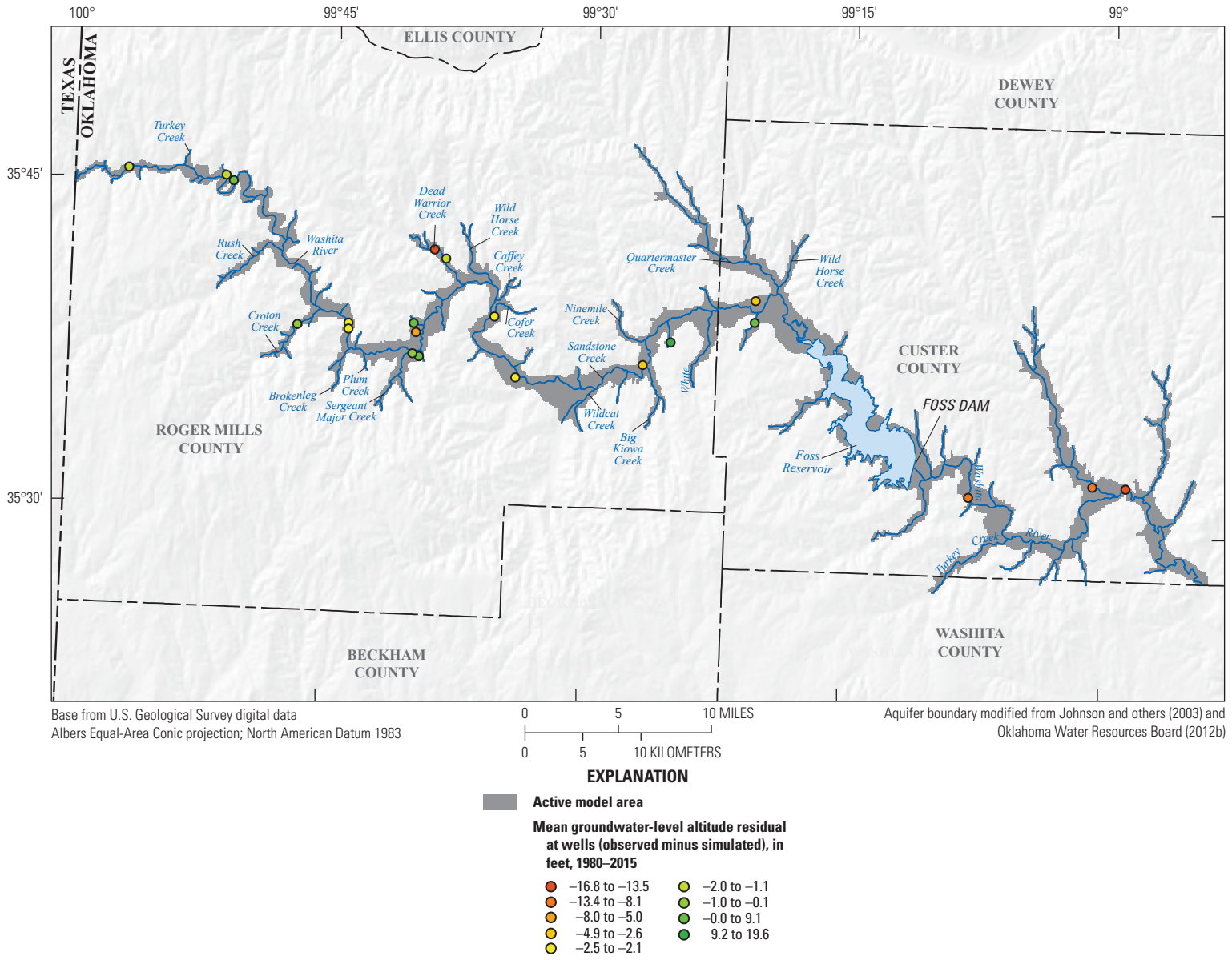

Figure 29. Spatial distribution of mean groundwater-level altitude residuals for the numerical groundwater-flow model of the Washita River alluvial aquifer, western Oklahoma, 1980–2015.

Table 10. Statistical summary of base-flow residuals for the numerical groundwater-flow model of the Washita River alluvial aquifer, western Oklahoma, 1980–2015.

[Residual is calculated as the observed value minus the simulated value; thus, a negative residual indicates higher simulated than observed values. All units are in cubic feet per second except where noted; USGS, U.S. Geological Survey; Min., minimum; Max., maximum; RMSE, root-mean-square error; ±, plus or minus]

USGS station number (fig. 1)	Short name for station (table 1; fig. 1)	Observed base flow			Simulated base flow			Base-flow residuals			RMSE range in observed base flow, in percent
		Min.	Mean	Max.	Min.	Mean	Max.	Mean	RMSE	75th percentile range	
07316500	Cheyenne streamgage	0.0	14.8	118.0	1.3	16.2	99.2	−1.4	6.8	±7.0	5.8
07324400	Hammon streamgage	0.0	40.0	463.4	0.0	23.7	152.4	16.3	42.0	±24.0	9.1
07324400	Foss streamgage	1.2	45.1	575.9	1.5	41.6	580.7	3.6	11.9	±5.7	2.1
07325000	Clinton streamgage	0.4	83.7	1,052.3	16.2	70.2	613.4	13.5	77.4	±26.2	7.4

about two-thirds of the total number of stress periods. For these stress periods when reservoir releases did not occur, the RMSE for the Clinton streamgage decreased by 55 percent; the 75-percent residual range decreased by 35 percent. Thus, the model generally simulates patterns in estimated base flow with more error present in months in which reservoir releases occur. Recharge processes, such as bank storage flow or interflow, that mostly operate on a submonthly time scale also could contribute to underpredicted base flows. Bank storage flows (Chen, 2003), by which floodwater infiltrates the aquifer and is released days to weeks after the floodwater recedes, may increase base flows during periods of no new recharge. The primary source of water to the aquifer is recharge, so large positive base-flow residuals also could be caused by underpredicted or incorrectly distributed recharge.

Reservoir Stage and Water Budget

The Foss Reservoir stage mean residual was −0.2 ft (table 11), indicating that the mean simulated stage was slightly higher than the mean observed stage (fig. 31*A*). The RMSE of Foss Reservoir stage residuals was 1.0 ft, and 75 percent of the simulated reservoir stage values were within ±0.9 ft of the observed stage values (table 11). The minimum simulated stage was 2 ft greater than the minimum observed stage, and the maximum simulated stage was 1 ft lower than the maximum observed stage. The largest Foss Reservoir stage residuals occurred in late 2014 and early 2015 when the observed reservoir stage was relatively low (fig. 31*A*).

Simulated storage in Foss Reservoir decreased by about 20,000 acre-ft during the study period (fig. 32*B*). Storage in Foss Reservoir between 2001 and 2007 reflected precipitation patterns, where large shifts in precipitation occurred during each subsequent year (fig. 32); thus, the stage and water budget in Foss Reservoir for these years tended to oscillate on a year-to-year basis more than in other periods. Stage in Foss Reservoir dropped to about 1,622 ft in 2014 (fig. 31*B*), or 40 percent of active conservation pool storage (fig. 32*B*), which is the lowest stage since 1965 (Bureau of Reclamation, 2018). This decrease in stage corresponds with a decrease in base flow in the Washita River during this period (table 2). More than half of the streamflow in the Washita River upstream from Foss Reservoir is from base flow from the aquifer (table 2); therefore, groundwater-level declines in the aquifer upgradient from Foss Reservoir affect stage and storage.

Calibrated Water Budget

The calibrated water budget for the Washita River alluvial aquifer model includes mean annual inflows and outflows for the simulation period (1980–2015) (table 12; figs. 33, 34*A*). Annual water budgets for the Washita River alluvial aquifer model are listed in table 13. A sub-accounting for areas upgradient and downgradient from Foss Reservoir was computed by using the ZONEBUDGET utility (Harbaugh, 1990). Simulated recharge was the largest inflow (49.0 percent); seepage from streams was 22.4 percent; lateral groundwater inflow was 19.6 percent, and lakebed seepage was 9.0 percent of total inflows. Seepage to streams was the largest outflow (57.6 percent); ETg was 28.0 percent, groundwater use was 8.5 percent, lakebed seepage was 4.1 percent, and lateral groundwater outflow was 1.8 percent of total outflows.

The mean annual recharge for the calibrated water budget (25,049 acre-ft/yr; table 12) was about 13 percent greater than that of the conceptual water budget (22,169 acre-ft/yr; table 5). This difference corresponds to a rate of 0.4 in/yr of recharge in the calibrated water budget compared to recharge in the conceptual water budget. Mean annual stream seepage for the calibrated water budget of 18,084 (shown as −18,084 acre-ft/yr in table 12) was about 18 percent smaller than that of the conceptual water budget (21,996 acre-ft/yr; table 5). Mean annual net lateral groundwater flow for the calibrated model

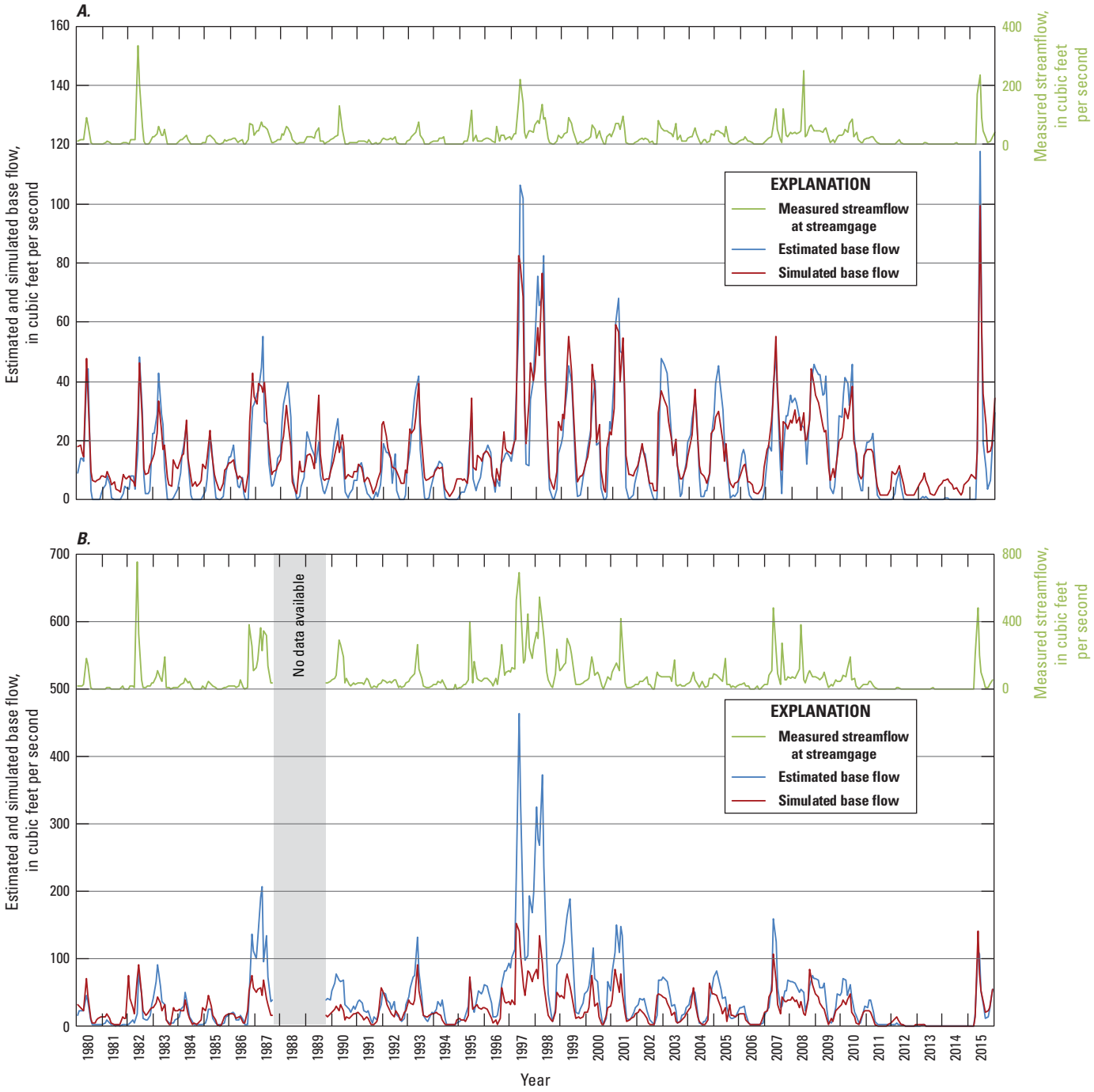

Figure 30. Observed and simulated base flow and total streamflow at U.S. Geological Survey streamgages *A,* 07316500 Washita River near Cheyenne, Okla.; *B,* 07324200 Washita River near Hammon, Okla.; *C,* 07324400 Washita River near Foss, Okla.; *D,* 07325000 Washita River near Clinton, Okla., used for the numerical groundwater-flow model of the Washita River alluvial aquifer, western Oklahoma, 1980–2015.

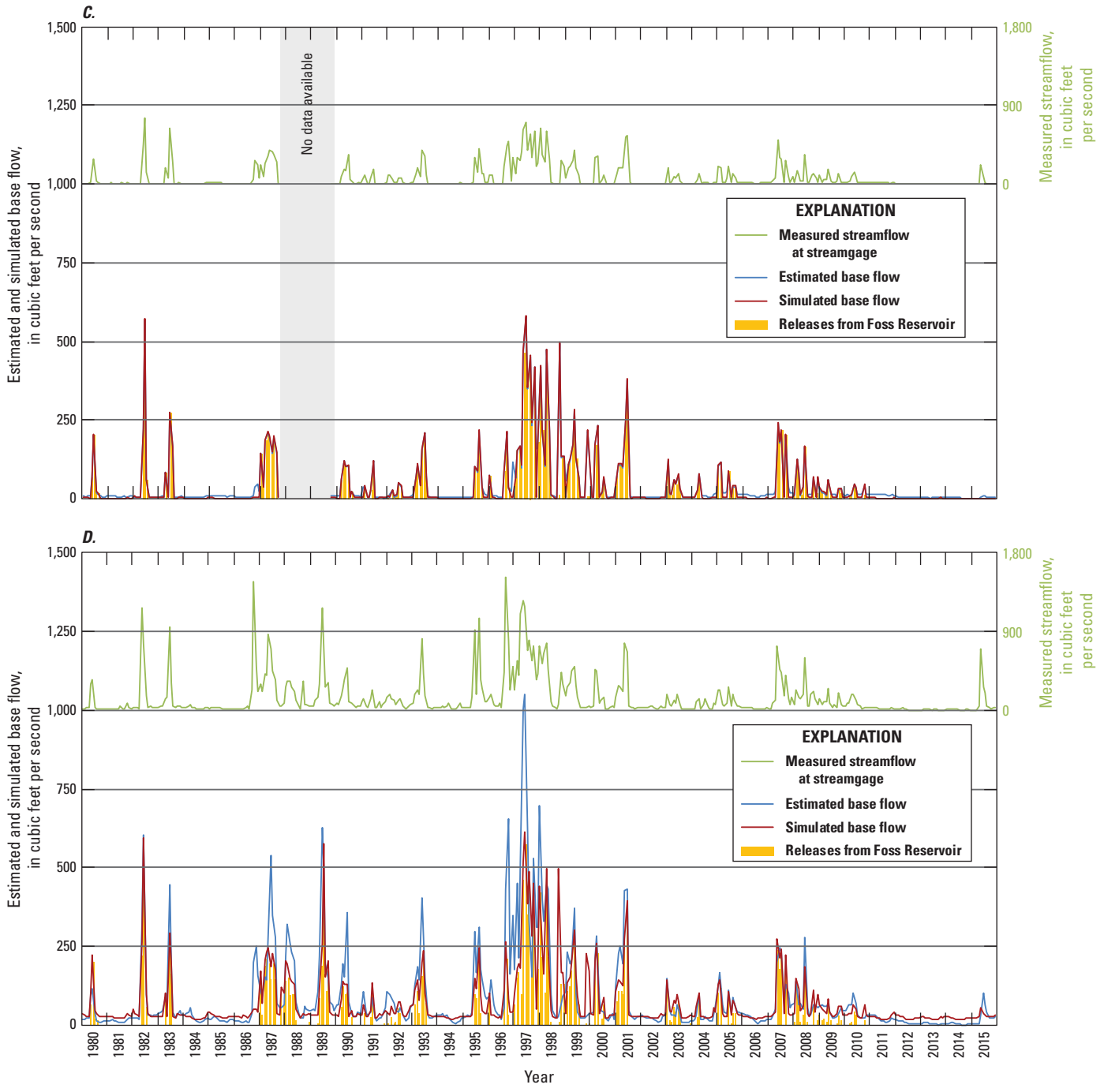

Figure 30. Observed and simulated base flow and total streamflow at U.S. Geological Survey streamgages *A,* 07316500 Washita River near Cheyenne, Okla.; *B,* 07324200 Washita River near Hammon, Okla.; *C,* 07324400 Washita River near Foss, Okla.; *D,* 07325000 Washita River near Clinton, Okla., used for the numerical groundwater-flow model of the Washita River alluvial aquifer, western Oklahoma, 1980–2015.—Continued

Table 11. Statistical summary of Foss Reservoir stage residuals for the numerical groundwater-flow model of the Washita River alluvial aquifer, western Oklahoma, 1980–2015.

[NAVD 88, North American Vertical Datum of 1988; RMSE, root-mean-square error; ±, plus or minus; --, not applicable]

Observation	Lake stage		
	Minimum	Mean	Maximum
Observed, in feet	1,622	1,639	1,648
Simulated, in feet	1,624	1,639	1,647
Mean residual, in feet	--	−0.2	--
RMSE, in feet	--	1.0	--
75th percentile residual range, in feet	--	±0.9	--

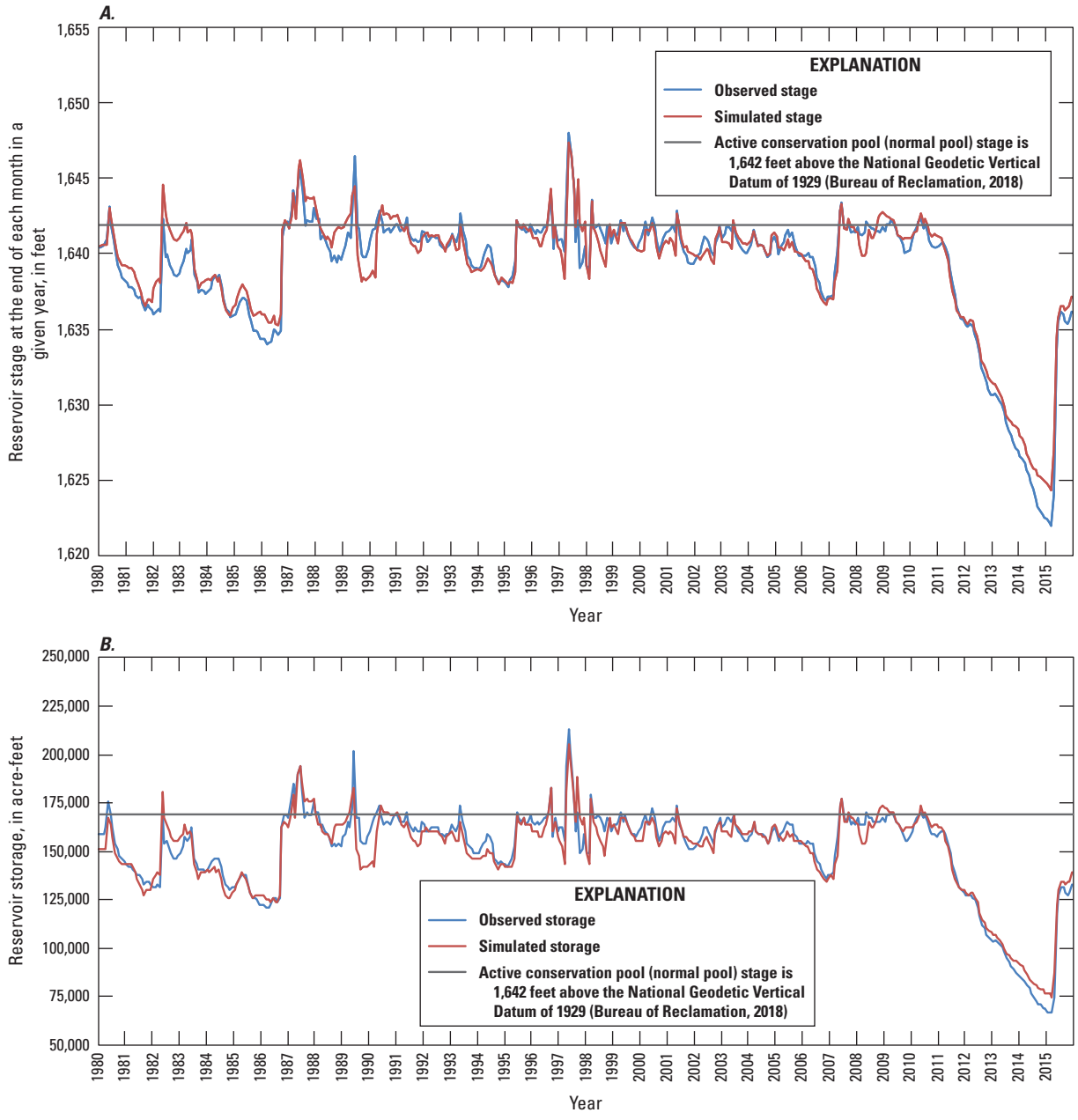

Figure 31. Observed and simulated *A*, stage and *B*, storage for Foss Reservoir for the numerical groundwater-flow model of the Washita River alluvial aquifer, western Oklahoma, 1980–2015.

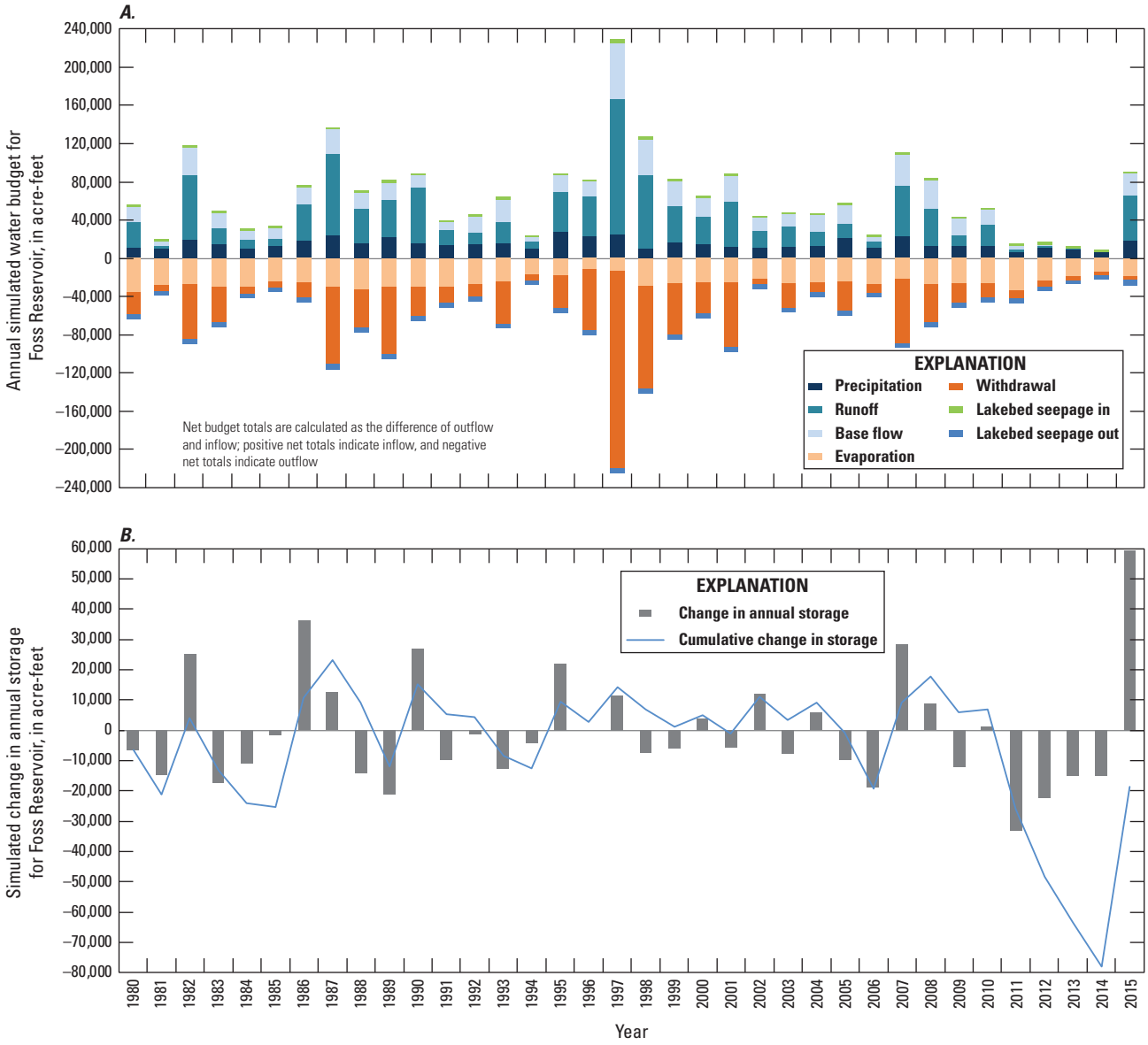

Figure 32. *A*, Annual simulated water budget for Foss Reservoir and *B*, simulated changes in storage for Foss Reservoir in the numerical groundwater-flow model of the Washita River alluvial aquifer, western Oklahoma, 1980–2015.

(9,117 acre-ft/yr; table 12) was about 47 percent less than that of the conceptual water budget (17,157 acre-ft/yr; table 5). Mean annual ETg for the calibrated model (14,377 acre-ft/yr; table 12) was about 22 percent greater than that of the conceptual water budget (11,828 acre-ft/yr; table 5). Because unreasonably long model run times are associated with larger ETg areas and rates, the area where ETg was simulated and the simulated ETg rate were decreased in the simulation. The mean simulated annual groundwater use (4,367 acre-ft/yr; table 12) was about 20 percent less than the conceptual water budget (5,502 acre-ft/yr; table 5) because of the threshold applied to simulated wells associated with 33 permits.

Simulated groundwater storage at the end of the simulation period (2015) was 587,252 acre-ft, and mean simulated groundwater storage for the simulation period was 589,423 acre-ft. Because of the difficulty associated with estimating total recoverable groundwater—whereby groundwater pumping cannot extract the entire volume of water from the aquifer—these simulated groundwater storage values represent theoretical volumes. However, these values are useful for comparisons of changes in groundwater storage caused by aquifer stresses. For the simulation period, mean annual simulated outflows exceeded inflows by 169 acre-ft/yr (table 12). This difference corresponds to a cumulative net storage decrease of about 6,000 acre-ft (fig. 34*B*), or a cumulative net groundwater-level decrease of about 0.5 ft.

Table 12. Mean annual calibrated water budget for the numerical groundwater-flow model of the Washita River alluvial aquifer, western Oklahoma, 1980–2015.

[--, not applicable; All units are in acre-feet per year. Net budget totals are calculated as the difference of outflow and inflow; therefore, positive net totals indicate inflow, and negative net totals indicate outflow to the Washita River alluvial aquifer]

Water-budget category	Upgradient from Foss Reservoir	Downgradient from Foss Reservoir	Total (acre-feet per year)	Percent of water budget
Inflow				
Recharge	16,811	8,239	25,049	49.0
Seepage from streams	9,209	2,243	11,452	22.4
Lateral groundwater inflow	33	9,990	10,023	19.6
Lakebed seepage inflow	29	4,570	4,599	9.0
Total inflow	26,082	25,041	51,123	100
Outflow				
Seepage to streams	11,276	18,259	29,536	57.6
Saturated-zone evapotranspiration	9,874	4,504	14,377	28.0
Groundwater use	3,984	383	4,367	8.5
Lakebed seepage outflow	1,018	1,088	2,106	4.1
Lateral groundwater outflow	1	904	905	1.8
Total outflow	26,153	25,139	51,292	100
Net water-budget totals				
Net stream seepage	−2,067	−16,017	−18,084	--
Net lateral flow	32	9,085	9,117	--
Net lakebed seepage	−989	3,482	2,493	--
Net change in groundwater storage	−71	−98	−169	--

Simulated annual groundwater storage changes reflect climatic patterns during the simulation period (fig. 16). From 1980 to 1985, cumulative storage was negative (fig. 34*B*) because of a period of generally lower than mean precipitation (fig. 16). A relatively long period of above-mean precipitation occurred between 1985 and 1997 (fig. 16), which resulted in a cumulative storage increase (fig. 34*B*). This period was followed by a period of generally below-mean precipitation between 2001 and 2006 (fig. 16), whereby cumulative storage decreased (fig. 34*B*). The drought conditions between 2009 and 2014 (fig. 16) resulted in a sustained decrease of groundwater in storage (fig. 34*B*).

Recharge composes 49 percent of the total simulated inflow to the aquifer (fig. 33; table 12). Therefore, precipitation changes—although moderated by the substantial part of inflows from lateral groundwater inflows (table 12)—affect groundwater storage and the annual water budget, which is several times larger in years with substantial precipitation events compared with years of below-mean precipitation. During extended periods of below-mean precipitation, groundwater use substantially increased—such as during 2013 and 2014, when groundwater use was nearly twice the mean fig. 6)—which compounded the effects on groundwater storage.

Mean simulated aquifer inflows, primarily from recharge and seepage from streams, tended to be greatest during May, June, and September (fig. 35*A*), which generally corresponds to months of above-mean recharge (fig. 17*B*). Mean simulated aquifer outflows, primarily from seepage to streams, ETg, and groundwater use, were greatest in June, July, and August (fig. 35*A*). During those summer months, seepage to streams was reduced by groundwater-level declines from large ETg outflows and groundwater use, which was primarily for irrigation. Mean monthly outflows exceeded mean monthly inflows in 4 of 12 months (fig. 35*B*).

Calibrated Parameter Values

The calibrated parameter values for the model represent updates to the initial values estimated from available hydraulic data or from the conceptual water budget and are available in Ellis and others (2020). Calibrated conductance values for the 25 GHB conductance zones were between 200 and 203 ft^2/d, respectively. The calibrated ETg rate multiplier was reduced to a value of 0.4 (40 percent) from the initial value in all areas where ETg was simulated. Although further increases in the ETg rate multiplier may have improved the calibration to base flows and groundwater levels, larger ETg rates could not be simulated without model stability issues. Because of

Table 13. Annual water budget for the simulation period for the Washita River alluvial aquifer, western Oklahoma, 1980–2015.

[GHB, general-head boundary; ET, evapotranspiration]

Year	INFLOWS (acre-feet per day)					OUTFLOWS (acre-feet per day)					
	Storage	GHB	Recharge	Stream seepage	Lake seepage	Storage	Well withdrawals	ET	GHB	Stream seepage	Lake seepage
1980	21,444	10,266	15,079	10,564	4,760	11,830	5,156	16,046	783	26,533	1,764
1981	13,988	10,982	11,487	13,276	4,112	9,161	4,843	17,107	645	19,694	2,395
1982	29,738	9,178	55,954	10,604	4,992	40,298	5,130	16,689	1,122	44,711	2,518
1983	17,186	10,313	19,215	11,552	4,448	15,461	3,493	13,566	741	26,945	2,508
1984	14,402	11,096	15,128	12,634	4,099	11,405	4,914	16,907	642	21,147	2,345
1985	15,777	10,317	18,384	12,027	4,080	13,056	4,765	13,696	789	26,167	2,112
1986	10,848	9,891	40,389	10,551	5,028	25,359	3,798	11,764	893	33,059	1,832
1987	20,831	8,842	25,203	8,939	6,183	15,400	3,536	14,168	1,154	34,828	912
1988	22,220	8,451	30,913	10,436	4,562	19,141	3,654	15,650	1,400	33,842	2,896
1989	22,107	8,643	35,341	9,720	4,569	22,409	3,113	13,458	1,448	36,354	3,599
1990	10,925	10,307	14,245	11,272	5,658	9,579	3,279	13,980	779	23,935	856
1991	10,703	10,554	23,959	13,046	4,656	17,895	3,173	15,427	711	24,188	1,522
1992	16,181	9,395	28,362	9,018	4,568	15,296	2,217	14,484	1,066	32,709	1,751
1993	24,816	8,448	31,187	8,031	4,284	18,107	2,193	13,157	1,534	38,613	3,163
1994	13,353	11,140	3,646	13,615	4,424	5,056	3,820	16,942	638	18,236	1,487
1995	16,682	9,144	45,396	10,328	4,944	29,021	5,280	13,817	1,131	35,884	1,361
1996	18,114	9,417	32,534	11,225	4,963	21,443	5,190	13,680	1,070	33,058	1,810
1997	29,524	7,041	78,460	5,657	5,119	42,523	1,888	9,676	2,174	65,295	4,247
1998	31,741	8,965	34,850	10,703	4,590	23,393	4,162	16,819	1,139	41,964	3,371
1999	19,414	10,109	19,489	10,599	4,594	11,570	4,197	13,397	783	31,820	2,439
2000	20,140	9,862	27,023	10,737	4,724	19,652	4,617	14,476	833	31,189	1,719
2001	20,025	9,835	25,435	10,631	4,690	17,706	3,895	15,179	844	31,176	1,816
2002	10,779	10,996	15,799	12,023	4,941	13,397	3,013	13,620	649	22,769	1,090
2003	10,609	10,957	3,178	13,358	4,804	3,644	2,932	14,789	632	19,990	918
2004	14,165	10,394	37,901	11,807	4,616	27,122	5,897	13,013	750	30,305	1,793
2005	21,112	9,807	19,266	10,745	4,411	13,198	4,846	13,771	898	29,740	2,887
2006	13,824	11,202	6,354	14,131	4,186	7,474	4,364	16,654	638	18,035	2,533
2007	19,703	9,401	45,499	8,088	5,116	30,364	4,009	10,499	1,002	40,262	1,671
2008	16,412	9,482	38,220	8,973	4,698	22,222	3,396	13,233	980	35,745	2,209
2009	15,896	10,419	8,207	12,351	4,715	5,615	4,464	14,571	772	24,514	1,652

Table 13. Annual water budget for the simulation period for the Washita River alluvial aquifer, western Oklahoma, 1980–2015.—Continued

[GHB, general-head boundary; ET, evapotranspiration]

Year	INFLOWS (acre-feet per day)					OUTFLOWS (acre-feet per day)					
	Storage	GHB	Recharge	Stream seepage	Lake seepage	Storage	Well withdrawals	ET	GHB	Stream seepage	Lake seepage
2010	11,157	11,011	12,224	13,127	4,941	8,924	4,803	14,222	642	22,716	1,152
2011	17,719	11,146	11,528	15,046	4,175	12,482	5,873	19,792	626	18,071	2,769
2012	20,096	11,028	2,828	15,511	3,529	7,143	7,177	17,810	680	17,226	2,957
2013	14,139	11,556	5,302	15,649	2,935	9,707	7,270	14,467	566	15,106	2,464
2014	13,839	11,666	3,142	15,427	2,485	7,121	7,167	15,417	551	14,018	2,284
2015	17,811	9,964	53,610	15,327	6,216	47,814	4,251	11,258	914	37,603	1,069
Average	17,706	10,034	24,854	11,576	4,606	17,527	4,327	14,533	906	29,374	2,107

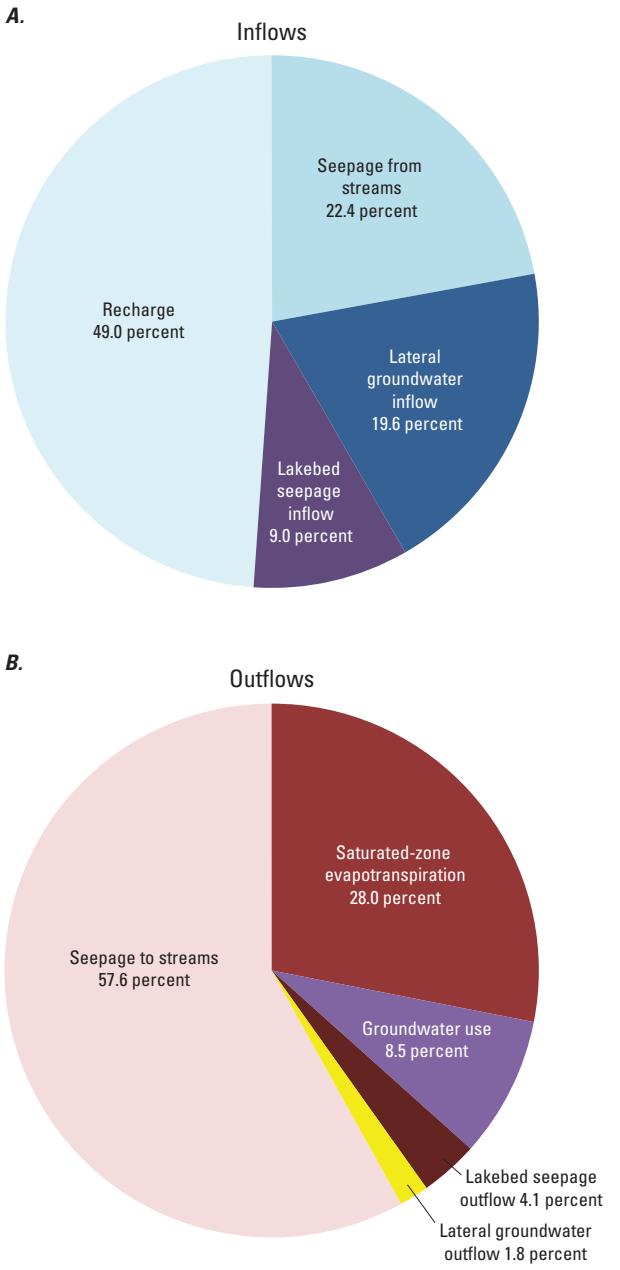

Figure 33. *A*, Inflows and *B*, outflows for the mean annual calibrated water budget for the numerical groundwater-flow model of the Washita River alluvial aquifer, western Oklahoma, 1980–2015.

these stability issues and extended run times during automated calibration, the following changes were made during calibration: (1) the ETg area—originally defined by using National Wetlands Inventory data (U.S. Fish and Wildlife Service, 2018)—was reduced to a narrower zone adjoining the simulated stream channel in the alluvium, and (2) an annual threshold of 95 in/yr was applied to the ETg rate.

Calibrated recharge was increased from the conceptual water budget by using recharge multipliers applied during the simulation period (Ellis and others, 2020) in approximately 40 percent of the monthly stress periods. Monthly mean calibrated recharge was greater than monthly mean precalibrated recharge for all months except July (fig. 36). With the exception of July, monthly mean calibrated recharge was 18–77 percent greater than the respective monthly mean precalibrated recharge. The increase in calibrated recharge was primarily used to match the stream base-flow observations at each streamgage. The increased recharge also improved the simulated water-table observation residuals in the terrace, which were typically less than the observed values.

Surface runoff and withdrawal inputs for Foss Reservoir were adjusted manually following the automated calibration. Because of the uncertainty inherent in estimating surface runoff to Foss Reservoir—particularly overland flows—surface runoff was varied between −30 and +30 percent in 329 of 432 transient stress periods. Foss Reservoir stage was generally underpredicted during summer months; thus, surface runoff was increased during these months. The required increase in surface runoff, particularly in May and June when precipitation was greatest (fig. 17*A*), indicates that this input was underestimated—or that ETg was overestimated—during the generation of inputs to the Lake package. Large reservoir releases during 5 of the 432 transient stress periods between 1997 and 2000 were reduced between 20 and 58 percent because of substantial declines in the simulated reservoir stage that occurred when the full release amount was simulated.

Sensitivity Analysis

Several analyses were performed to ensure that the parameters used were effective in reducing the objective function and to evaluate the correlation among parameters and identify parameters informed by the calibration process. During automated calibration, PEST++ computed the sensitivities of each parameter with respect to all observations by using 1-percent changes in parameters, which are contained in the Jacobian matrix used to record the response or sensitivity of each observation to an adjustment in a parameter. Doherty and Hunt (2010, p. 4) explain: “the Jacobian matrix consists of the sensitivities of all specified model outputs to all adjustable model parameters; each column of the Jacobian matrix contains the sensitivity of all model outputs for a single adjustable parameter. Individual parameters, or combinations of parameters, that are deemed to be estimable on the basis of the calibration dataset constitute the calibration solution space.” These sensitivities are a dimensionless measure of the change in residuals affected by adjustments to a parameter; thus, calibration-target residuals are more easily reduced by parameters with larger sensitivities. Sensitivities were calculated by using the Jacobian matrix output from PEST++ (Ellis and others, 2020) and summed for each parameter group (fig. 37).

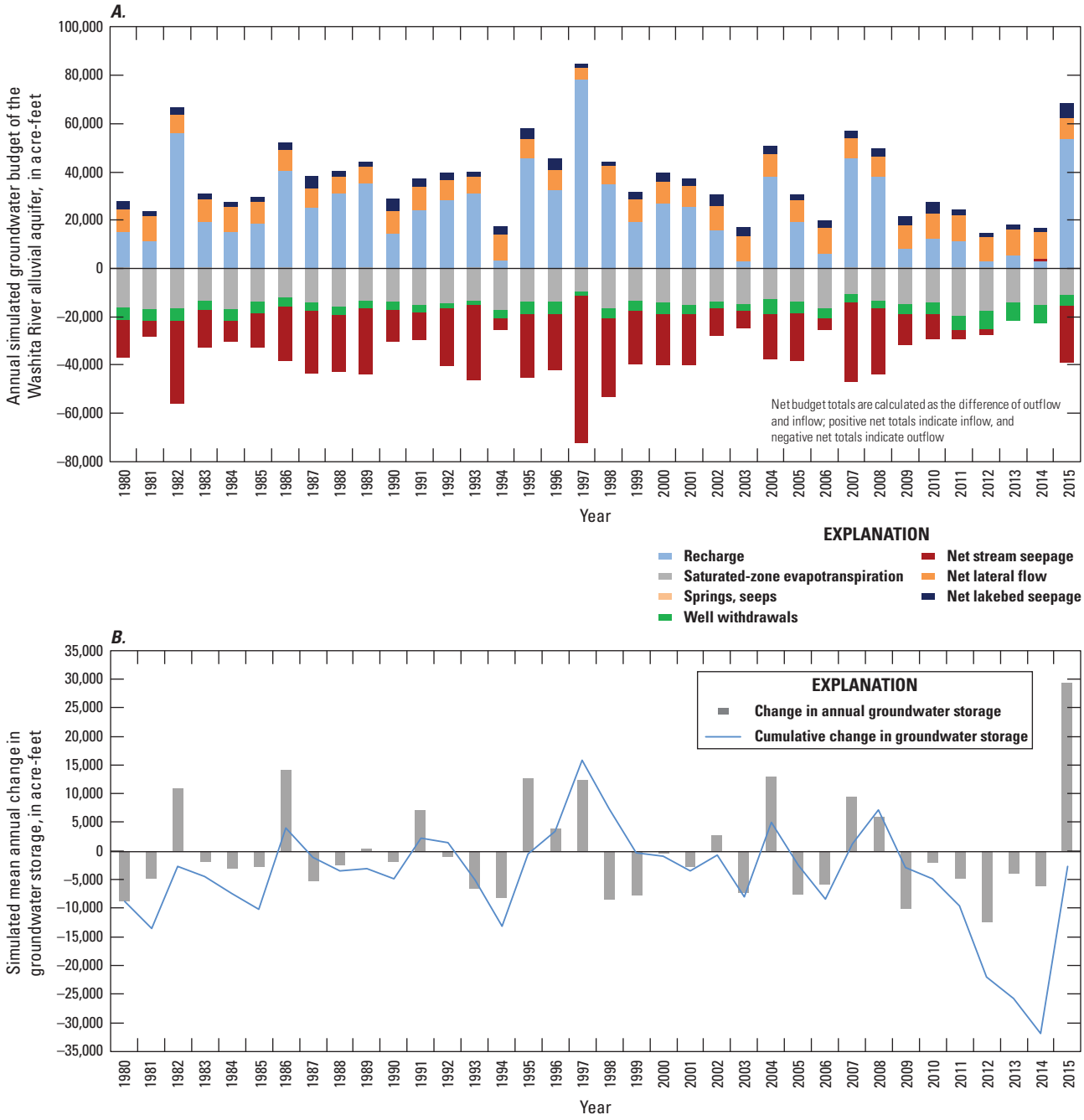

Figure 34. *A*, Mean annual simulated groundwater water budget and *B*, simulated mean annual change in groundwater storage for the numerical groundwater-flow model of the Washita River alluvial aquifer, western Oklahoma, 1980–2015.

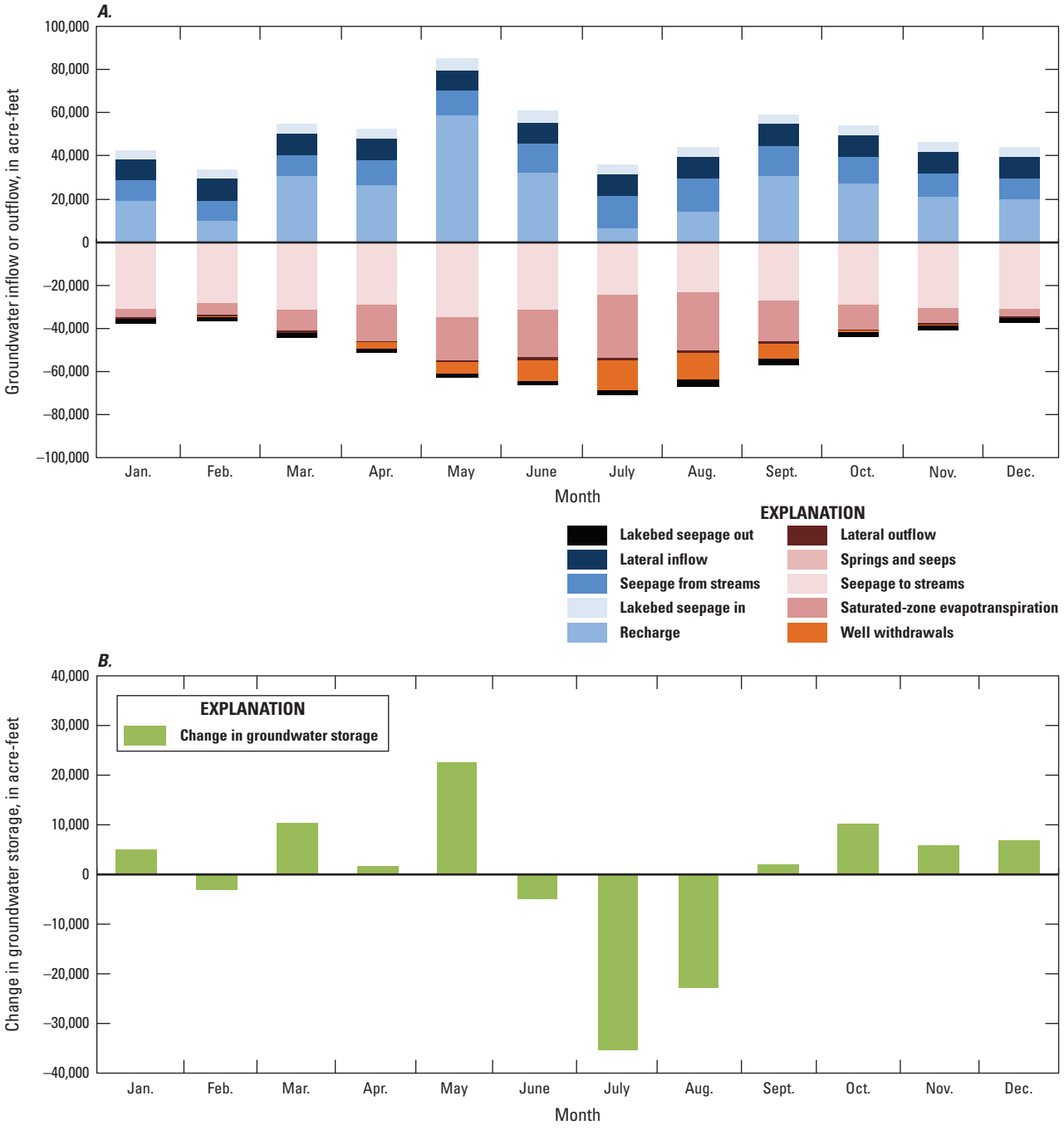

Figure 35. *A*, Mean monthly groundwater inflows and outflows and *B*, mean monthly change in groundwater storage for the Washita River alluvial aquifer, western Oklahoma, 1980–2015.

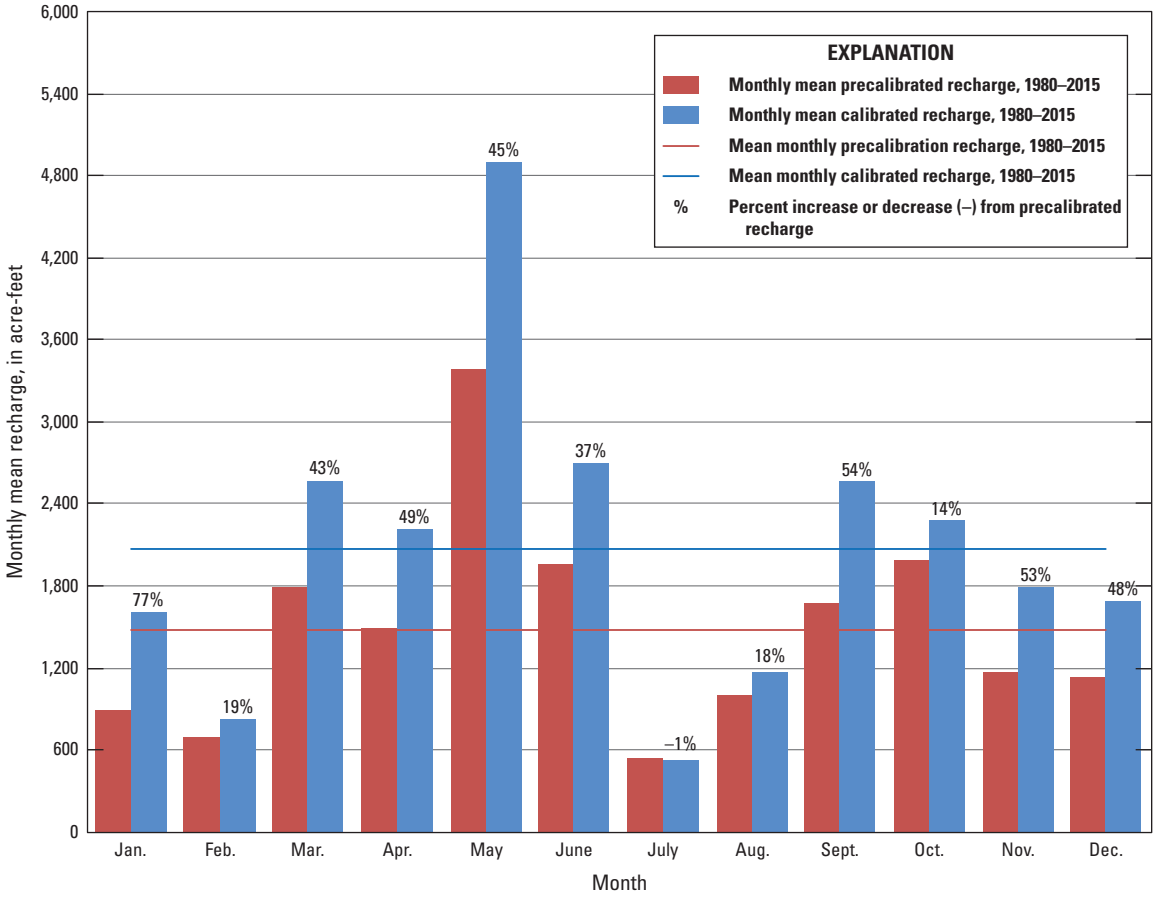

Figure 36. Monthly mean precalibration recharge and monthly mean calibrated recharge for the numerical groundwater-flow model of the Washita River alluvia aquifer, 1980–2015.

The observation groups were generally most sensitive to changes in recharge, ETg, and hydraulic conductivity (fig. 37). Recharge was the largest aquifer inflow (table 12), which—along with the pilot points used to adjust hydraulic conductivity and specific yield—affected the groundwater levels, base flows, stream seepage, and reservoir stage throughout the model. Estimated base-flow observations (1,684) were more numerous than the groundwater-level observations (168) (table 7). Therefore, changes in ETg applied to the alluvium had a lesser effect than recharge on groundwater-level observations because most of the observations are distant from Evapotranspiration package cells compared to base-flow observations at the four model-area streamgages. For matching the Foss Reservoir stage observations, the model was less sensitive to changes in ETg than to changes in recharge because stream inflows contributed a large percentage of inflow to this reservoir. The GHB cells in the model were only located downgradient from Foss Reservoir (fig. 22); therefore, the sensitivity of most observation groups to changes in the GHB conductance values was reduced. The reservoir-stage observation group typically had the greatest sensitivity of the four observation groups; this observation group was most sensitive to the lake parameter group but also to recharge and least sensitive to GHB conductance (fig. 37).

Groundwater-Availability Scenarios

Three types of scenarios were formulated for the calibrated groundwater model. These scenarios were used to (1) estimate the EPS pumping rate that retains a saturated thickness that meets the minimum 20-year life of the aquifer, (2) quantify the effects of projected groundwater-use rates on groundwater storage over a 50-year period, and (3) evaluate the effects of projected pumping rates extended 50 years into the future and sustained hypothetical drought conditions over a 10-year period on base flow and groundwater in storage. Additionally, an uncertainty analysis was performed for the EPS scenario.

Equal-Proportionate Share

The EPS for the Washita River alluvial aquifer was defined as the pumping rate at which fresh groundwater can be withdrawn so that, after a minimum of 20 years of continuous EPS withdrawals, 50 percent of the aquifer retains a saturated thickness of at least 5 ft. To compute the EPS for the Washita River alluvial aquifer, a similar approach to that of the model calibration was implemented. Whereas automated calibration

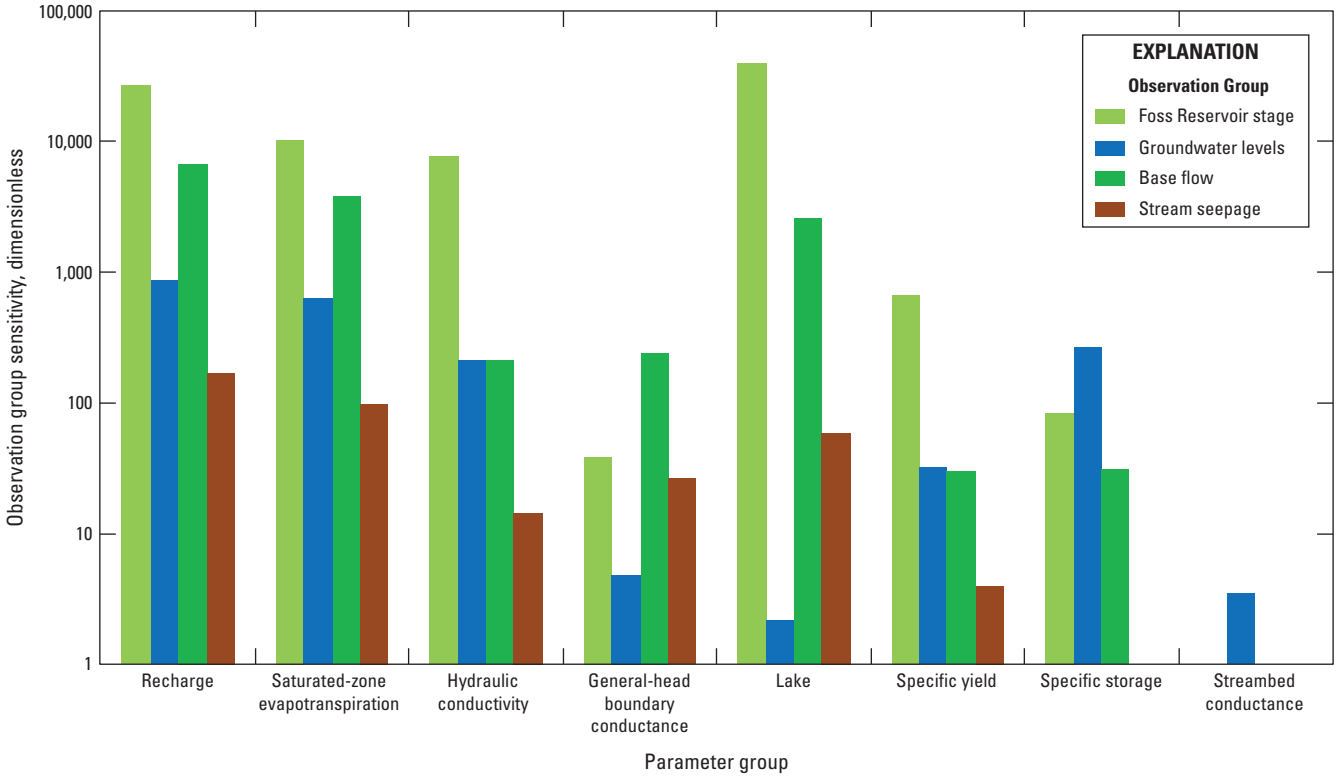

Figure 37. Observation group sensitivity by parameter group in the numerical groundwater-flow model of the Washita River alluvial aquifer, western Oklahoma.

of the Washita River alluvial aquifer model involved the adjustment of many model parameters based on available calibration targets, the determination of the EPS was based only on a uniform pumping rate parameter and an aquifer saturated thickness calibration target (5 ft). The EPS pumping rate parameter was composed of a hypothetical well placed in each active cell in layer 1. During each iteration of the calibration process, the pumping rate parameter was adjusted until the objective function was zero—when 50 percent of the basin retained a saturated thickness of 5 ft. The EPS was computed for time periods of 20, 40, and 50 years into the future. The 20-year time period was chosen by the OWRB to align with the MAY ensuring a minimum 20-year life of the groundwater basin. The OWRB also requested analyses for additional time periods of 40 and 50 years.

Annual stress periods with calibrated model mean stresses were used in the EPS scenarios instead of monthly stress periods to (1) shorten transient simulation run times, (2) minimize the iterative variability in the EPS pumping rate caused by monthly or seasonal stresses, and (3) improve model stability. The 2015 simulated water table from the calibrated groundwater model was used as the starting water table in each EPS scenario. The calibrated model mean annual recharge is referred to as "normal recharge." To account for potential climate variability, the EPS scenarios were run with recharge alternatively increased and decreased by 10 percent.

The 20-, 40-, and 50-year EPS pumping rates under normal recharge conditions were 1.7, 1.6, and 1.6 (acre-ft/acre)/yr, respectively (table 14). Given the aquifer area used for modeling purposes (84,366 acres), these rates correspond

Table 14. Equal-proportionate-share (EPS) pumping rates for the Washita River alluvial aquifer, western Oklahoma, 1980–2015.

Period (number of years)	EPS pumping rate (acre-feet per acre per year)		
	Normal recharge[1]	Recharge reduced by 10 percent	Recharge increased by 10 percent
20	1.7	1.6	1.8
40	1.6	1.5	1.7
50	1.6	1.5	1.7

[1]The calibrated model mean annual recharge is referred to as "normal recharge."

to annual yields of about 143,423, 134,986, and 134,986 acre-ft/yr, respectively. Increasing and decreasing recharge by 10 percent resulted in 20-year EPS pumping rates of 1.8 (5.9-percent increase) and 1.6 (acre-ft/acre)/yr (5.9-percent decrease), respectively. Increasing and decreasing recharge by 10 percent resulted in 40-year EPS pumping rates of 1.7 (6.2-percent increase) and 1.5 (acre-ft/acre)/yr (6.3-percent decrease), respectively. Increasing and decreasing recharge by 10 percent resulted in 50-year EPS pumping rates of 1.7 (6.2-percent increase) and 1.5 (acre-ft/acre)/yr (6.3-percent decrease), respectively.

At the end of the 20-year EPS scenario, saturated thickness (figs. 11 and 12) remained unchanged primarily in the eastern parts of the aquifer and along the thickest areas of the active alluvium near the center of the stream channel (fig. 38). Most of the terrace material upland from the alluvial deposits was unsaturated except for areas where a shallow hydraulic gradient occurred. Streamflow in the Washita River upstream from Foss Reservoir was sustained mostly from the inflows from the Washita River in Texas. As a result, the Washita River alluvial aquifer deposits upgradient from Croton Creek remained saturated, whereas most other alluvial deposits between this location and Foss Reservoir generally had minimal or no saturation at the end of the EPS scenarios (fig. 38). Downgradient from Foss Reservoir, saturated thickness was sustained by lateral inflow from the Rush Springs aquifer simulated by the general-head boundary cells (fig. 22) and by releases from Foss Reservoir. Saturated thickness greater than 5 ft also remained along Turkey, Barnitz, Beaver, and Turtle Creeks, which was sustained by simulated SFR2 inflows.

In the 20- and 40-year EPS scenarios, substantial percentages of groundwater storage were removed by the simulated wells in each model cell (fig. 39). Annual EPS groundwater pumping decreased as the thinner areas of the aquifer, including most of the alluvium and terrace, were dewatered and saturated thickness dropped below 5 ft, or the areas went dry (figs. 38 and 39). Annual groundwater storage changes decreased as annual EPS groundwater pumping decreased, but groundwater storage changes were more moderate during the last 3 years of each scenario (fig. 39).

Groundwater storage at the end of the 20-year EPS scenario was about 281,000 acre-ft, or about 306,000 acre-ft (52 percent) less than the starting storage (fig. 39). Considering the 84,366-acre area used for modeling purposes and using a specific yield of 0.12, this decrease in storage was equivalent to a mean groundwater-level decline of about 30 ft. This groundwater-level decline was greater than the aquifer thickness in some areas of the model where the aquifer was dewatered (fig. 38).

At the end of the 20-year EPS scenario, base flow had decreased to 0 ft^3/s at the Cheyenne and Hammon streamgages (fig. 38). Downstream from Foss Reservoir, base flow was sustained at the Clinton streamgage as a result of SFR2 inflows from Foss Reservoir releases and GHB inflows from the Rush Springs. The groundwater-level altitude in the aquifer was below the altitude of the streambed during most of the EPS scenarios, thus promoting seepage from streams to the aquifer. Except for streams receiving base-flow inflows from outside the active model area and except for the Washita River downstream from Foss Reservoir, the majority of streams in the study area were dry at the end of the 20-year EPS scenario (fig. 38).

Foss Reservoir stage was below the dead-pool stage of 1,597 ft after about 7 years of pumping in the 20-year EPS scenario (fig. 40). The loss of any remaining usable water in the reservoir in this scenario was caused by (1) the cessation of stream inflows from the Washita River—which constituted about one-fourth of inflows to Foss Reservoir (fig. 32)—after the first year, and (2) the decline of groundwater levels around the reservoir compared to the calibrated model (fig. 38), resulting in large lakebed seepage outflows to the aquifer. Surface-water inflows composed a larger percentage of the total reservoir inflow than lakebed seepage; thus, the precipitous decline in reservoir stage in the first 7 years is largely the result of the cessation of flow from the Washita River. Precipitation and evaporation also decreased as cells representing Foss Reservoir became dry, but these decreases tended to offset each other.

Projected (50-Year) Groundwater Use

Projected 50-year groundwater-use scenarios were used to simulate the effects of selected well withdrawal rates on groundwater storage in the Washita River alluvial aquifer. The effects of well withdrawals were evaluated by comparing changes in groundwater storage among four 50-year scenarios using (1) no groundwater use, (2) groundwater use at the 2015 pumping rate, (3) mean groundwater use for the simulation period, and (4) increasing groundwater use.

The increasing-use scenario assumed a 38-percent increase in pumping over 50 years based on 2010–60 demand projections for west-central Oklahoma (West Central Region, OWRB, 2012b). Model stresses were configured as the mean of stresses in each month from the calibrated model, and the scenarios assumed that future climate conditions were similar to those of the 1980–2015 simulation period. The projected storage calculation uses the same method as the EPS scenarios, whereby the model specific yield is multiplied by the saturated thickness in each active model cell.

Groundwater storage after 50 years with no groundwater use was 545,249 acre-ft, or 693 acre-ft (0.1 percent) greater than the initial groundwater storage; this groundwater storage increase is equivalent to a mean groundwater-level increase of 0.1 ft (table 15). Groundwater storage at the end of the 50-year period with the 2015 groundwater-pumping rate applied was 543,831 acre-ft, or 723 acre-ft (0.1 percent) less than the initial storage; this groundwater storage decrease is equivalent to a mean groundwater-level decrease of 0.1 ft. Groundwater storage after 50 years with the mean pumping rate for the study period was 543,202 acre-ft, or 1,349 acre-ft (0.2 percent) less than the initial groundwater storage; this groundwater storage

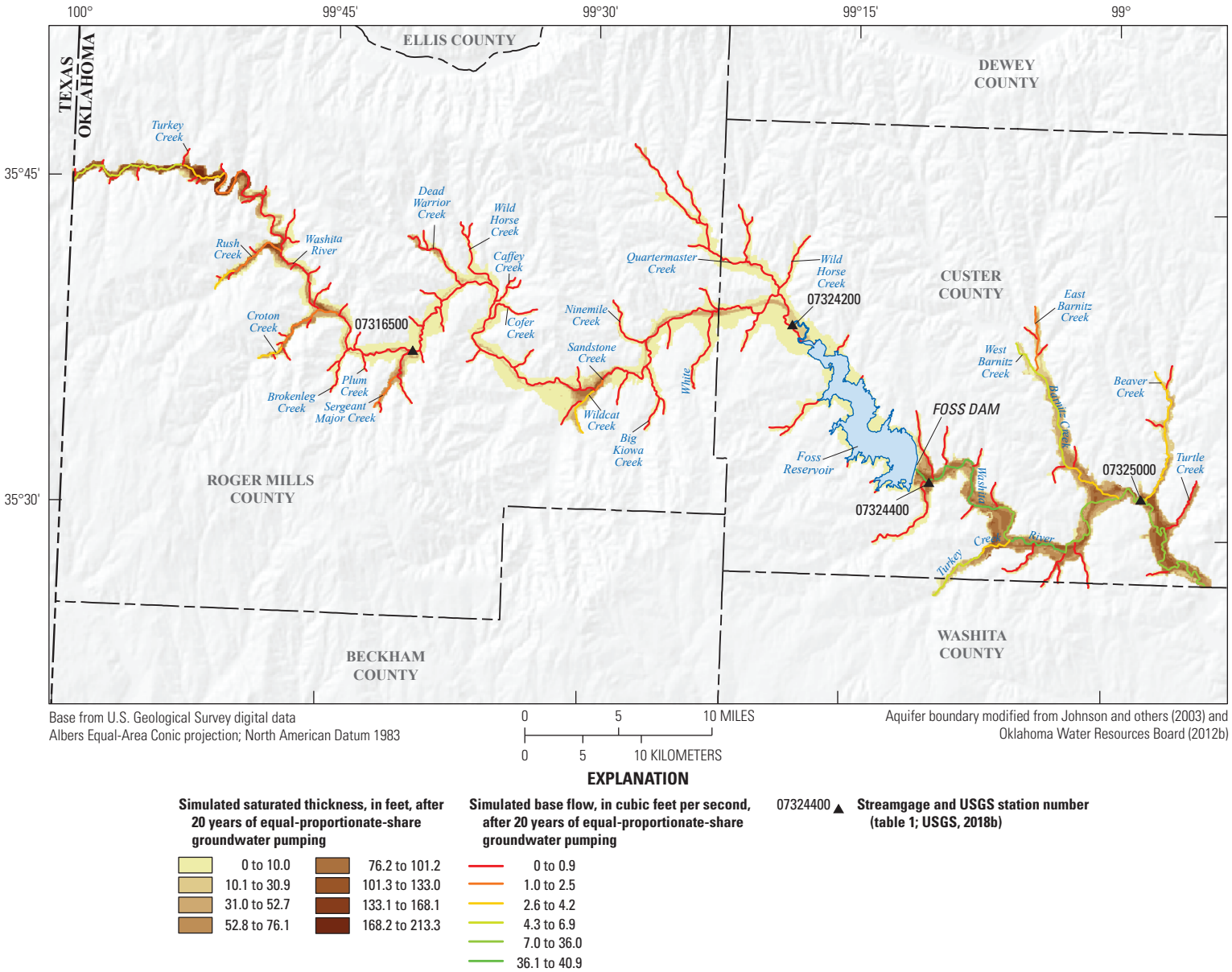

Figure 38. Simulated saturated thickness and simulated base flow after 20 years of continuous equal-proportionate-share groundwater pumping in the Washita River alluvial aquifer, western Oklahoma, 1980–2015.

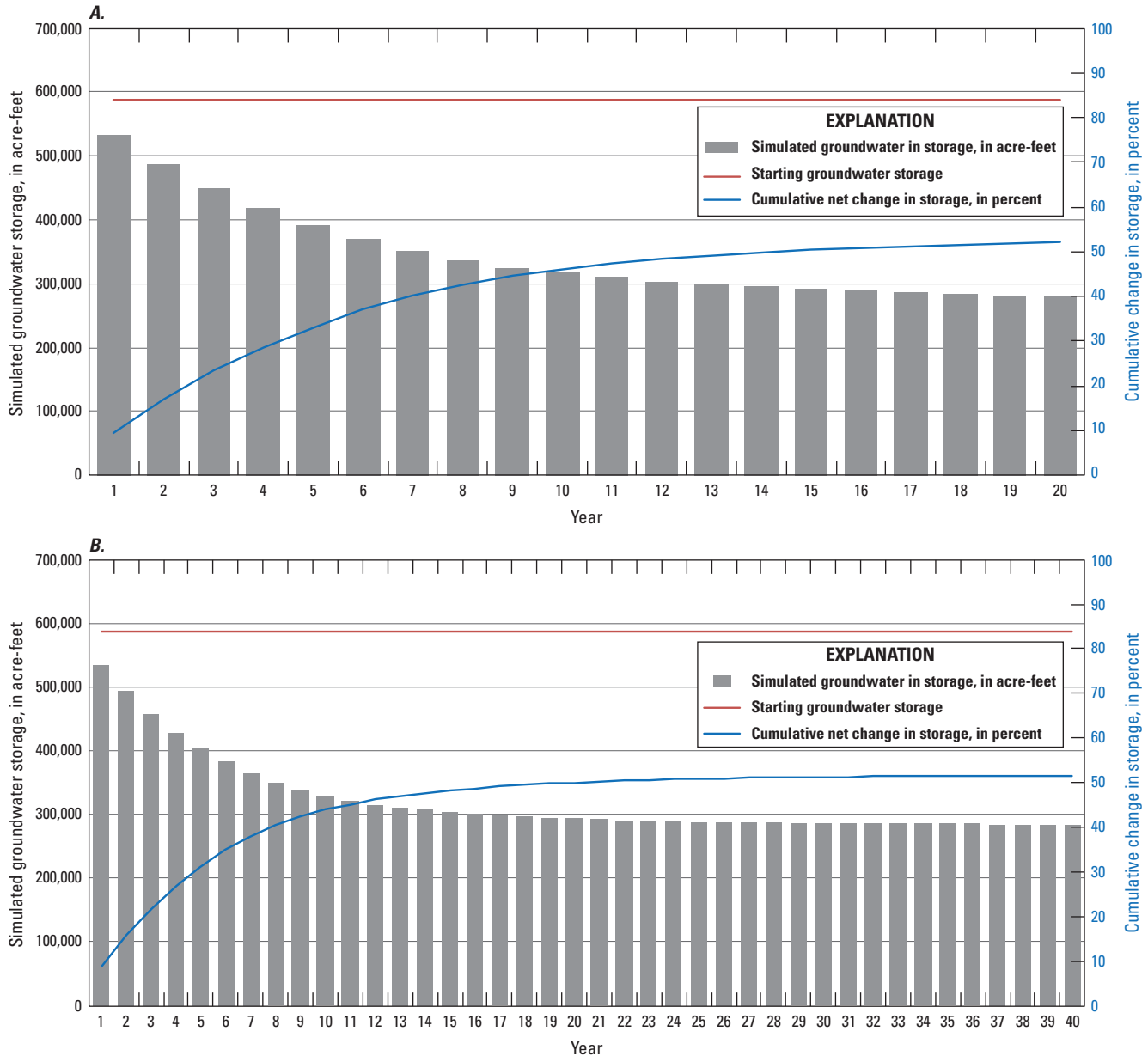

Figure 39. Changes in simulated groundwater storage during *A*, 20, and *B*, 40 years of continuous equal-proportionate-share groundwater pumping in the Washita River alluvial aquifer, western Oklahoma, 1980–2015.

decrease is equivalent to a mean groundwater-level decrease of 0.1 ft. Groundwater storage at the end of the 50-year period with an increasing demand pumping rate was 542,584 acre-ft, or 1,967 acre-ft (0.4 percent) less than the initial storage; this groundwater storage decrease is equivalent to a mean groundwater-level decrease of 0.2 ft.

Mean annual base flow simulated at the Cheyenne streamgage decreased 0.49 ft^3/s (2.4 percent) after 50 years with no pumping and decreased 1.7 ft^3/s (9.4 percent) after 50 years of an increasing demand groundwater-pumping rate (table 16). Mean annual base flow simulated at the Hammon streamgage decreased 0.2 ft^3/s (0.6 percent) after 50 years with no pumping and decreased 3.6 ft^3/s (12.9 percent) after 50 years of an increasing demand groundwater-pumping rate. Mean annual base flow simulated at the Clinton streamgage decreased 0.3 ft^3/s (0.5 percent) after 50 years with no pumping and decreased 0.6 ft^3/s (0.9 percent) after 50 years of an increasing demand groundwater-pumping rate (table 16). Decreasing base flow and decreasing groundwater storage during these projected groundwater use scenarios indicate that pumping across the aquifer depletes streamflow before groundwater levels and storage are appreciably affected by this pumping.

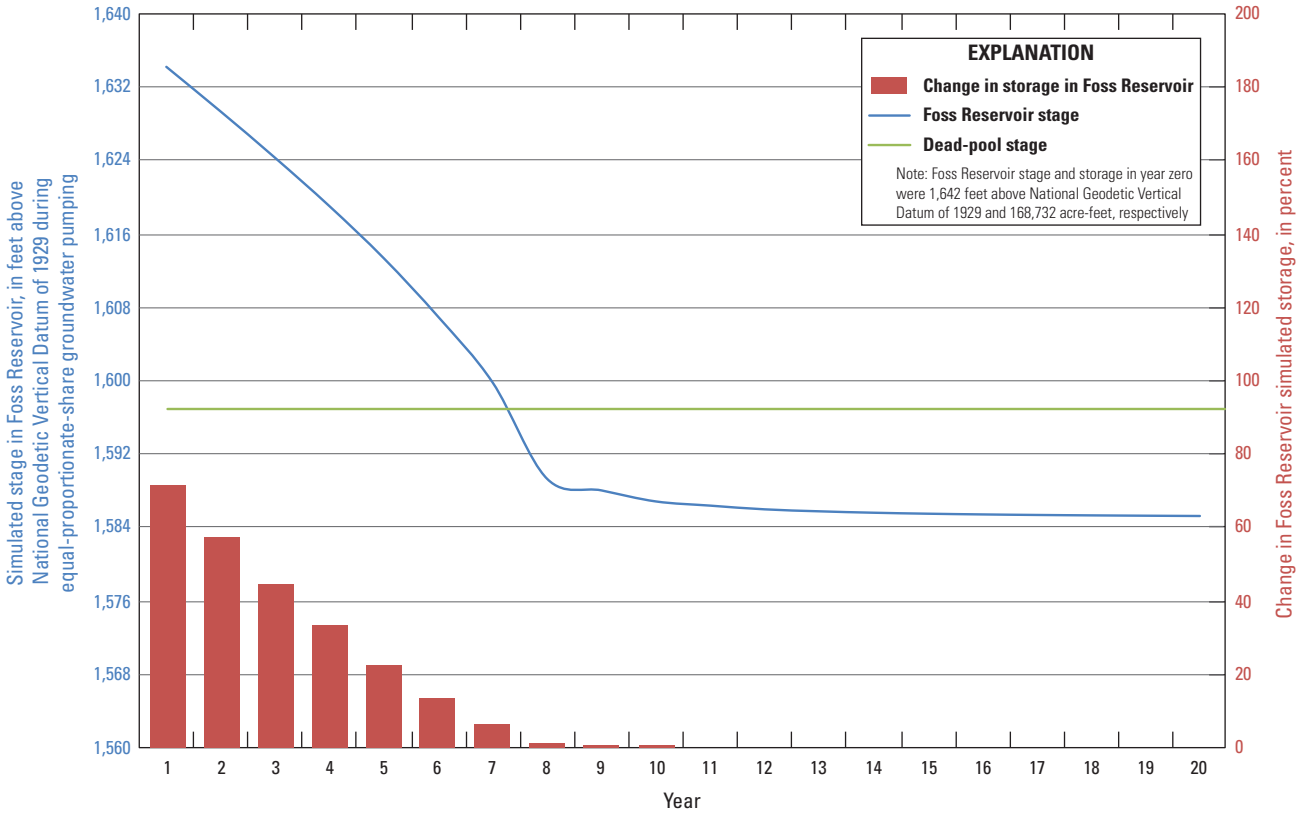

Figure 40. Simulated stage and change in simulated storage in Foss Reservoir during 20 years of continuous equal-proportionate-share groundwater pumping in the Washita River alluvial aquifer, western Oklahoma.

Table 15. Changes in groundwater storage after 50 years of groundwater use at different pumping rates for the Washita River alluvial aquifer, western Oklahoma.

50-year groundwater-use scenario	Groundwater storage at beginning of scenario, in acre-feet	Groundwater storage for last year of scenario, in acre-feet	Change in groundwater storage, in acre-feet	Change in groundwater storage, in percent	Mean change in groundwater levels, in feet
No groundwater use	544,556	545,249	693	0.1	0.1
2015 groundwater-pumping rate	544,554	543,831	−723	−0.1	−0.1
Mean groundwater-pumping rate, 1980–2015	544,551	543,202	−1,349	−0.2	−0.1
Increasing demand groundwater-pumping rate (38-percent increase compared to 2015)	544,551	542,584	−1,967	−0.4	−0.2

Table 16. Changes in simulated mean annual base flow after 50 years of groundwater use at different pumping rates for the Washita River alluvial aquifer, western Oklahoma.

[ft^3/s, cubic foot per second; See table 1 and figure 1 for streamgage information and location]

50-year groundwater-use scenario	Mean base flow for first year of scenario (ft^3/s)	Mean base flow for last year of scenario (ft^3/s)	Change in base flow (ft^3/s)	Change in base flow (percent)
Mean annual base flow at the Cheyenne streamgage (07316500)				
No groundwater use	20.2	19.8	0.49	−2.4
2015 groundwater-pumping rate	19.1	18.5	0.69	−3.6
Mean groundwater-pumping rate, 1979–2015	18.5	17.6	0.9	−4.9
Increasing demand groundwater-pumping rate (38-percent increase compared to 2015)	18.5	16.8	1.7	−9.4
Mean annual base flow at the Hammon streamgage (07324200)				
No groundwater use	32.5	32.3	0.2	−0.6
2015 groundwater-pumping rate	28.5	27.3	1.1	−4.0
Mean groundwater-pumping rate, 1979–2015	28.2	26.6	1.6	−5.6
Increasing demand groundwater-pumping rate (38-percent increase compared to 2015)	28.2	24.5	3.6	−12.9
Mean annual base flow at the Clinton streamgage (07325000)				
No groundwater use	65.3	65.0	0.3	−0.5
2015 groundwater-pumping rate	65.2	64.8	0.4	−0.6
Mean groundwater-pumping rate, 1979–2015	64.9	64.5	0.4	−0.6
Increasing demand groundwater-pumping rate (38-percent increase compared to 2015)	64.9	64.4	0.6	−0.9

Hypothetical (10-Year) Drought

A hypothetical (10-year) drought scenario was used to simulate the effects of a prolonged period of reduced recharge on groundwater storage in the Washita River alluvial aquifer and Foss Reservoir stage and storage. January 1983 to December 1992 was chosen as the drought period because mean annual base flows and recharge for that period were similar to those of the simulation period. Drought effects were quantified by comparing the results of the drought scenario to the calibrated model (no drought). To simulate the hypothetical drought, recharge in the calibrated model was reduced by 50 percent during the simulated drought period. Upstream inflows to the Washita River and associated tributaries were reduced by 37 percent, which was the mean decrease in annual base flow during the drought from 1976 to 1981 (Shivers and Andrews, 2013). The simulation was continued 15 years past the end of the drought period through 2007 to assess the recovery of groundwater storage in the Washita River alluvial aquifer.

The rates of precipitation, evaporation, and surface runoff to Foss Reservoir were unchanged from the calibrated groundwater model. Observed reservoir releases for each month prior to and during the drought period were included in the simulation. To assess the recovery of Foss Reservoir stage following the drought period, reservoir releases were suspended until the stage reached the top of the active conservation pool (1,642 ft). Once this stage was reached, reservoir releases were again included in the simulation.

Groundwater storage at the end of the drought period in December 1992 was about 562,000 acre-ft, or about 36,000 acre-ft (6 percent) less than the groundwater storage of the calibrated groundwater model (about 598,000 acre-ft) (fig. 41). Based on the 84,366-acre area used for modeling purposes and specific yield of 0.12, this change in groundwater storage was equivalent to a mean groundwater-level decline of 3.6 ft. By comparison, the drought conditions of 2009–14 resulted in a mean simulated groundwater-level decline of 5.6 ft between January 2009 and December 2014, which can be seen in the mean annual change in groundwater

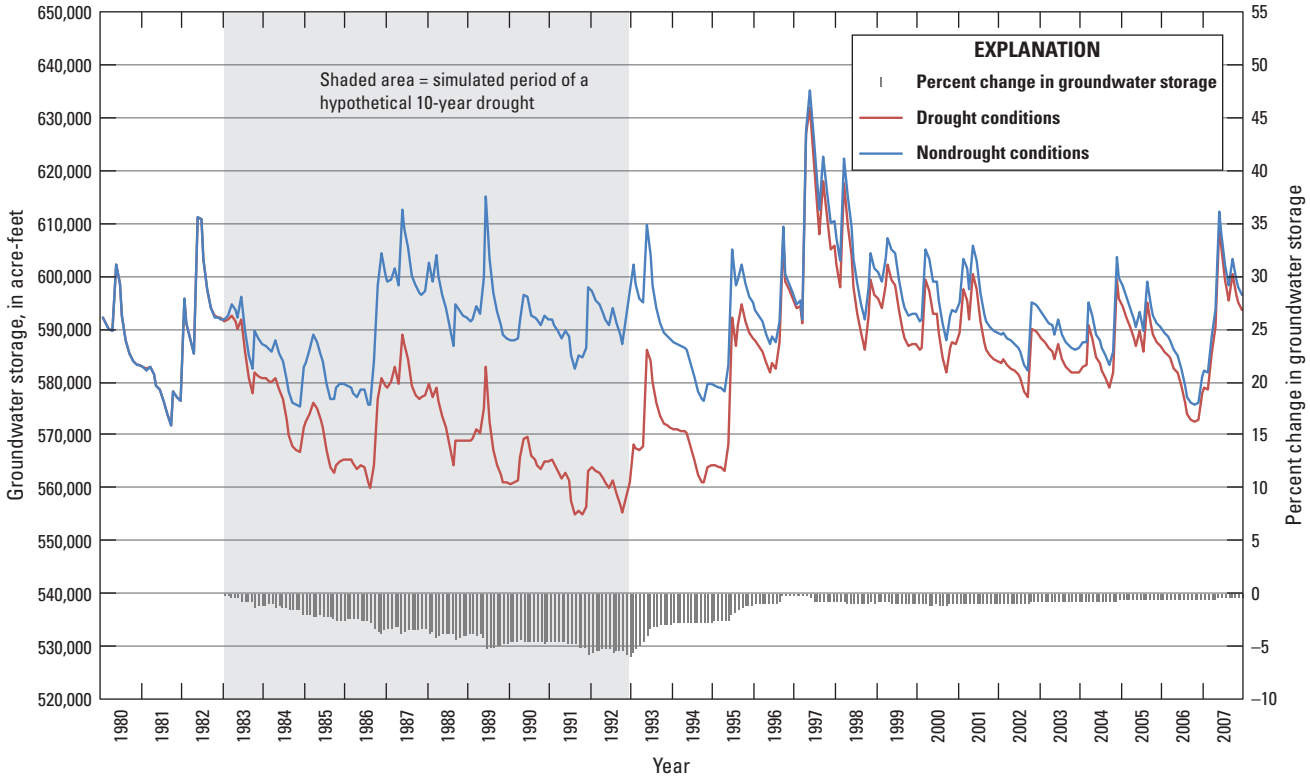

Figure 41. Change in groundwater storage resulting from a hypothetical 10-year drought for the Washita River alluvial aquifer, western Oklahoma.

storage in figure 34*B*. Mean annual recharge during the hypothetical drought (1.3 in/yr) was greater than the mean annual recharge during the 2009–14 drought (0.7 in/yr) (fig. 34*A*).

At the end of the hypothetical drought, the largest changes in saturated thickness (as great as 43.5 ft) were in the area upgradient from Foss Reservoir, particularly in the terrace at the model boundary (fig. 42). Groundwater storage in the upgradient terrace was supplied entirely by recharge, so decreases in recharge have substantial effects on groundwater-level altitudes in the terrace areas. The decreased saturated thickness in some areas of the terrace caused a reduction in simulated well withdrawals as compared to the calibrated groundwater model. The saturated thickness of areas near the streams and associated tributaries changed little during the hypothetical drought; however, simulated base flows decreased at the Cheyenne, Hammon, and Clinton streamgages (fig. 43). Downgradient from Foss Reservoir, groundwater storage declines were moderated by GHB inflow from the Rush Springs aquifer and were typically less than 5 ft (fig. 42).

After 12 months of the hypothetical drought, simulated base flows at the Cheyenne, Hammon, and Clinton streamgages had decreased by about 45, 57, and 21 percent, respectively (fig. 43). At the end of the 10-year hypothetical drought period, simulated base flows at the Cheyenne, Hammon, and Clinton streamgages had decreased by about 55, 73, and 42 percent, respectively. Simulated low-flow conditions in some months may be overpredicted during the drought scenario because periods of nearly zero flow periodically occur in the simulation period that could not be reproduced in the calibrated groundwater model.

Substantial decreases in the Foss Reservoir stage began during the fall of 1985 (fig. 44*A*) in conjunction with base-flow decreases of up to 100 percent at the Hammon streamgage (fig. 43*B*). These lake-stage declines outpaced groundwater-level declines in the surrounding aquifer. Annual lakebed seepage for Foss Reservoir was similar for the first 5 years of the hypothetical drought compared to the nondrought conditions. The minimum stage in Foss Reservoir was 1,623 ft in March 1990 (fig. 44*A*), near the end of the hypothetical drought period, indicating a storage capacity of 42 percent of active conservation pool storage. The minimum Foss Reservoir storage simulated during the drought period was 77,954 acre-ft, which was a decrease of 46 percent from the nondrought storage. Large precipitation events totaling 11 in. during April and May 1993 (fig. 5) resulted in a stage recovery to 1,632 ft at Foss Reservoir by June 1993 (Bureau of Reclamation, 2018). Stage recovery to the top of the conservation pool did not occur until August 1996.

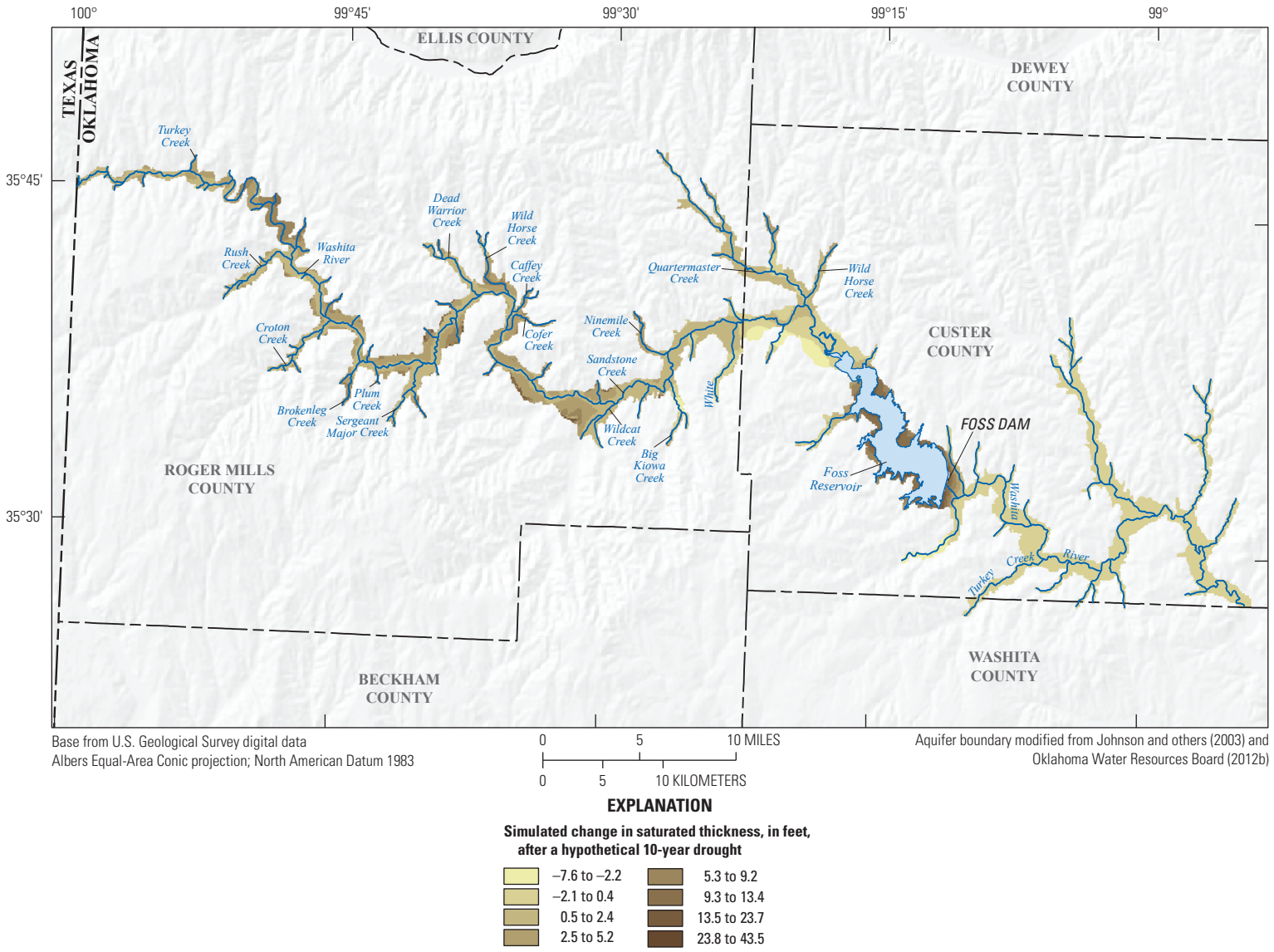

Figure 42. Simulated change in saturated thickness after a hypothetical 10-year drought for the Washita River alluvial aquifer, western Oklahoma.

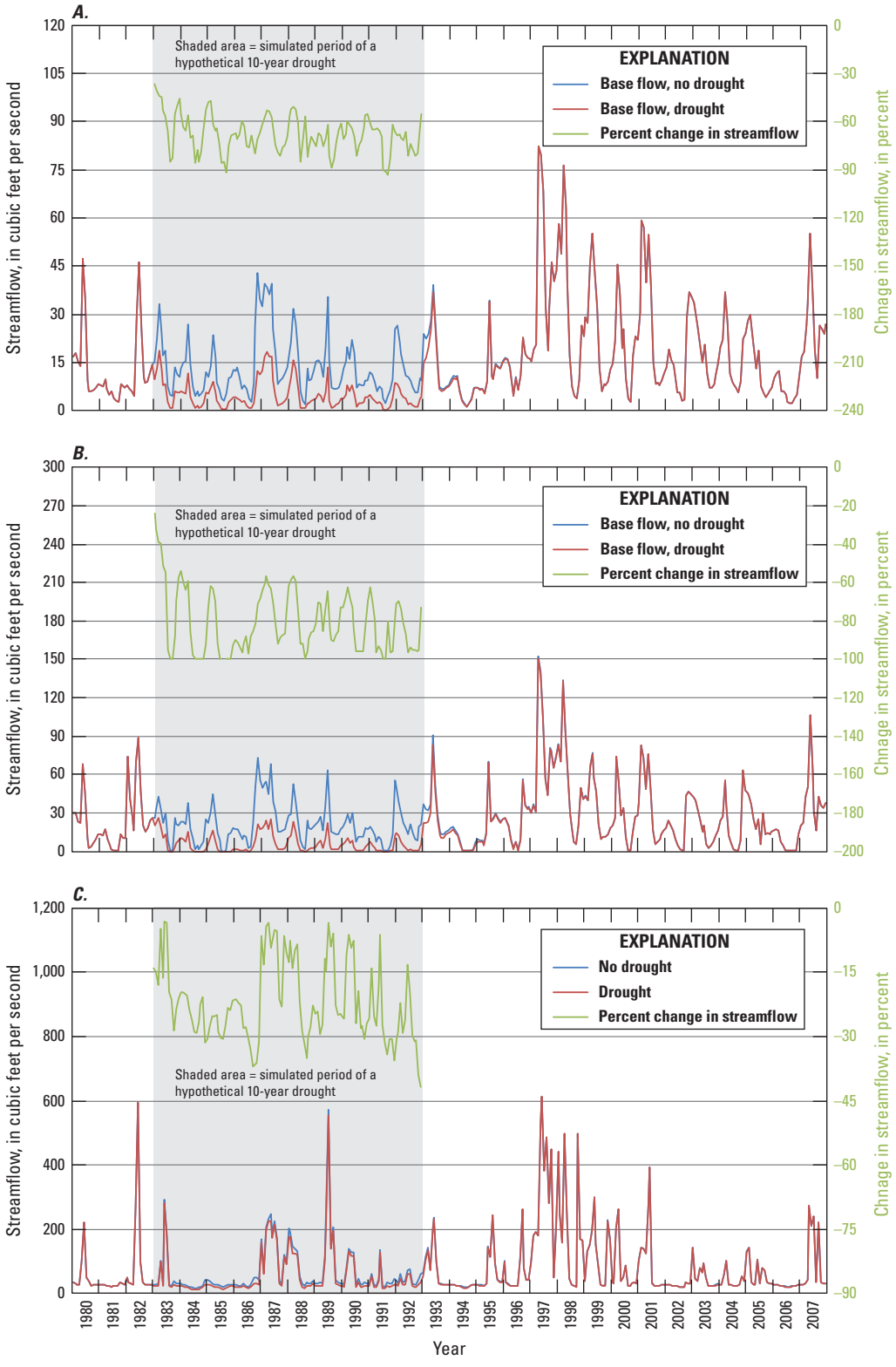

Figure 43. Changes in simulated streamflow and base flow for the numerical groundwater-flow model of the Washita River alluvial aquifer at U.S. Geological Survey streamgages *A*, 07316500 Washita River near Cheyenne, Okla.; *B*, 07324200 Washita River near Hammon Okla.; and *C*, 07325000 Washita River near Clinton, Okla., western Oklahoma, 1980–2007.

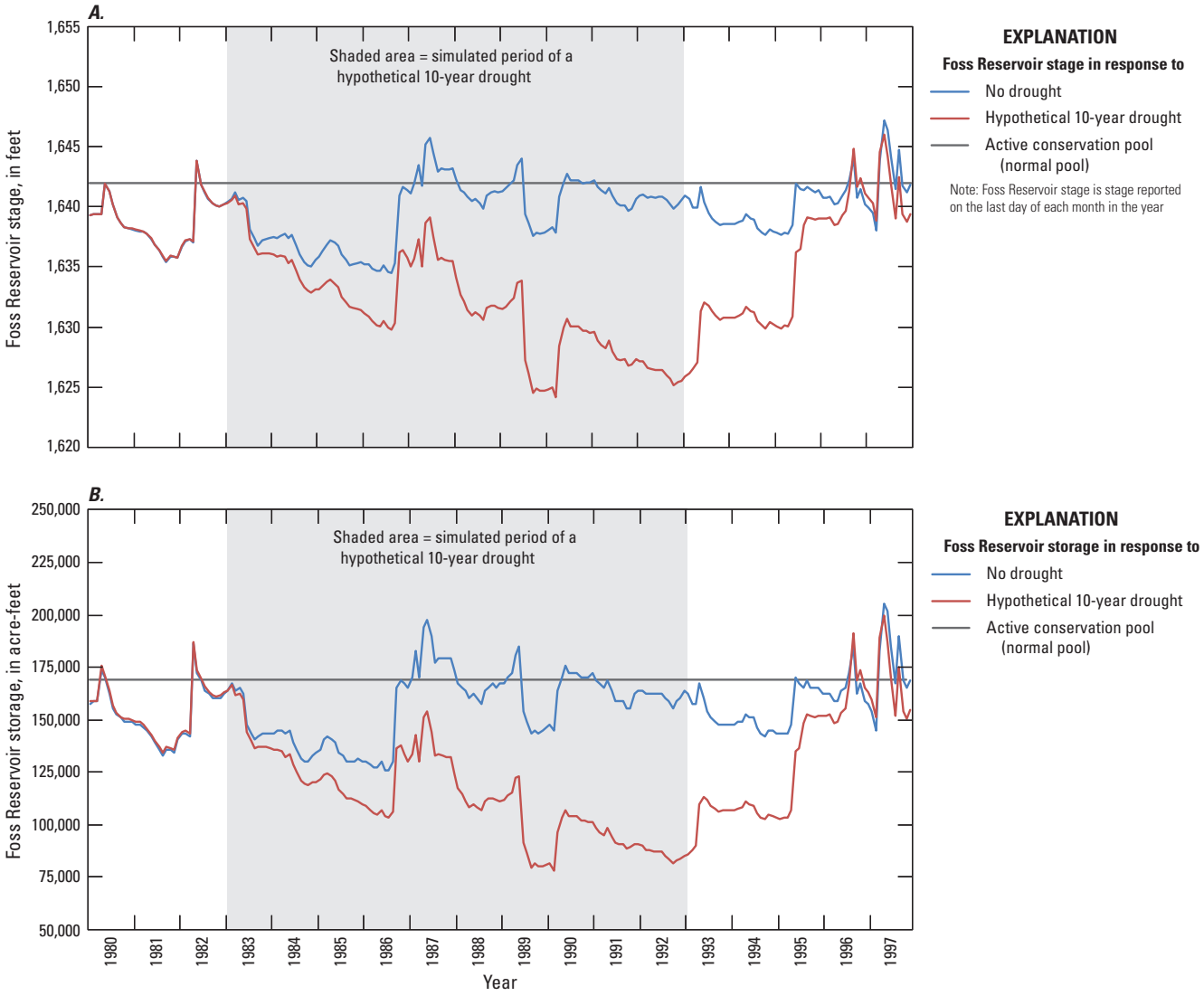

Figure 44. Changes in *A*, stage and *B*, storage for Foss Reservoir in response to a hypothetical 10-year drought for the Washita River alluvial aquifer, 1980–2007.

Model Limitations

The Washita River alluvial aquifer groundwater model is a simplification of a complex groundwater-flow system and, therefore, incorporates necessary limitations and assumptions. The model contains features such as the Streamflow-Routing package, the Lake package, and a grid size that may represent localized features, but the model is best used to support groundwater management decisions at a regional to sub-regional scale. The 36-year simulation period included hydrologic and climatic variability; however, results from the groundwater model may not be accurately representative of the variability found in past hydrologic conditions or representative of future climatic variability.

An uneven spatial and temporal distribution of water-table-altitude observations caused data gaps in the calibration data. Although the simulated water table in areas with a small number of observations occurs in a likely water-table-altitude range, more site-specific and local calibration-target data could facilitate a more detailed characterization of water-table conditions. Additionally, GHB inflows from the Rush Springs aquifer were based on the simulated water table of the Rush Springs aquifer (Ellis, 2018), and these inflows could be in error because relatively few groundwater-level observations were available for the Rush Springs aquifer adjacent to the Washita River alluvial aquifer.

The stream network used in the numerical model is a simplification of the actual stream geometry and hydraulic properties. Refined measurement of the stream channel width and streambed conductance at the local scale might improve the numerical model calibration because these factors control the amount of streambed seepage exchange with the aquifer. The numerical model was calibrated primarily to base-flow estimates; therefore, collection of more streamflow and base-flow data during other hydrologic conditions also could further reduce uncertainty in local-scale simulation results.

Exact amounts of annual groundwater use are unknown because groundwater wells are not metered, and groundwater-use data are based on estimates submitted to the OWRB by permit holders. Additionally, groundwater use by domestic wells, although assumed to be relatively small, was not included in the numerical model.

Summary

The Washita River alluvial aquifer is a saturated sand and gravel alluvial deposit along the valley of the Washita River in western Oklahoma that provides a productive source of groundwater for agricultural irrigation and water supply and is subdivided into reaches for appropriation. The Oklahoma Water Resources Board (OWRB) issued an order on November 13, 1990, that established the maximum annual yield (MAY; 120,320 acre-feet per year [acre-ft/yr]) and equal-proportionate-share (EPS) pumping rate (2.0 acre-feet per acre per year) for reach 1 of the Washita River alluvial aquifer. The MAY and EPS were based on hydrologic investigations that evaluated the effects of potential groundwater withdrawals on groundwater availability in the Washita River alluvial aquifer. Every 20 years, the OWRB is statutorily required to update the hydrologic investigation on which the MAY and EPS were based. Because 30 years have elapsed since the last order was issued, the U.S. Geological Survey (USGS), in cooperation with the OWRB, conducted an updated hydrologic investigation and evaluated the effects of potential groundwater withdrawals on groundwater flow and availability in the Washita River alluvial aquifer.

The Washita River alluvial aquifer is a long, narrow surficial aquifer that underlies the Washita River valley in Oklahoma from the western border with Texas southeast to near Lake Texoma, covering approximately 110 square miles (71,000 acres). The OWRB has designated the westernmost section of the aquifer in Roger Mills and Custer Counties, Okla., as reach 1 of the Washita River alluvial aquifer. The Washita River is the primary source of inflow to Foss Reservoir, a Bureau of Reclamation reservoir constructed in 1961 for flood control, water supply, and recreation; the reservoir provides water for Bessie, Clinton, New Cordell, and Hobart, Okla. During 1967–2015, nearly 98 percent of the total groundwater use from the Washita River alluvial aquifer was for irrigation, while other uses of groundwater in the study area include public supply, mining, and agriculture.

A hydrogeologic framework was developed for the Washita River alluvial aquifer and included the physical characteristics of the aquifer, the geologic setting, the characteristics and hydraulic properties of hydrogeologic units, the potentiometric surface, and groundwater-flow directions at a scale that captures the regional controls on groundwater flow. The Washita River alluvial aquifer consists of alluvium and terrace deposits that were transported primarily by water and range from clay to gravel in size. The terrace includes windblown deposits of silt size and, in some cases, contains gravel laid down at several levels along former courses of present-day rivers. Underlying the alluvium and terrace deposits in the westernmost part of the study area, the Ogallala Formation of Tertiary age consists of fine- to medium-grained brown to light tan sand with some clay, silt, gravel, volcanic ash, and caliche beds, with some beds locally cemented by calcium carbonate. Underlying the Washita River alluvial aquifer in the eastern part of the study area are bedrock units of Permian age that are reddish-brown and consist of the Elk City Member, Doxey Shale, Cloud Chief Formation, and Rush Springs Formation.

A conceptual flow model is a simplified description of the aquifer system that includes hydrologic boundaries, major inflow and outflow sources of the groundwater-flow system, and a conceptual water budget with the estimated mean flows between those hydrologic boundaries. Mean annual groundwater withdrawals (water use), predominantly from agricultural irrigation, during the study period 1980–2015 totaled 5,502 acre-ft/yr, or 14 percent of aquifer outflows. When applied across the 132-square-mile area used for modeling purposes (84,366 acres), mean annual recharge of 3.15 inches per year corresponds to a mean annual recharge volume of 22,169 acre-ft/yr, or 56 percent of aquifer inflows. If 16 percent (11,828 acres) of the active alluvium area (73,584 acres) had similar cover and depths to water, this rate would correspond to the annual saturated-zone evapotranspiration outflow of 11,828 acre-ft/yr for the Washita River alluvial aquifer, or about 30 percent of aquifer outflows. For the Washita River alluvial aquifer, lateral flow was 17,157 acre-ft/yr, or 44 percent of the aquifer inflows. Lake seepage between Foss Reservoir and the Washita River alluvial aquifer is likely a small amount in terms of an aquifer budget and was not quantified for this study. The conceptual flow model and hydrogeologic framework were used to conceptualize, design, and build the numerical groundwater-flow model.

A numerical groundwater-flow model of the Washita River alluvial aquifer was constructed by using MODFLOW-2005. The Washita River alluvial aquifer groundwater-model grid was spatially discretized into 384 rows and 927 columns containing 350-foot (ft) cells. Two layers were used to represent geologic units in the study area; layer 1 represented the undifferentiated alluvium and terrace deposits of Quaternary age with variable thickness determined from the hydrogeologic framework, and layer 2 represented the bedrock of Permian age which was given a uniform nominal thickness of 100 ft. The groundwater-simulation period was temporally discretized into 433 monthly transient stress periods with one time step each, representing the period January 1980 to December 2015. The monthly transient stress periods were used to capture seasonally variable processes such as recharge, saturated-zone evapotranspiration, and groundwater use. An initial 365-day steady-state stress period was configured to represent mean annual inflows and outflows from the Washita River alluvial aquifer for the study period. The groundwater-flow model was calibrated manually and by automated adjustment of model inputs using PEST++; both processes adjust initial model input values to improve the fit between model-simulated data and observed or estimated data (calibration targets). Calibration targets for the Washita River alluvial aquifer model included groundwater-level and reservoir-stage observations, as well as base-flow and stream-seepage estimates.

Three groundwater-availability scenarios were formulated for the calibrated groundwater model. These scenarios were used to (1) estimate the EPS pumping rate that retains the saturated thickness that meets the minimum 20-year life of the aquifer, (2) quantify the effects of projected pumping rates on groundwater storage over a 50-year period, and (3) evaluate the effects of projected pumping rates extended 50 years into the future and sustained hypothetical drought conditions over a 10-year period on base flow and groundwater in storage. The results of the groundwater-availability scenarios could be used by the OWRB to reevaluate the established MAY of groundwater from the Washita River alluvial aquifer.

EPS scenarios for the Washita River alluvial aquifer were run for periods of 20, 40, and 50 years. The 20-, 40-, and 50-year EPS pumping rates under normal recharge conditions were 1.7, 1.6, and 1.6 acre-feet per acre per year, respectively. Given the aquifer area used for modeling purposes (84,366 acres), these rates correspond to annual yields of about 142,579, 134,986, and 134,986 acre-ft/yr, respectively. Groundwater storage at the end of the 20-year EPS scenario was about 281,000 acre-feet (acre-ft), or about 306,000 acre-ft (52 percent) less than the starting storage. Considering the 84,366-acre model area and using a specific yield of 0.12, this decrease in storage was equivalent to a mean groundwater-level decline of about 30 ft. This groundwater-level decline was greater than the aquifer thickness in some areas of the model where the aquifer was dewatered. The groundwater-level altitude in the aquifer was below the altitude of the streambed during most of the EPS scenarios, thus promoting seepage from streams to the aquifer. The Washita River downstream from Foss Reservoir and most of streams in the study area were dry at the end of the 20-year EPS scenario. Foss Reservoir stage was below the dead-pool stage of 1,597 ft after about 7 years of pumping in the 20-year EPS scenario.

Projected 50-year groundwater-use scenarios were used to simulate the effects of selected well withdrawal rates on groundwater storage in the Washita River alluvial aquifer. The effects of withdrawals from wells were evaluated by comparing changes in groundwater storage among four 50-year scenarios using (1) no groundwater use, (2) groundwater use at the 2015 pumping rate, (3) mean groundwater use for the simulation period, and (4) increasing groundwater use. The increasing-use scenario assumed a 38-percent increase in pumping over 50 years based on 2010–60 demand projections for west-central Oklahoma. Groundwater storage after 50 years with no groundwater use was 545,249 acre-ft, or 693 acre-ft (0.1 percent) greater than the initial groundwater storage; this groundwater storage increase is equivalent to a mean groundwater-level increase of 0.1 ft. Groundwater storage at the end of the 50-year period with 2015 pumping rates was 543,831 acre-ft, or 723 acre-ft (0.1 percent) less than the initial storage; this groundwater storage decrease is equivalent to a mean groundwater-level decrease of 0.1 ft. Groundwater storage after 50 years with the mean pumping rate for the study period was 543,202 acre-ft, or 1,349 acre-ft (0.2 percent) less than the initial groundwater storage; this groundwater storage decrease is equivalent to a mean groundwater-level decrease of 0.1 ft. Groundwater storage at the end of the 50-year period with an increasing demand groundwater-pumping rate, which was 38 percent greater than the 2015 groundwater-pumping rate, was 542,584 acre-ft, or 1,967 acre-ft (0.4 percent) less than the initial storage; this groundwater storage decrease is equivalent to a mean groundwater-level decrease of 0.2 ft.

Mean annual base flow simulated at the USGS streamgage 07316500 Washita River near Cheyenne, Okla. (Cheyenne streamgage) decreased 0.49 ft^3/s (2.4 percent) after 50 years with no pumping and decreased 1.7 ft^3/s (9.4 percent) after 50 years with an increasing demand pumping rate. Mean annual base flow simulated at the USGS streamgage 07324200 Washita River near Hammon, Okla. (Hammon streamgage) decreased 0.2 ft^3/s (0.6 percent) after 50 years with no pumping and decreased 3.6 ft^3/s (13 percent) after 50 years with an increasing demand pumping rate. Mean annual base flow simulated at the USGS streamgage 07325000 Washita River near Clinton, Okla. (Clinton streamgage) decreased 0.3 ft^3/s (0.5 percent) after 50 years with no pumping and decreased 0.6 ft^3/s (0.9 percent) after 50 years with an increasing demand pumping rate.

A hypothetical (10-year) drought scenario was used to simulate the effects of a prolonged period of reduced recharge on groundwater storage in the Washita River alluvial aquifer and Foss Reservoir stage and storage. Drought effects were quantified by comparing the results of the drought scenario to the calibrated model (no drought). To simulate the hypothetical drought, recharge in the calibrated model was reduced by 50 percent during the simulated drought period (1983–1992). Upstream inflows to the Washita River and associated tributaries were reduced by 37 percent, which was the mean decrease in annual base flow during the drought of 1976–81. The simulation was continued 15 years past the end of the drought period through 2007 to assess the recovery of groundwater storage in the Washita River alluvial aquifer. Groundwater storage at the end of the drought period in December 1992 was 562,000 acre-ft, or 36,000 acre-ft (6 percent) less than the groundwater storage of the calibrated groundwater model (598,000 acre-ft). This decrease in groundwater storage is equivalent to a mean water-table-altitude decline of 3.6 ft. By comparison, the drought conditions of 2009–14 resulted in a mean simulated groundwater-level decline of 5.6 ft between January 2009 and December 2014. At the end of the hypothetical drought, the largest changes in saturated thickness (as great as 43.5 ft) were in the area upgradient from Foss Reservoir, particularly in the terrace at the model boundary, whereas changes in saturated thickness downgradient from Foss Reservoir were moderated by inflow from the Rush Springs aquifer. After 12 months of the hypothetical drought, simulated base flows at the Cheyenne, Hammon, and Clinton streamgages had decreased by about 46, 57, and 21 percent, respectively. At the end of the 10-year hypothetical drought period, simulated base flows at these streamgages had decreased by about 55, 73, and 42 percent, respectively.

Substantial decreases in the Foss Reservoir stage began during the fall of 1985 in conjunction with base-flow decreases of up to 100 percent at the Hammon streamgage. These lake-stage declines outpaced groundwater-level declines in the surrounding aquifer.

Selected References

Bard, P.Y., and SESAME-Team, 2004, Guidelines for the implementation of the H/V spectral ratio technique on ambient vibrations-measurements, processing and interpretations: SESAME European research project EVG1-CT-2000-00026, deliverable D23.12.

Barlow, P.M., Cunningham, W.L., Zhai, T., and Gray, M., 2015, U.S. Geological Survey Groundwater Toolbox, a graphical and mapping interface for analysis of hydrologic data (version 1.0)—User guide for estimation of base flow, runoff, and groundwater recharge from streamflow data: U.S. Geological Survey Techniques and Methods, book 3, chap. B10, 27 p., accessed January 1, 2019, at https://doi.org/10.3133/tm3B10.

Barlow, P.M., and Leake, S.A., 2012, Streamflow depletion by wells—Understanding and managing the effects of groundwater pumping on streamflow: U.S. Geological Survey Circular 1376, 84 p., accessed May 1, 2019, at https://doi.org/10.3133/cir1376.

Becker, M.F., and Runkle, D.L., 1998, Hydrogeology, water quality, and geochemistry of the Rush Springs aquifer, western Oklahoma: U.S. Geological Survey Water-Resources Investigations Report 98–4081, 37 p., accessed April 1, 2019, at https://doi.org/10.3133/wri984081.

Bureau of Reclamation, 2018, Reservoir release, storage, evaporation, and precipitation data for Foss Reservoir, Oklahoma, accessed August 15, 2018, at https://www.usbr.gov/gp-bin/custom.pl?SWE221A&foss.

Burns & McDonnell Engineering Company, Inc., 2015, Hydrogeologic Investigation Report for the City of Clinton, Oklahoma, Project No. 81878: Kansas City, Mo., Burns & McDonnell Engineering Company, Inc., 210 p.

Carr, J.E., and Bergman, D.L., 1976, Reconnaissance of the water resources of the Clinton quadrangle, west-central Oklahoma: Oklahoma Geological Survey Hydrologic Atlas 5, 4 sheets.

Chandler, V.W., and Lively, R.S., 2014, Evaluation of the horizontal-to-vertical spectral ratio (HVSR) passive seismic method for estimating the thickness of Quaternary deposits in Minnesota and adjacent parts of Wisconsin: Minnesota Geological Survey Open File Report 14-01, 52 p.

Chen, X., 2003, Stream water infiltration, bank storage, and storage zone changes due to stream-stage fluctuations: Journal of Hydrology, v. 280, no. 1-4, p. 246–264. [Also available at https://doi.org/10.1016/S0022-1694(03)00232-4.]

Condor Team, 2012, Condor version 7.6.6 manual: Madison, Wis., University of Wisconsin.

Cunningham, W.L., and Schalk, C.W., 2011, Groundwater technical procedures of the U.S. Geological Survey: U.S. Geological Survey Techniques and Methods book 1, chap. A1, 151 p., accessed March 1, 2019, at https://doi.org/10.3133/tm1A1.

Doherty, J.E., and Hunt, R.J., 2010, Approaches to highly parameterized inversion—A guide to using PEST for groundwater-model calibration: U.S. Geological Survey Scientific Investigations Report 2010–5169, 59 p., accessed June 1, 2019, at https://doi.org/10.3133/sir20105169.

Dugan, J.T., and Zelt, R.B., 2000, Simulation and analysis of soil-water conditions in the Great Plains and adjacent areas, central United States, 1951–80: U.S. Geological Survey Water-Supply Paper 2427, 81 p., accessed May 1, 2019, at https://doi.org/10.3133/wsp2427.

Ellis, J.H., 2018, Simulation of groundwater flow and analysis of projected water use for the Rush Springs aquifer, western Oklahoma: U.S. Geological Survey Scientific Investigations Report 2018–5136, 156 p., accessed March 1, 2019, at https://doi.org/10.3133/sir20185136.

Ellis, J.H., Mashburn, S.L., Graves, G.M., Peterson, S.M., Smith, S.J., Fuhrig, L.F., Wagner, D.L., and Sanford, J.E., 2017, Hydrogeology and simulation of groundwater flow and analysis of projected water use for the Canadian River alluvial aquifer, western and Central Oklahoma: U.S. Geological Survey Scientific Investigations Report 2016–5180, 64 p., accessed March 1, 2019, at https://doi.org/10.3133/sir20165180.

Ellis, J.H., Ryter, D.W., Fuhrig, L.F., Mashburn, S.L., and Rogers, I., 2020, MODFLOW-NWT model used in simulation of groundwater flow, and analysis of projected water use for the Washita River alluvial aquifer, western Oklahoma: U.S. Geological Survey data release, https://doi.org/10.5066/P9PKMG6U.

Esri, Inc., 2015, An overview of the Spatial Analyst Toolbox, accessed January 28, 2015, at http://resources.arcgis.com/en/help/main/10.2/index.html#/An_overview_of_the_Spatial_Analyst_toolbox/009z00000003000000/.

Fay, R.O., 1978, Stratigraphy and general geology of Custer County, *in* Fay, R.O., and Hart, D.L., 1978, Geology and mineral resources (exclusive of petroleum) of Custer County, Oklahoma: Oklahoma Geological Survey Bulletin 114, 88 p.

Fay, R.O., 2010, Preliminary geologic map of the Foss Reservoir 30′ × 60′ quadrangle, Beckham, Custer, Dewey, Ellis, and Roger Mills Counties, Oklahoma; Oklahoma Geological Survey Geologic Quadrangle Map OGQ-78A, scale 1:100,000, accessed August 31, 2019, at http://ogs.ou.edu/docs/OGQ/OGQ-78A-color.pdf.

Fay, R.O., and Hart, D.L., 1978, Geology and mineral resources (exclusive of petroleum) of Custer County, Oklahoma: Oklahoma Geological Survey Bulletin 114, 88 p.

Ferrari, R.L., 2011, Foss Reservoir 2009 sedimentation survey: Bureau of Reclamation Technical Report No. SRH-2011-01, 26 p., accessed August 15, 2018, at https://www.usbr.gov/tsc/techreferences/reservoir/Foss%20Reservoir%202009%20Sedimentation%20Survey.pdf.

Fry, J.A., Xian, G., Suming, J., Dewitz, J.A., Homer, C.G., Yang, L., Barnes, C.A., Herold, N.D., and Wickham, J.D., 2011, Completion of the 2006 National Land Cover Database for the conterminous United States: Photogrammetric Engineering and Remote Sensing, v. 77, no. 9, p. 858–864.

Griley, H.L., 1933, Subdivision of Quartermaster formation of Oklahoma, and its relationship to known Triassic of Texas Panhandle (abs.): Pan-Amercian Geologist, v. 59, no. 3, p. 234–235.

Gutentag, E.D., Heimes, F.J., Krothe, N.C., Luckey, R.R., and Weeks, J.B., 1984, Geohydrology of the High Plains aquifer in parts of Colorado, Kansas, Nebraska, New Mexico, Oklahoma, South Dakota, Texas, and Wyoming: U.S. Geological Survey Professional Paper 1400-B, 63 p., accessed May 1, 2020, at https://doi.org/10.3133/pp1400B.

Harbaugh, A.W., 1990, A computer program for calculating subregional water budgets using results from the U.S. Geological Survey Modular Three-Dimensional Finite-Difference Ground-Water Flow Model: U.S. Geological Survey Open-File Report 90–392, 46 p., accessed February 1, 2019, at https://doi.org/10.3133/ofr90392.

Harbaugh, A.W., 2005, MODFLOW-2005, the U.S. Geological Survey modular ground-water model—The ground-water flow process: U.S. Geological Survey Techniques and Methods, book 6, chap. A16, variously paged, accessed February 1, 2019, at https://doi.org/10.3133/tm6A16.

Hargreaves, G.H., and Samani, Z.A., 1985, Reference crop evapotranspiration from temperature: Applied Engineering in Agriculture, v. 1, no. 2, p. 96–99. [Also available at https://doi.org/10.13031/2013.26773.]

Hart, D.L., Jr., 1978, Ground water in Custer County, *in* Fay, R.O., and Hart, D.L., 1978, Geology and mineral Resources (exclusive of petroleum) of Custer County, Oklahoma: Oklahoma Geological Survey Bulletin 114, 88 p.

Healy, R.W., and Cook, P.G., 2002, Using groundwater levels to estimate recharge: Hydrology Journal, v. 10, p. 91–109.

Heran, W.D., Green, G.N., and Stoeser, D.B., 2003, A digital geologic map database for the State of Oklahoma: U.S. Geological Survey Open-File Report 03–247, 10 p., accessed June 1, 2019, at https://doi.org/10.3133/ofr03247.

Holland, A.A., 2015, Preliminary fault map of Oklahoma: Oklahoma Geological Survey Open File Report, OF3-2015, 1 p., accessed September 24, 2020, at http://ogs.ou.edu/docs/openfile/OF3-2015.pdf.

Horizon Systems Corporation, 2015, National Hydrography Dataset Plus (NHDPlus): Horizon Systems Corporation, accessed August 1, 2018, at http://www.horizon-systems.com/nhdplus/.

Johnson, K.S., Stanley, T.M., and Miller, G.W., 2003, Geologic map of the Elk City 30' × 60' quadrangle, Beckham, Custer, Greer, Harmon, Kiowa, Roger Mills, and Washita Counties, Oklahoma: Oklahoma Geological Survey Geologic Quadrangle Map OGQ-44, scale 1:100,000, accessed October 5, 2017, at http://ogs.ou.edu/docs/OGQ/OGQ-44-color.pdf.

Keese, K.E., Scanlon, B.R., and Reedy, R.C., 2005, Assessing controls on diffuse groundwater recharge using unsaturated flow modeling: Water Resources Research, v. 41, no. 6, W06010, accessed June 1, 2020, at https://doi.org/10.1029/2004WR003841.

Kent, D.C., Neafus, R.J., Patterson, J.W., Jr., and Schipper, M.R., 1984, Evaluation of aquifer performance and water supply capabilities of the Washita River alluvium in Oklahoma: Final Report to the Oklahoma Water Resources Board, 49 p.

Kottek, M., Grieser, J., Beck, C., Rudolf, B., and Rubel, F., 2006, World map of the Köppen-Geiger climate classification updated: Meteorologische Zeitschrift, v. 15, no. 3, p. 259–263. [Also available at https://doi.org/10.1127/0941-2948/2006/0130.]

Lane, J.W., White, E.A., Steele, G.V., and Cannia, J.C., 2008, Estimation of bedrock depth using the horizontal-to-vertical (H/V) ambient-noise seismic method, *in* Symposium on the Application of Geophysics to Engineering and Environmental Problems, April 6–10, 2008, Philadelphia, Pennsylvania, Proceedings: Denver, Colorado, Environmental and Engineering Geophysical Society, 13 p. [Also available at https://doi.org/10.3997/2214-4609-pdb.177.170.]

Leonard, A.R., Davis, L.V., and Stacy, B.L., 1958, Ground water in the alluvial deposits of the Washita River and its tributaries in Oklahoma: U.S. Geological Survey Open-File Report 58–63, 10 p., accessed February 1, 2019, at https://doi.org/10.3133/ofr5863.

McMahon, P.B., Böhlke, J.K., and Carney, C.P., 2007, Vertical gradients in water chemistry and age in the northern High Plains aquifer, Nebraska, 2003: U.S. Geological Survey Scientific Investigations Report 2006–5294, 58 p., accessed June 1, 2019, at https://doi.org/10.3133/sir20065294.

McMahon, P.B., Plummer, L.N., Böhlke, J.K., Shapiro, S.D., and Hinkle, S.R., 2011, A comparison of recharge rates in aquifers of the United States based on groundwater-age data: Hydrogeology Journal, v. 19, no. 4, p. 779–800. [Also available at https://doi.org/10.1007/s10040-011-0722-5.]

Merritt, M.L., and Konikow, L.F., 2000, Documentation of a computer program to simulate lake-aquifer interaction using the MODFLOW ground-water flow model and the MOC3D solute-transport model: U.S. Geological Survey Water-Resources Investigations Report 00–4167, 146 p., accessed June 1, 2019, at https://doi.org/10.3133/wri004167.

Microsoft Corporation, 2017, Bing maps imagery API, accessed May 1, 2019, at https://msdn.microsoft.com/en-us/library/ff701721.aspx.

Miller, G.W., and Stanley, T.M., 2004, Geologic map of the Anadarko 30' × 60' quadrangle, Caddo, Canadian, Custer, Grady, Kiowa and Washita Counties, Oklahoma: Oklahoma Geological Survey Geologic Quadrangle Map OGQ-58, scale 1:100,000, accessed August 31, 2019, at http://ogs.ou.edu/docs/OGQ/OGQ-58-color.pdf.

Morris, D.A., and Johnson, A.I., 1967, Summary of hydrologic and physical properties of rock and soil materials, as analyzed by the hydrologic laboratory of the U.S. Geological Survey, 1948–60: U.S. Geological Survey Water Supply Paper 1839–D, 42 p., accessed May 20, 2020, at https://doi.org/10.3133/wsp1839D.

National Agricultural Statistics Service, 2019, CropScape—Cropland data layers, 2008–18, accessed November 1, 2019, at https://nassgeodata.gmu.edu/CropScape/.

National Climatic Data Center, 2018, Climate data online, accessed August 16, 2018, at https://www7.ncdc.noaa.gov/CDO/CDODivisionalSelect.jsp.

Natural Resources Conservation Service [NRCS], 2018, Geospatial Data Gateway, accessed September 23, 2018, at https://datagateway.nrcs.usda.gov/.

Neel, C.R., Wagner, D.L., Correll, J.S., Sanford, J.E., Hernandez, R.J., Spears, K.W., and Waltman, P.B., 2018, Hydrologic investigations report of the Rush Springs aquifer in west-central Oklahoma: Oklahoma Water Resources Board, accessed August 2, 2018, at http://www.owrb.ok.gov/reports/studies/RushSprings2015.pdf.

Niswonger, R.G., Panday, S., and Ibaraki, M., 2011, MODFLOW-NWT, A Newton formulation for MODFLOW-2005: U.S. Geological Survey Techniques and Methods, book 6, chap. A37, 44 p., accessed June 1, 2019, at https://doi.org/10.3133/tm6A37.

Niswonger, R.G., and Prudic, D.E., 2005, Documentation of the streamflow-routing (SFR2) package to include unsaturated flow beneath streams—A modification to SFR1: U.S. Geological Survey Techniques and Methods, book 6, chap. A13, 47 p., accessed June 1, 2019, at https://doi.org/10.3133/tm6A13.

Oklahoma Climatological Survey, 2017a, Daily time series using cooperative observer (COOP) data, accessed November 1, 2017, at http://climate.ok.gov/cgi-bin/public/climate.timeseries.one.cgi.

Oklahoma Climatological Survey, 2017b, The climate of Roger Mills County, accessed December 1, 2017, at http://climate.ok.gov/county_climate/Products/County_Climatologies/county_climate_roger_mills.pdf.

Oklahoma Mesonet, 2018, Daily data retrieval, accessed August 16, 2018, at http://www.mesonet.org/index.php/weather/daily_data_retrieval.

Oklahoma Senate, 2019, Title 82—Waters and water rights, Section 1020.5, Determination of maximum annual yield, accessed August 18, 2020, at https://oksenate.gov/sites/default/files/2019-12/os82.pdf.

Oklahoma Water Resources Board [OWRB], 2012a, Oklahoma Comprehensive Water Plan Executive Report, 159 p. [Also available at http://www.owrb.ok.gov/supply/ocwp/pdf_ocwp/WaterPlanUpdate/draftreports/OCWP Executive Rpt FINAL.pdf.]

Oklahoma Water Resources Board [OWRB], 2012b, Oklahoma comprehensive water plan: West-Central Watershed Planning Region Report, 168 p.

Oklahoma Water Resources Board [OWRB], 2015, Water Well Record Search, accessed January 1, 2015, at http://www.owrb.ok.gov/wd/search/search.php?type=wl.

Oklahoma Water Resources Board [OWRB], 2017a, 2017 Oklahoma groundwater report—Beneficial Use Monitoring Program: Oklahoma Water Resources Board, 172 p., accessed March 15, 2019, at https://www.owrb.ok.gov/quality/monitoring/bump/pdf_bump/Reports/GMAPReport.pdf.

Oklahoma Water Resources Board [OWRB], 2017b, Taking and use of groundwater, Title 785, Chapter 30, accessed November, 2017, at https://www.owrb.ok.gov/rules/pdf/current/Ch302019.pdf.

Oklahoma Water Resources Board [OWRB], 2018, Data & maps—Groundwater: Oklahoma Water Resources Board, accessed February 2017 at http://www.owrb.ok.gov/maps/pmg/owrbdata_GW.html.

Patrignani, A., Godsey, C.B., Ochsner, T.E., and Edwards, J.T., 2012, Soil water dynamics of conventional and no-till wheat in the southern Great Plains: Soil Science Society of America Journal, v. 76, no. 5, p. 1768–1775, accessed December 11, 2017, at https://doi.org/10.2136/sssaj2012.0082.

Piper, A.M., 1944, A graphic procedure in the geochemical interpretation of water-analyses: Eos (Washington, D.C.), v. 25, no. 6, p. 914–928, accessed October 8, 2020, at https://doi.org/10.1029/TR025i006p00914.

Rantz, S.E., and others, 1982, Measurement and computation of streamflow—Volume 1. Measurement of stage and discharge: U.S. Geological Survey Water-Supply Paper 2175, 284 p., accessed March 1, 2019, at https://doi.org/10.3133/wsp2175.

Roark, D.M., and Healy, D.F., 1998, Quantification of deep percolation from two flood-irrigated alfalfa fields, Roswell basin, New Mexico: U.S. Geological Survey Water-Resources Investigations Report 98–4096, 32 p., accessed June 1, 2019, at https://doi.org/10.3133/wri984096.

Ryter, D.W., and Correll, J.S., 2016, Hydrogeological framework, numerical simulation of groundwater flow, and effects of projected water use and drought for the Beaver-North Canadian River alluvial aquifer, northwestern Oklahoma: U.S. Geological Survey Scientific Investigations Report 2015–5183, 63 p., accessed May 1, 2019, at https://doi.org/10.3133/sir20155183.

Scanlon, B.R., Reedy, R.C., Stonestrom, D.A., Prudic, D.E., and Dennehy, K.F., 2005, Impact of land use and land cover change on groundwater recharge and quality in the southwestern U.S: Global Change Biology, v. 11, no. 10, p. 1577–1593, accessed July 1, 2019, at https://doi.org/10.1111/j.1365-2486.2005.01026.x.

Schipper, M.R., 1983, A ground-water management model of the Washita River aquifer in Roger Mills and Custer Counties, Oklahoma: Stillwater, Okla., Oklahoma State University, Master of Science Thesis, 147 p.

Scholl, M., Christenson, S., Cozzarelli, I., Ferree, D., and Jaeschke, J., 2005, Recharge processes in an alluvial aquifer riparian zone, Norman Landfill, Norman, Oklahoma, 1998–2000: U.S. Geological Survey Scientific Investigations Report 2004–5238, 54 p., accessed July 5, 2017, at https://doi.org/10.3133/sir20045238.

Shivers, M.J., and Andrews, W.J., 2013, Hydrologic drought of water year 2011 compared to four major drought periods of the 20th century in Oklahoma: U.S. Geological Survey Scientific Investigations Report 2013–5018, accessed July 1, 2019, at https://doi.org/10.3133/sir20135018.

Smith, S.J., Ellis, J.H., Wagner, D.L., and Peterson, S.M., 2017, Hydrogeology and simulated groundwater flow and availability in the North Fork Red River aquifer, southwest Oklahoma, 1980–2013: U.S. Geological Survey Scientific Investigations Report 2017–5098, 107 p., accessed August 1, 2019, at https://doi.org/10.3133/sir20175098.

Smith, S.J., and Esralew, R.A., 2010, StreamStats in Oklahoma—Drainage-basin characteristics and peak-flow frequency statistics for ungaged streams: U.S. Geological Survey Scientific Investigations Report 2009–5255, 59 p., accessed June 1, 2019, at https://doi.org/10.3133/sir20095255.

Stanton, J.S., Peterson, S.M., and Fienen, M.N., 2010, Simulation of groundwater flow and effects of groundwater irrigation on stream base flow in the Elkhorn and Loup River Basins, Nebraska, 1895–2055—Phase two: U.S. Geological Survey Scientific Investigations Report 2010–5149, 78 p., accessed August 1, 2019, at https://doi.org/10.3133/sir20105149.

Stanton, J.S., Ryter, D.W., and Peterson, S.M., 2012, Effects of linking a soil-water-balance model with a groundwater-flow model: Groundwater, v. 51, no. 4, p. 613–622, accessed August 20, 2019, at https://doi.org/10.1111/j.1745-6584.2012.01000.x.

Strahler, A.N., 1952, Hypsometric (area-altitude) analysis of erosional topology: Geological Society of America Bulletin, v. 63, no. 11, p. 1117–1142. [Also available at https://doi.org/10.1130/0016-7606(1952)63[1117:HAAOET]2.0.CO;2.]

Thornthwaite, C.W., and Mather, J.R., 1957, Instructions and tables for computing potential evapotranspiration and the water balance: Centerton, N.J., Laboratory of Climatology, Publications in Climatology, v. 10, no. 3, p. 185–311.

Tonkin, M.J., and Doherty, J., 2005, A hybrid regularized inversion methodology for highly parameterized environmental models: Water Resources Research, v. 41, no. 10, W10412, accessed July 10, 2017, at https://doi.org/10.1029/2005WR003995.

Tortorelli, R.L., Cooter, E.J., and Schuelin, J.W., 1991, Oklahoma—Floods and droughts, *in* Paulson, R.W., Chase, E.B., Roberts, R.S., and Moody, D.W., comps., 1991, National water summary 1988–89: U.S. Geological Survey Water-Supply Paper 2375, p. 451–458, accessed June 5, 2019, at https://doi.org/10.3133/wsp2375.

Trescott, P.C., Pinder, G.F., and Larson, S.P., 1976, Finite difference model for aquifer simulation in two dimensions with results of numerical experiments: U.S. Geological Survey Techniques of Water-Resources Investigations, book 7, chap. C1, 116 p., accessed June 5, 2019, at https://doi.org/10.3133/twri07C1.

Tromino, 2012, Tromino portable ultra-light acquisition system for seismic noise and vibrations—User's manual: Treviso, Italy, Micromed, 139 p.

Tromino, 2017, Tromino Grilla software introduction, accessed December 12, 2017, at http://www.tromino.it/soft-database.htm.

U.S. Census Bureau, 2017, American FactFinder: U.S. Census Bureau database, accessed October 2017 at https://factfinder.census.gov/faces/nav/jsf/pages/index.xhtml.

U.S. Environmental Protection Agency, 1986, Method 9100—Saturated hydraulic conductivity, saturated leachate conductivity, and intrinsic permeability, Revision 0, 57 p.

U.S. Environmental Protection Agency, 2020, Drinking water regulations and contaminants: accessed March 24, 2020, at https://www.epa.gov/sdwa/drinking-water-regulations-and-contaminants.

U.S. Fish and Wildlife Service, 2018, National Wetlands Inventory—Download seamless wetlands data by State, accessed August 16, 2018, at https://www.fws.gov/wetlands/Data/State-Downloads.html.

U.S. Geological Survey [USGS], 2013, National Hydrography Dataset, accessed January 2013 at https://nhd.usgs.gov/data.html.

U.S. Geological Survey [USGS], 2016, Earth Explorer LIDAR dataset: U.S. Geological Survey database, accessed March 2016 at https://earthexplorer.usgs.gov/.

U.S. Geological Survey [USGS], 2018a, National Elevation Dataset, accessed August 16, 2018, at https://ned.usgs.gov/index.html.

U.S. Geological Survey [USGS], 2018b, USGS water data for the Nation: U.S. Geological Survey National Water Information System database, accessed August 16, 2018, at https://doi.org/10.5066/F7P55KJN.

Wahl, K.L., and Wahl, T.L., 1995, Determining the flow of Comal Springs at New Braunfels, Texas, *in* Proceedings of Texas Water '95, A Component Conference of the First International Conference on Water Resources Engineering, San Antonio, Tex., August 16–17, 1995: American Society of Civil Engineers, p. 77–86.

Water Data for Texas, 2020, Texas Water Development Board glossary, accessed June 30, 2020, at https://waterdatafortexas.org/reservoirs/glossary.

Welter, D.E., White, J.T., Hunt, R.J., and Doherty, J.E., 2015, Approaches in highly parameterized inversion—PEST++ Version 3, a Parameter ESTimation and uncertainty analysis software suite optimized for large environmental models: U.S. Geological Survey Techniques and Methods, book 7, chap. C12, 54 p., accessed August 1, 2019, at https://doi.org/10.3133/tm7C12.

Wentworth, C.K., 1922, A scale of grade and class terms for clastic sediments: The Journal of Geology, v. 30, no. 5, p. 377–392. [Also available at https://doi.org/10.1086/622910.]

Westenbroek, S.M., Kelson, V.A., Dripps, W.R., Hunt, R.J., and Bradbury, K.R., 2010, SWB—A modified Thornthwaite-Mather Soil-Water-Balance code for estimating groundwater recharge: U.S. Geological Survey Techniques and Methods 6-A31, 60 p., accessed June 5, 2019, at https://doi.org/10.3133/tm6A31.

White, W.N., 1932, A method for estimating ground-water supplies based on discharge by plants and evaporation from soil—Results of investigations in Escalante Valley, Utah: U.S. Geological Survey Water Supply Paper 659A, 115 p., accessed March 1, 2019, at https://doi.org/10.3133/wsp659A.

For more information about this publication, contact
Director, Oklahoma-Texas Water Science Center
U.S. Geological Survey
1505 Ferguson Lane
Austin, Texas 78754-4501

For additional information, visit
https://www.usgs.gov/centers/tx-water/

Publishing support provided by
Lafayette Publishing Service Center

USGS

Ellis and others—**Hydrogeology, Numerical Simulation of Groundwater Flow, and Effects of Water Use and Drought, Washita River Alluvial Aquifer**—SIR 2020–5118

ISSN 2328-0328 (online)
https://doi.org/10.3133/sir20205118